Effect of taphonomy and methodological decisions on inferences of spatio-temporal distribution of molluscan assemblages and its paleobiological implications

A thesis

Submitted in partial fulfillment of the requirements

Of the degree of

Doctor of Philosophy

By

Madhura Bhattacherjee

ID:20193637

Research Supervisor: **Dr. Devapriya Chattopadhyay**

INDIAN INSTITUTE OF SCIENCE EDUCATION AND RESEARCH PUNE

2022

Dedicated to my grandfather

Late Rabindra Nath Bhattacherjee

Certificate

Certified that the work incorporated in the thesis entitled “Effect of taphonomy and methodological decisions on inferences of spatio-temporal distribution of molluscan assemblages and its paleobiological implications” submitted by **Mrs. Madhura Bhattacherjee** was carried out by the candidate, under my supervision. The work presented here or any part of it has not been included in any other thesis submitted previously for the award of any degree or diploma from any other University or institution.

Date: 3.11.2022

Dr. Devapriya Chattopadhyay
(Supervisor)

Declaration

I declare that this written submission represents my ideas in my own words and where others' ideas have been included, I have adequately cited and referenced the original sources. I also declare that I have adhered to all principles of academic honesty and integrity and have not misrepresented or fabricated or falsified any idea/data/fact/source in my submission. I understand that violation of the above will be cause for disciplinary action by the Institute and can also evoke penal action from the sources which have thus not been properly cited or from whom proper permission has not been taken when needed.

Madhura Bhattacherjee

Date: 2nd November 2022

Mrs. Madhura Bhattacherjee

ID:20193637

Acknowledgements

Undertaking this PhD has been truly a life-changing experience for me and it would not have been possible to do it without the support and guidance that I received from many people.

First and foremost, I would not have been able to complete this work without the support of my supervisor Dr. Devapriya Chattopadhyay (DC). This space does not even seem sufficient to express my immense gratitude towards her. DC has been with me since my masters' days in IISER Kolkata. I joined her for my master's dissertation at IISER Kolkata and continued to work under her supervision for my PhD. It was a great learning experience ever since my masters when I hardly had any knowledge about how the field of research works, she made sure I develop the habit of reading papers and learn to think and develop our own ideas. During my PhD tenure, we had to shift our lab three time, but she made sure everything happened smoothly so that our work was not hampered too much in the process. She worked with us, guided us during planning and execution of all my project endeavours and field trips. Whenever she accompanied us on our field trips, she made sure that we finish our work and have fun at the same time. It was her patience to go through and review multiple drafts of my papers, chapters and presentations that has helped me acquire the necessary skills today. She has always been there to talk to regarding whenever I have faced any academic or personal issues. Her confidence in me made me push my limits and work harder and do things which I thought I wasn't capable of. Apart from the academician that I have become, I owe her a lot to the person that I am today.

I wish to express my earnest gratitude to all my teachers at IISER Kolkata and IISER Pune for leading me to the path of science. I am thankful to my RAC committee members, Dr. Shreyas Managave and Dr. Sudipta Sarkar for their help, support and constructive recommendations during my research work. I wish to thank Dr. Kalyan Halder who was part of my research progress committee at IISER Kolkata for sharing his immense knowledge and inputs on the first research project that I worked on. I am immensely grateful to my collaborator as well as mentor, Dr. Satyaki Mazumder for helping me learn the statistical methods and develop the algorithm for statistical modelling using analytical software required as a part of my Ph.D. work. Inspite of his busy schedule being a faculty at maths department of IISER Kolkata, he has guided me whenever I have reached out to him.

I am thankful to my collaborators Bidisha Som and Ammu Shankar for their contribution during sampling and fieldwork in the first chapter of my thesis. A substantial part of my thesis required taxonomic identification of a huge number of shells and I wish to thank Sai Kulkarni who was a project student in our lab, for her significant contribution to the identification part.

I am thankful to my previous lab seniors Deepjay Sarkar, Debarati Chattopadhyay and Saurav Dutta for providing me with their help and support and creating a comfortable space during the first two years of my PhD tenure. I thank my present lab mate who is more like a younger brother to me, KS Venu Gopal for being the friend that everybody needs. I would also thank my other lab mate Avinash Dahakey and all the BS- MS (present and past) and project students of our lab for the stimulating discussions and constructive inputs during lab meetings and for all the fun we have had in all these years. This long and tedious journey of PhD would not have been possible without the amazing friends that I made during this phase. I am blessed with friends like Shreya, Dilip, Rashi, Pragyant, Piya di, Ritesh, Chirantan, Farzan and Ammu who were with me through my ups and downs of my PhD life and made my stay in both IISERs pleasant and memorable.

I also got the opportunity to attend the Analytical Paleobiology workshop, during the second year of my PhD and had the privilege of learning from some of the best minds in Paleontology. I will always stay grateful to Prof. Michal Kowalewski and Dr. Rafal Nawrot for conducting such intensive and helpful courses. I have utilized the statistical methods learnt during those courses in almost every aspect of data analysis in my PhD work. I was extremely lucky to have met the people who had attended the workshop and got to learn a lot from their work ethics towards science.

I want to extend my sincere gratitude to my family members. No words will ever be enough to thank the contribution of my parents, my father Mr Deb Kumar Bhattacherjee, my mother Mrs. Bulbul Bhattacherjee who have always supported me and stood as a silent pillar to help me flourish and grow through thick and thin. I am also thankful to my husband Squadron Leader Saurish Ganguly, for standing by me and serving as a constant source of motivation. His encouragement and support helped me to cross the ups and downs during the final phase of my PhD.

Lastly, I would remain ever thankful to IISER Kolkata and the doctoral fellowship of IISER Pune for funding all my research expenses from the day I joined to till date.

Table of Contents

Page

Abstract

Marine biodiversity changes through time and space. Identifying the drivers of such change is becoming especially important in the context of recent anthropogenic biodiversity loss. Shallow marine molluscan assemblages have long been recognized as good indicators of overall marine biodiversity and the health of the ecosystem at a regional scale. Their long geologic span and abundance in the fossil record also make useful diversity indicators of past ecosystems. Their complex ecosystem and durable shells enable their fossil record to be a reliable indicator of ecological interactions including predation and competition. A comparison of live assemblage (LA) and time-averaged death assemblage (DA) also provides important ecological insight into the changes in the molluscan community through time. Before one can use these signals for inferring spatio-temporal patterns from molluscan fossil assemblage, however, it is important to recognize that various taphonomic and methodological artifacts can potentially affect the accurate ecological signal. In this thesis, I tried to assess the influence of taphonomy and methodological decisions (such as sampling protocol, analytical method, and data categorization) on ecological inferences using time-averaged molluscan death assemblages. Using statistical modeling, I also proposed ways to recognize such influences and account for them.

The first research problem explored how the degree of spatial live-dead similarity of an assemblage (spatial fidelity) is affected by the degree of post-mortem transportation in a tropical marine setting with a high sedimentation rate and high frequency of storms. Shells can be transported both within and out-of-habitat depending on the energy conditions of the surrounding habitats. Largescale mixing is more common in siliciclastic settings with a narrow shelf, high sedimentation rate, and those that are frequented by episodically high-energy events. By studying the live-dead (L-D) fidelity and modeling size-frequency distribution of the molluscan fauna from Chandipur-on-sea on the east coast of India, I attempted to evaluate the contribution of ‘‘out-of-habitat’’ versus ‘‘within-habitat’’ mixing in developing the molluscan death assemblages. The tropical cyclones originating above 15°N cause a high degree of lateral transport explained by the high compositional similarity of species within this latitudinal extent. The results indicate that those death assemblages are not likely to be a product of within-habitat mixing and they probably received considerable input via regional transport, facilitated by frequent tropical cyclones.

The second research problem of the thesis explored how the spatial diversity of an assemblage is affected by the scale of the study and the choice of diversity index. Beta diversity or between-habitat diversity can be driven by various factors such as environmental,

historical processes, and biotic interactions. The factors determining variability in composition at a small spatial scale are different from the determinant processes at larger scales. I tried to assess how the spatial scale of sampling can influence the nature of beta diversity of molluscs at a regional scale using LA and DA from the west coast of India. I developed a statistical approach to test if the observed variation in beta diversity is explained by the unequal spatial scale (grain size) of sampling. A realistic null model was developed by generating a beta diversity pattern with progressively increasing spatial scale using the observed data of DA and LA over 14 latitude bins. Our observed beta diversity pattern is significantly different from the null model pattern, implying that the unequal grid size of sampling does not explain the spatial variation in beta diversity in this region. Our results also demonstrate that the choice of the beta diversity index and the design of the null model can significantly influence the inference of spatial patterns of diversity. By choosing a combination of the robust models and indices (thereby reducing the effect of methodological artifacts), we could identify the responsible oceanographic variables shaping the regional beta diversity along the west coast of India. This study provides an approach for evaluating the effect of variable sampling scales on comparing regional beta diversity. It emphasizes the importance of understanding the role of sampling and spatial standardization while inferring about processes driving diversity changes.

The third research problem of the thesis evaluated how the sampling intensity and evenness of an assemblage can alter ecological inferences regarding biotic interactions such as predation. Predation is an important evolutionary driver and predation estimates play an important role in understanding its role in shaping the molluscan ecosystem through time. The reliability of the inferences is dependent on the assumption that it is not influenced by other processes or methodological artifacts. Using a resampling technique, I evaluated the effect of evenness and sampling intensity of a community on the inferred predation estimates in molluscs. Theoretically simulated model communities representing different levels of evenness, predation intensity, and predatory behavior (selective, non-selective) were resampled without replacement. The variation in the inferred predation intensity and the number of prey species was noted. The results demonstrate that communities with highly selective predation are sensitive to evenness and sampling intensity. For non-selective predation, sampling intensity heavily influences communities with low evenness and low predation intensity. I also proposed a standardization protocol and validated it using predation data from four Plio-Pleistocene molluscan assemblages. Our approach highlights the importance of these methodological choices in influencing the predation estimates of fossil and recent assemblages.

The findings reported in my thesis highlight the influence of factors such as taphonomy and sampling on the ecological inferences of molluscan assemblages. It also provides critical insights into how such influences can be recognized in recent and fossil assemblages. This will enable future researchers to standardize the data collected from spatio-temporally separated molluscan assemblages before using them for evaluating important ecological hypotheses.

List of figures Page

List of tables Page

CHAPTER 1

Introduction

1. 1 Introduction

The spatio-temporal patterns of biodiversity change have fascinated paleontologists and ecologists since Darwin (Darwin 1909). It provides crucial insight into the long- and short-term processes shaping the distribution of living organisms (Tittensor et al. 2010). The fossil record is the avenue to study long-term processes responsible for the spatio-temporal distribution of organisms. In the context of the recent climate changes, identifying the mechanisms for ecological variation is of primary importance to quantify the processes which may potentially cause an ecosystem collapse (Jablonski 1998; Olszewski and Patzkowsky 2001; Bonelli et al. 2006; Clapham et al. 2006; Clapham and James 2008; Heim 2009). At the same time, various operational decisions about sampling protocols, analytical methods, and data categorization can significantly affect the inferred biological signal (Jurasinski 2007). Appreciation of such factors that may obscure the ecological pattern is essential before concluding spatio-temporal patterns from any fossil assemblage.

Molluscs, with their taphonomically durable shells, are one of the most abundant groups in the shallow marine environment (Kidwell 2001; Kowalewski et al. 2003; Giribet 2008; Khan et al. 2010). Their high abundance in various ecological niches at shallow marine and coastal regions makes them an interesting proxy for tracking their spatial and morphological response to environmental fluctuations occurring along the coasts at a regional scale (Ponder and Lindberg 2008; Sarkar et al. 2019). They have a remarkably documented fossil record with around 60,000 fossil species which dates far back to early Cambrian (Lee et al. 2014). Predation traces such as drill holes and repair scars recording successful and failed predation attempts on molluscs are one of the most abundant predation traces preserved in the fossil record (Alexander and Dietl 2003*a*; Kelley and Hansen 2003; Alexander and Dietl 2005; Klompmaker and Kelley 2015; Klompmaker et al. 2019). As a result, many such large scale quantitative palaeoecological studies rely on molluscan fossil record for evaluating evolutionary hypotheses and inferring ecological patterns through space and time (Hutchinson and Hawkins 1992; Gray 2000; McClain and Rex 2001; McClain et al. 2012; Sarkar et al. 2019). Therefore, we chose molluscs as a proxy for our study to evaluate the role of these operational decisions on the derived paleobiological inferences.

Fossil assemblage represents a subset of a paleocommunity that got favorable conditions to be preserved under the action of taphonomic processes (Staff et al. 1986). Assessing the quality of fossil records as a reliable source of biological information is an

ongoing concern when it comes to the reconstruction of past ecosystems and diversity (Boucot 1953; Kowalewski and Bambach 2008; Patzkowsky and Holland 2012). Before deriving conclusions about macroevolutionary processes, one needs to quantify the extent to which the composition of an ancient community is represented by the fossil assemblages. Actuopaleontology is the study of patterns of distribution and the processes occurring between death and burial of paleontologically relevant organisms in the present time (W Schäfer 1962; Gerhard C Cadée 1991). Examination of their dead remains can provide valuable insights about how taphonomy can impact their fossil record (Behrensmeyer et al. 2000; Kidwell and Holland 2002). Alteration of dead remains can occur after death of an organism depending on the depositional environment, energy conditions of the region and preservation potential of the taxonomic group (Behrensmeyer 1978; Behrensmeyer et al. 2000; Kidwell and Holland 2002). Live-Dead studies, evaluate the extent to which modern death assemblages resemble their living counterpart in terms of their community composition and has been conducted on a number of groups including mammals (Behrensmeyer 1978; Behrensmeyer et al. 2000; Western and Behrensmeyer 2009; Terry 2010; Miller et al. 2014), marine invertebrates such as molluscs (Kidwell 2007; Tomašových and Kidwell 2009*a*, *b*, 2010*a*; Yanes 2012; Kidwell 2013), brachiopods (Tomašových 2004; Tomašových and Kidwell 2010*b*) and also ostracods (Tomašových and Kidwell 2010*b*). This approach has proved to be particularly important to develop critical insight about preservation potential of specific groups, role of environment in preservation, nature of sedimentation and impact of time-averaging (Kowalewski et al. 2003; Tomašových 2004; Tomašových and Kidwell 2009*b*, *a*, 2010*a*, *b*; Kidwell 2013; Cheng et al. 2021).

The rich fossil record of molluscan assemblages prompted paleontologists to study the fidelity of modern marine shelly assemblages (Kidwell 2001). Dead shelly assemblages can be different from live ones because of accumulation of dead remains with time (Fürisch and Aberhan 1990; Kidwell and Bosence 1991; Kowalewski 1996) and degradation due to taphonomic processes such as abrasion, fragmentation, chemical dissolution and cementation (Smith and Nelson 2003; Kosnik et al. 2009; Powell et al. 2011). Post-mortem transportation causing influx and removal of dead shells from different areas depending on the sedimentation rate and wave energy of the region can also impact the formation of dead shell and fossil assemblages (Fürisch and Aberhan 1990; Kidwell and Bosence 1991; Pandolfi 1992; Parsons-Hubbard et al. 1999; Powell et al. 2002, 2008, 2011).There is growing evidence against the generalizations made from molluscan live-dead fidelity studies performed at sampling sites which are mostly situated in regions with a wide shelf, lower

sedimentation rate and with low rates of large scale post-mortem transportation events. These associated biases and underlying assumptions need to be quantified with respect to the area that is being studied.

Apart from taphonomy, the biological signal inferred from the fossil data could be significantly dependent on the protocols followed during data collection and further analyses. Researchers employ a variety of methods for collection, compilation, identification and analysis of fossil assemblages. The inferences derived from these studies are considered reliable biological signal and used for testing various ecological and evolutionary hypotheses in both marine and terrestrial flora and fauna (Kitchell and Kitchell 1980; Vermeij et al. 1981; Harrison et al. 1992; Kelley and Hansen 1993; Vermeij 1993; McNamara 1994; Ellingsen 2001; Ellingsen and Gray 2002; Davidar et al. 2007; Jankowski et al. 2009; Budd and Mann 2019). Only a small number of studies explicitly quantified the impact of methodological differences on the outcome of paleobiological observations including live-dead fidelity (Kidwell 2002), predation (Kowalewski and Hoffmeister 2003; Budd and Mann 2019), diversity and community composition (Rahel 1990; Redman et al. 2007; Anderson et al. 2011; Barton et al. 2013; Budd and Mann 2019). The impact of sampling strategies on inferred faunal composition differ in spatial and temporal scale. Forcino et al. (2010) tested the sensitivity of inferences about faunal composition to operational decisions about sampling and data processing (e.g. taxa to be included, taxonomic resolution). They had observed a consistent signal irrespective of similarity measure and data categorization being used. In contrast, a study on temporal change of molluscan assemblage showed a significant effect of sampling strategies (e.g. data format, analytical approach, and rare data exclusion) on the interpretation of faunal persistence (Visaggi and Ivany 2010). Patchiness among samples affects fine-scale patterns of biological variation, because compositional variation among localities depends on the composition of the patch sampled (Bennington 2003; Webber 2005). Smaller replicate samples within a single bed or unit remove patchiness within samples and produce more robust patterns than one large bulk sample (Lafferty et al. 1994; Zuschin et al. 2006; Zambito et al. 2008). Forcino (2013) observed that increased temporal sampling within multiple stratigraphic units was more informative as compared to increased lateral sampling across a single stratigraphic unit. Therefore, it is also important to evaluate what level of sampling is adequate so that one does not spend valuable time and effort on over-collecting.

Another operational decision which we make while performing modern as well as paleoecological studies is the spatial scale of the study. While studying the biodiversity of a

region, the spatial scale at which we make ecological observations plays a major role in our understanding of ecosystem functioning (Mac Arthur and Wilson 1967; Pandolfi 2002; Hewitt et al. 2005; Tokeshi 2009). Beta diversity, also known as the within- habitat diversity is used to quantify the spatial variation in community composition among localities (Harrison et al. 1992; Gray 2000; Anderson et al. 2011). In comparison to terrestrial communities, beta diversity of marine communities are relatively poorly studied with the exception of reefal communities such as fishes and benthic invertebrates (Hewitt et al. 2005; Harborne et al. 2006; Josefson 2009; Belley and Snelgrove 2016; Roden et al. 2020; Souza et al. 2021). Even though there has been an explosion in terms of reviews and literature highlighting important issues of analytical methods and appropriate terminologies regarding beta diversity, conceptual issues surrounding scale dependence in the patterns and processes producing variation in beta diversity remain (Baselga 2010; Tuomisto 2010; Anderson et al. 2011).The level of habitat heterogeneity will depend on the scale of observation, with increasing resolution (finer scales), more detail can be observed (Senft et al. 1987; With and Crist 1995; Goodsell and Connell 2002). While studying paleo communities, it is important to check the effect of ecological processes on the community composition over variable spatio-temporal scales, before making any statements what processes are truly driving the palaeoecological signal (Fleishman et al. 2003; Becking et al. 2006; Forcino 2013). The factors that will determine variability in composition at a small spatial scale (site-scale or point-based studies) will be different from the determinant processes at larger scales. Most studies have focused on finding drivers of beta diversity over an environmental or latitudinal gradient at global scales (Bustamante and Branch 1996; Melo et al. 2009; Baselga et al. 2012; Maxwell et al. 2022) and small (local) scales are mostly assumed to be homogenous (Whittaker and Likens 1975; Gaston 1994). Recently some progress has been made in observing spatial heterogeneity at smaller scales (point based or site scale) (Downes et al. 1993; Boström and Bonsdorff 1997; Hereu et al. 2008). Athough the importance of global pattern is appreciated, previous researchers also highlighted the role of physical drivers (such as temperature, seasonality and productivity) and the variation of habitats observed at an intermediate regional scale that may have significant effect of the variability in composition (Broitman et al. 2001; Ellingsen 2001; Ellingsen and Gray 2002; Astorga et al. 2014). Studies on terrestrial woody plants have shown that beta diversity changes across a latitudinal or elevational gradient can also simply be caused by sampling due to changes in the size of species pools and not by variable mechanisms of community assembly at temperate vs tropical systems (Kraft et al. 2011). However regional scale studies exploring the effect of variable scale of sampling within a certain spatial extent on spatial heterogeneity is still relatively unexplored.

Despite the significant problems associated with spatial scaling across heterogenous ecosystems, the analytical methods and model designing of ecological studies have been fairly unchanged (Hewitt et al. 2007; Barton et al. 2013).

Apart from faunal composition, different sampling strategies may impact inferences of other important paleoecological processes such as biotic interaction. Biotic interaction, such as predation is an important driver of evolutionary changes through time and predation traces from past and present assemblages are often used to test specific evolutionary hypothesis (Vermeij 1977; Vermeij et al. 1981; Signor and Brett 1984; Langerhans 2007; Stanley 2008; Barnes et al. 2010; Gorzelak et al. 2012; Kotta et al. 2018; Petsios et al. 2021). Researchers have been relying on traces of predation events preserved in the fossil record to assess evolutionary impact of predation in deep time (Vermeij et al. 1981; Alexander and Dietl 2003*b*; Kelley and Hansen 2003). Drill holes and repair scars are one of the abundantly preserved predation traces in the fossil record and hence they are commonly used for various paleoecological studies. The reliability of the inferences are dependent on the premise that it is not influenced by other processes or methodological artefacts. Targeted sampling of specific size-class or a taxon also impacts the inferred predation patterns derived from a sample (Kowalewski and Hoffmeister 2003; Kosloski et al. 2008; Ottens et al. 2012; Hattori et al. 2014; Chattopadhyay et al. 2016; Hausmann et al. 2018). Studies which evaluate the predation trends through space and time are however often forced to use predation data from various discrete assemblages that differ in sample size, community structure, and the type of predation selectivity (Harper 2016). Previous studies have shown analytical techniques to evaluate predation measures and to compare temporally distinct groups often impact the inferences (Kowalewski 2002; Leighton 2002; Grey et al. 2006; Stafford and Leighton 2011; Dietl and Kosloski 2013; Smith et al. 2018; Budd and Mann 2019). Therefore, standardization of protocol for sampling, data categorization and analyses are necessary before concluding about ecological signals such as predation trends and variability in composition of a taxon, especially in studies across variable spatiotemporal scales and meta-analyses (Forcino 2013).

In this thesis, I tried to evaluate the role of taphonomy and sampling on various paleobiological inferences including live-dead fidelity, beta diversity and predation patterns using recent marine molluscan assemblages.

Post-mortem transportation is one of the processes which can impact the accumulation of dead shells and their spatial fidelity with respect to the live assemblages.

Shells can be transported both within and out-of-habitat depending on energy conditions of the surrounding habitats (Kidwell and Bosence 1991). Previous studies suggest that out-of-habitat transport (Kidwell and Flessa 1995; Behrensmeyer et al. 2000) characterized by a large number of shells transported over great distances is thought to play a rather insignificant role in ordinary level bottom sublittoral environments with gentle slopes and they mostly experience within habitat transportation. Narrow, steep continental shelves, in contrast, have more potential for post-mortem transportation (Donovan 2002). However, high energy catastrophic events such as storms and turbidity current can transport shells over large distances and carry them to a low energy environment where they are eventually buried (Dominici and Zuschin 2005). Rate of sedimentation is also an important factor in controlling the rate of mixing by transportation and high rates of sedimentation yield high spatial fidelity (Zuschin and Stanton 2002; Keen et al. 2004). In 2nd chapter of my thesis, I explored the nature of post mortem transportation which is affecting the spatial fidelity in a tropical marine setting with high sedimentation rate and high frequency of storm events such as Chandipur, Orissa. By studying the live-dead fidelity and modelling the size-frequency distribution of the fauna, I attempted to evaluate the contribution of ‘‘out-of-habitat’’ versus ‘‘within-habitat’’ mixing in developing the molluscan death assemblages.

In the third Chapter of my thesis, I tried to investigate how methodological factors such as the grid size of sampling might affect nature of inferred beta diversity patterns at a regional scale. Tropical habitats are known for their high diversity and environmental heterogeneity. Beta diversity or between habitat diversity can be driven by various factors such as environmental, historical processes, biotic interactions. The coastal part of India bordering the eastern Arabian Sea having a latitudinal spread of 14 ° (8–23°N) presents a unique scenario to evaluate the effect of spatial resolution and sampling on beta diversity of bivalves at a regional scale (Sarkar et al. 2019). Using data from our collection of dead assemblages from west coast as well as live assemblages reported from the existing literature, I devised a numeric null model to check if the variation in the beta diversity along the west coast can be explained by unequal spatial scales of sampling . I tried to compare the results of this null model using various beta diversity measures to check if the choice of distance measure has any effect on the patterns. Finally, I tried to evaluate what environmental variables are driving the beta diversity pattern if it is not being affected by methodological factors.

Lastly in the fourth Chapter of my thesis, I evaluated the effect of sampling intensity and nature of prey community structure on inferred predation pattern. Various aspects of prey

community such as evenness, predation selectivity may influence quantification of predation at the community level, such as predation intensity, prey selection. Sampling intensity and selective sampling of a specific size group may significantly impact the results obtained. Using theoretical simulation based on a resampling technique, I attempted to develop a methodological framework to understand the effect of community evenness, sampling intensity, and the nature of predation selectivity on inferred predation estimates. The effect of these parameters was observed on the pattern of inferred predation intensity and the number of prey species. In addition to that, I proposed a method of post-facto standardization to validate our approach using predation data from drill holes and repair scars from four Plio-Pleistocene fossil assemblages of Florida.

In summary, the motivation of this study to understand the effect of various underlying processes and methodological decisions to discover the true biotic and abiotic responses of marine communities from fossil records and modern assemblages.

CHAPTER 2

Molluscan live-dead fidelity of a storm-dominated shallow-marine setting and its implications

Molluscan live-dead fidelity of a storm-dominated shallow-marine setting and its implications

ABSTRACT

Actualistic studies are important for evaluating the fidelity of fossil assemblages in representing the living community. Poor live-dead (LD) fidelity in molluscan assemblages may result from transport-induced mixing. Large-scale mixing is more common in siliciclastic settings with a narrow shelf, high sedimentation rate, and those that are frequented by episodically high-energy events. Chandipur-on-sea, on the east coast of India has an optimal setting to promote such conditions. By studying the LD fidelity and modeling size-frequency distribution (SFD) of the fauna, we attempted to evaluate the contribution of "out-of-habitat" versus "within-habitat" mixing in developing the molluscan death assemblage. The correlation between the composition of live (LA) and death assemblages (DA) was insufficient; unlike LAs, the DAs do not show environmental partitioning in ordination space. A numerical simulation of the shell size frequency distribution (SFD) for DAs from LAs was compared with the observed SFD of the DAs. The results of this simulation indicate that DAs are not likely to be a product of within-habitat mixing. DAs probably received considerable input via regional transport, facilitated by frequent tropical cyclones affecting the coast of Odisha. Chandipur receives a large proportion of cyclones originating above 15°N, which causes a high degree of lateral transport and shell mixing between 15° to 21°N, explained by the high compositional similarity of species within this latitudinal extent. Our study highlights the significance of out-of-habitat transport in shaping the regional distribution of marine fossil assemblages, especially in storm dominated siliciclastic shallow-marine settings.

Keywords: Out-of-habitat transport, tropical cyclone, spatial fidelity, taphonomy

2.1 INTRODUCTION

Actualistic studies are an important tool to understand the taphonomic processes. Live-dead (LD) fidelity is used to evaluate the impact of the taphonomic processes in shaping the fossil record (Behrensmeyer et al. 2000). Marine molluscan assemblages were used for a large number of LD fidelity studies because of their high preservation potential and the resultant paleontological relevance (Kidwell and Bosence 1991). LD fidelity can be affected by multiple processes including time averaging (Fürisch and Aberhan 1990; Kidwell and Bosence 1991; Kowalewski 1996), taphonomic degradation (Smith and Nelson 2003; Kosnik et al. 2009; Powell et al. 2011), and shell mixing due to post-mortem transportation (Zenetos 1990; Parsons and Brett 1991; Callender et al. 1992). Spatial fidelity of molluscan assemblages, in particular, is largely affected by post-mortem transportation (Kidwell and Bosence 1991), both within- and out-of-habitat. Dead shells in siliciclastic environments are more prone to undergo post-mortem transportation as compared to carbonate environments due to lower cementation rate and lower taphonomic degradation by bio-erosion in siliciclastic environments (Tomašových and Kidwell 2009a; Kidwell and Tomasovych 2013; Weber and Zuschin 2013; Korpanty and Kelley 2014; Zuschin and Ebner 2015). Therefore, siliciclastic settings are appropriate to evaluate the effect of post-mortem transportation on the final distribution of dead assemblages.

The susceptibility of dead shells to transportation depends on the energy condition of the surrounding habitats to which the shells are exposed. Experimental flume studies on mollusks have shown that the entrainment velocity is affected by various aspects of morphology such as shell size (Spencer 1963; Olivera and Wood 1997; Dey 2003), shape (Chattopadhyay et al. 2013*a*), and presence of predation marks (Chattopadhyay et al. 2013*b*; Molinaro et al. 2013). Consequently, the original and the transported assemblage may have a different composition (Chattopadhyay et al. 2013*a*, *b*). This may explain the fact that death assemblages (DAs) often capture environmental gradients reflecting habitat-specific taphonomic processes, including between-habitat differences in transportation (Fürsich and Flessa 1987; Powell et al. 2008).

Out-of-habitat transport (Kidwell and Flessa 1995; Behrensmeyer et al. 2000) characterized by a large number of shells transported over great distances by mass (or bulk) flow (Kidwell and Bosence 1991) is thought to play a rather insignificant role in the ordinary level-bottom sublittoral environments as suggested by actualistic taphonomic studies. It is

only considered to play an important role in settings characterized by a steep slope, high sedimentation rate, or settings frequented by very high-energy events (Kidwell and Bosence 1991). In level-bottom sublittoral environments, however, most of the lateral transport is "within-habitat" with influx of exotic species from adjacent habitats (Kidwell and Bosence 1991). The high spatial fidelity found in the majority of actualistic studies could, therefore, be attributed to the preferential selection of sampling sites which are situated on a wide shelf, with low rates of sedimentation and are largely unaffected by high energy events. Narrow, steep continental shelves, in contrast, have more potential for post-mortem transportation (Donovan 2002). Studies conducted in steep slopes tend to show low fidelity due to increased transportation (Hubbard 1992; Hohenegger and Yordanova 2001) and hence, could lead to greater taphonomic bias in benthic marine records. Dominici and Zuschin (2005) emphasized the importance of high energy catastrophic events in the geologic record and argued that the potential of shell transport even in the gently sloping shelves might be greatly altered by catastrophic events such as major storms or turbidity currents—events that are geologically frequent although historically rare. These events may transport skeletal remains into a low-energy environment at depth, bury it with transported sediments over a long period and thereby, lead to eventual preservation (Bries et al. 2004). Rate of sedimentation can also play an important role in controlling the mixing rate of shells during post-mortem transportation. Reworking through intense bioturbation in low-sedimentation areas often strips the event beds of their unique features (Zuschin and Stanton Jr 2002; Keen et al. 2004). Modern assemblages, characterized by high sedimentation rates leading to time-averaged shell beds yield high spatial fidelity (Kowalewski and Bambach 2008; Tyler and Kowalewski 2017). Lower sedimentation, in contrast, would result in low spatial-fidelity of fossil assemblages. In fact, in a comprehensive study based on molluscan datasets from modern open shelf settings, signatures of post-mortem transportation (such as presence of allochthonous shells) are detected in some datasets of the shoreface on wide shelves, that receive high sediment input with transported specimens from adjacent habitats such as estuaries (Kidwell 2008).

There is growing evidence against the general assumption of low probability of "out-of-habitat" transport for fossil assemblages that has been formed by generalizing the results from actualistic studies of selected environments (Dominici and Zuschin 2005) . It is, therefore, worth exploring the nature of spatial fidelity from areas characterized by high sedimentation rate and that are frequented by high energy events.

The eastern coast of the peninsular India is characterized by extremely high sediment influx (> 1350 million tons of suspended sediments/year) brought by the Ganges-

Brahmaputra River systems together with other rivers to the Bay of Bengal, especially towards the north (Milliman and Meade 1983; Subramanian et al. 1985). Chandipur-on-sea is a coastal town in northern Odisha, India (Fig. 2.1A). The state of Odisha has experienced 128 tropical cyclones in the last 109 years (Mohanty et al. 2004). Its coastline is characterized by a siliciclastic marine setting with different habitats including a tidal flat, a beach, a restricted embayment, and an estuary within a small geographic extent. Using the species composition and size frequency distribution of live and dead molluscan assemblages from various habitats of the Chandipur-on-sea, we evaluated the nature of spatial fidelity in a tropical marine setting with high sedimentation rate and high frequency of storm events. We tried to assess the nature of post-mortem transportation processes at small scales (< 200 kms from Chandipur) and large scales (>200 kms from Chandipur) influencing the spatial fidelity of Chandipur by addressing the following questions:

First, is the habitat specific LA-DA fidelity consistent with transportation-induced mixing? We expect significant compositional dissimilarity between habitat specific LAs and DAs as a consequence of storm-induced "within" and "out-of-habitat" transport. Moreover, habitat specific LAs should have lower compositional variation compared to habitat specific DAs. This can be explored with samples from the tidal flat and restricted embayment because these were the only habitats where live specimens were found.

Second, is the shell mixing a result of within-habitat transportation? We expect good agreement between the size-frequency distribution (SFD) of pooled LA and DA if the DAs are developed by transporting LAs after they are dead, within short distances and accumulating over time. Disagreement between the observed DA and the simulated DA created from the pooled LA, however, would point to the low probability of developing DA by within-habitat mixing of live populations. This can be explored with samples from all of the four habitats (i.e., tidal flat, beach, restricted embayment, and estuary).

Finally, is the regional record of high-energy events indicative of the extent of out-of-habitat transport? If the high-energy events are restricted to specific regions, we expect a high degree of shell transport and resultant mixing within that region. This would eventually lead to high compositional similarity of shells within such regions compared to those unaffected by high-energy events. This can be explored using the published data on high energy events and species occurrence from the Chandipur region.

2.2 MATERIALS AND METHODS

The studied coastal region of Chandipur on-sea (21°27′27.01″N, 87°03′25.09″E) represents a 5 km long tropical siliciclastic shallow marine setting (Fig. 2.1) composed of a variety of habitats, including a tidal flat, a sandy beach, an estuary, and a restricted embayment (Figs. 2. 1, 2.2).

2.2.1 Collection Protocol:

Molluscan specimens from four different habitats (beach, tidal flat, restricted embayment, and estuary) were collected during three visits (October 2015, July 2016, September 2016) (Table 2.1). The sampling was conducted with a metal box sediment corer of dimensions 30 cm × 30 cm × 5 cm. After placing the corer, the top sediments within the frame were scooped out with a spatula and the specimens were sieved using a sieve of mesh size 0.3 mm and washed before collecting in separate jars. Using Rose Bengal staining, live specimens were identified and picked. We found live specimens only on the tidal flat and in the restricted embayment. The specimens were identified to the species level using available literature sources (Apte 1998; Rao 2017). The taxonomic information was verified using the World Register of Marine Species (WoRMS). The number of individuals was estimated by counting intact shells and making necessary adjustments for disarticulated valves of bivalves by taking the higher number of left or right valves (total = articulated shells + higher number of left or right valves). After identification, specimens were photographed and cataloged. Sites represented by less than 25 dead specimens were excluded from further analyses (Table 2.1).

Using digital calipers, we measured the length and height of seven individuals (the largest, the smallest, and five random specimens) for each species from live and dead assemblages of each site. The log-transformed (base 2) geometric mean of length and height is used as a measure of size for all subsequent analyses (Kosnik et al. 2006).

2.2.2 Statistical analyses:

2.2.2.1 Live-Dead Fidelity

Univariate analyses were performed on the live and dead assemblages within two habitats (tidal flat and restricted embayment) and the rest of the habitats were not included

due to the lack of live fauna. We calculated F1 (the percentage of species found in LAs occurring in DAs) and F2 (the percentage of species found in DAs occurring in LAs) indices (Kidwell and Bosense 1991; Ritter and Erthal 2013). To evaluate live-dead agreement, we calculated probability of interspecific encounter (PIE) using the calc_PIE() function (Hurlbert 1971), ΔS (Olszewski and Kidwell 2007), and Chao's Jaccard similarity index (Chao et al. 2005). The PIE is also an indicator of beta diversity and consequently for spatial mixing (Olszewski 2004). The difference between the evenness of the death assemblage (dead PIE) and that of the living community (live PIE), called ΔPIE is used for quantifying live-dead agreement in evenness (Olszewski and Kidwell 2007) and can range from +1 to –1. Spearman rank-order correlation of species relative abundance was used as an indicator of similarity between LAs and DAs (Kidwell 2001). The normality of the size distribution of species was evaluated using the Shapiro-Wilk test. Indices were calculated using 'diversity' and 'vegdist' functions in the 'vegan' packages in the statistical programming language R. To visualize the compositional similarity of LA and DA between all samples and habitats, NMDS plots were performed based on the Bray-Curtis similarity indices on Wisconsin-standardized square root transformed proportional abundances using the 'metaMDS' function in R.

2.2.2.2 Size Distribution Model

The extent of post-mortem transport that a shell undergoes primarily depends on the size/mass of the shell and the energy of the carrying medium (Spencer 1963; Allen 1984; Chattopadhyay et al. 2013*a*). A habitat specific size frequency distribution (SFD) depends on the species proportion of a habitat and the body-size of those species (Tomasovych 2004; Kosnik et al. 2006). To test the probability of creating the characteristic size distribution of the DA of each habitat from a common pool of live samples, we designed the SFD model. We first created the SFD of the live population by considering the size data for each species present in the LA. Instead of measuring all live specimens (N) of a species, we developed a representative ontogenetic trend (linear) between length (L) and width (W) for each species from measured specimens (m). Because of small sample size of our measured specimens for certain species, we compared our results with those from a larger collection (S. Mondal's collection from the same locality). The species-specific ontogenetic trend remains the same. Moreover, the larger dataset demonstrates a normal distribution of L for all species except one (Shapiro-Wilk test, p-value > 0.05) (See Appendix Figure 2.S1). After confirming the normality of an observed species-specific SFD, we generated a simulated species-specific

SFD by randomly drawing p (= N-m) number of L values from a normal distribution bounded between the measured minimum and maximum value of L for a particular species. The log transformed (base 2) geometric mean of the Ls and the inferred W (from the species-specific linear trend) was used to create the final SFD of a species. The same process is performed to develop SFDs for all species that are present in the live assemblage. The SFD of pooled live assemblage (SP_L) is generated by combining the SFDs of all the species present in the live assemblage with their observed proportion.

Using this SFD of pooled live data, we developed a model for simulating a distribution of dead shells for each of the different habitats by randomly sampling the size-distribution of the pooled live assemblage. Let's consider that the pooled size data of live assemblage is a vector SP_L with n elements where n is larger than the DA of any habitat. The number of dead shells in a sample from a specific habitat is SB_D. We resampled SB_D from SP_L with replacement and generated a distribution of the simulated dead shells. We calculated the K-S distance and the corresponding p-value between the distribution of observed and simulated dead using the ks.test () function in R. We repeated this step 10,000 times to get Bootstrap densities of K-S distances and p-values.

If dead shells of a given habitat are produced by small-scale mixing as a result of post-mortem transportation of the live assemblages of different habitats, then the above method should show good agreement between the simulated and the observed dead samples. Disagreement between the observed and the simulated dead, however, would point to a low probability of developing the dead assemblage by within-habitat mixing of live populations. A variant of the model is also developed restricting the sampling only to species shared between LA and DA.

Because the entrainment velocity of shells is primarily controlled by shell size and each habitat is characterized by a specific energy, we can calculate a characteristic maximum velocity for each habitat (Spencer 1963; Allen 1984; Olivera and Wood 1997; Dey 2003). We calculated the entrainment velocity of shells in each habitat by using its grain-size range from the Hjulström-Sundborg Diagram (Sundborg 1956). The maximum shell size that can be entrained by the hydrodynamic energy of a habitat was calculated using empirical results (Chattopadhyay et al. 2013*a*; Molinaro et al. 2013; Fick et al. 2020). From the sizes calculated for each habitat using the above equation, a maximum size constraint is applied to the live data. We generated a simulated dead size distribution from the live data with a velocity filter, using the same analysis described previously. For some empirically derived equations (Molinaro et al. 2013; Fick et al. 2020), the maximum size constraint is smaller

than the smallest of the observed value and hence, does not affect the velocity filter and the final distribution.

2.2.2.3 Regional Record of the Storm and Shell Distribution

The cyclone record of Chandipur was developed based on the global-tropical-extratropical cyclone climatic atlas from the U.S. Navy National Climate Data Center cyclone records. We identified the frequency of VSCS (very severe cyclonic storms) and CS (cyclonic storms) that passed within a radius of 200 km around Chandipur in the last 40 years (1977 to 2017). A compilation of published bivalve occurrences from 15 latitudinal bins spanning from 8° to 22°N along the east coast of India was reported by Sarkar et al. (2019). These data of 1927 occurrences representing 417 bivalve species were used to evaluate the compositional similarity with the Chandipur assemblage using an occurrence-based Bray-Curtis similarity index.

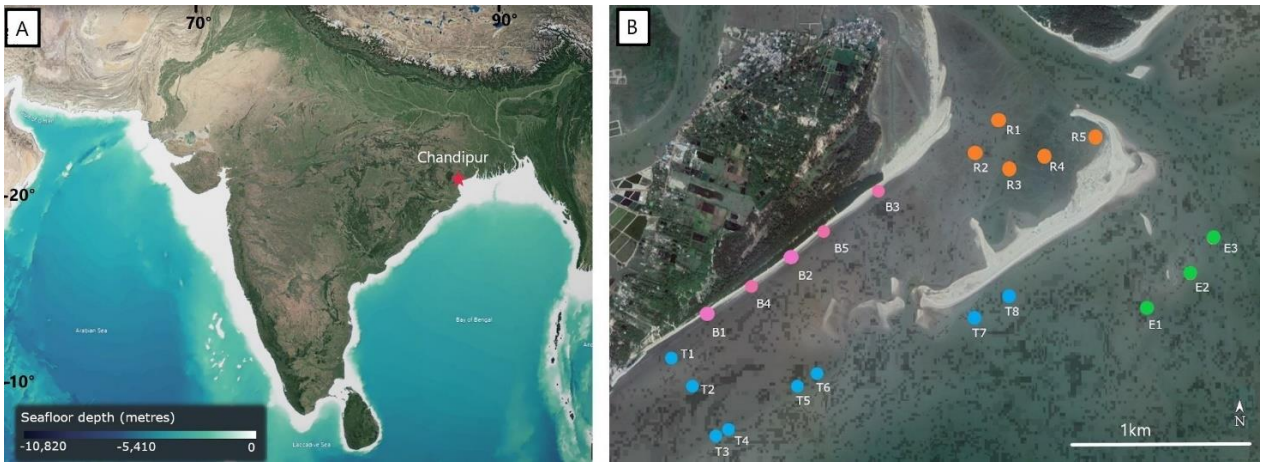

Figure 2.1. Study area. **A**) The location of Chandipur in India (Source: Google Earth Image, National Geophysical Data Center, NOAA). **B**) Location of the sampling sites in Chandipur. Colors represent different habitats: pink = beach; blue = tidal flat; orange = restricted embayment; green = estuary

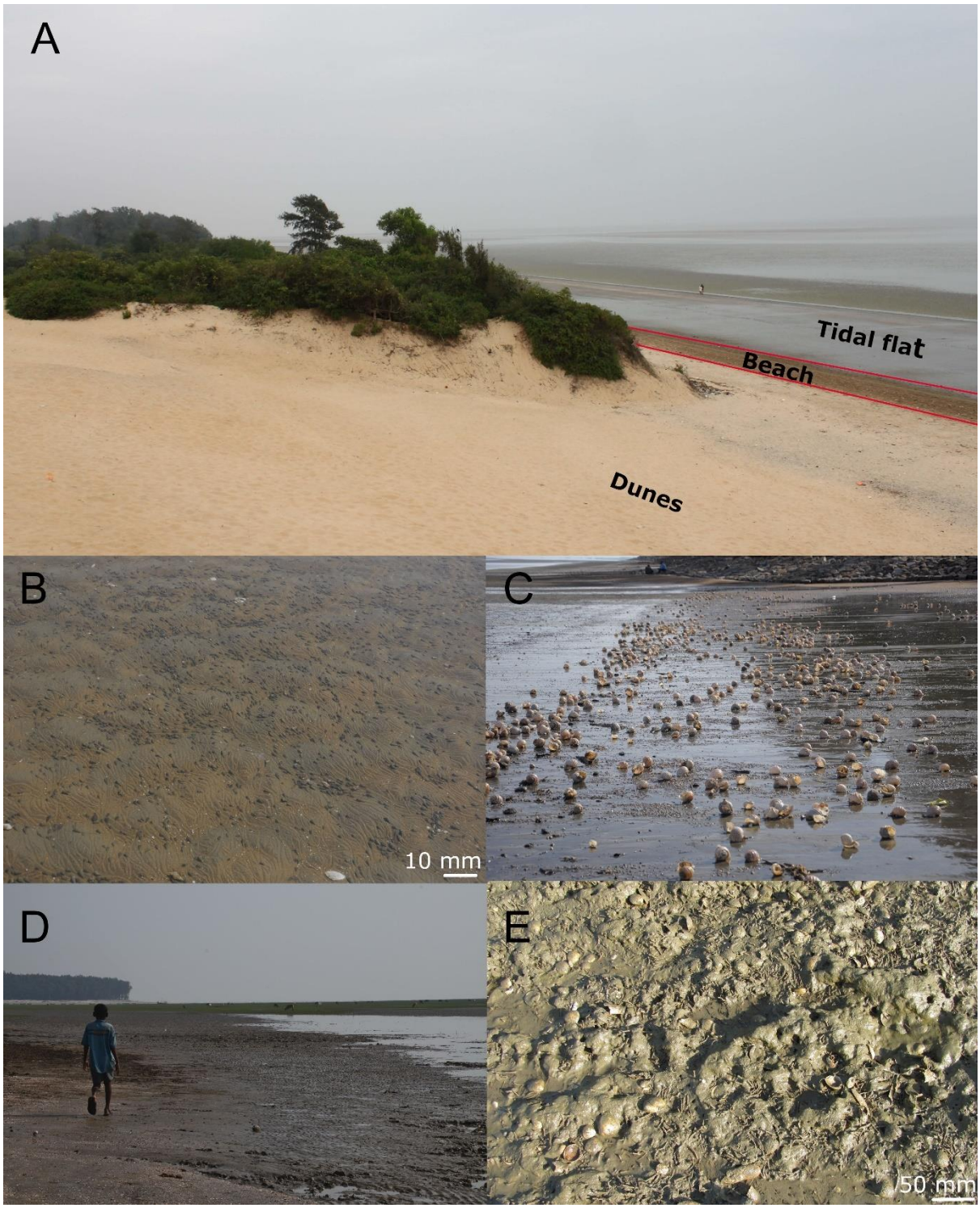

Figure 2.2. Different habitats around Chandipur. (A) Overall view of the backshore, foreshore, and intertidal regions. (B) Live molluscan assemblage, consisting virtually exclusively of gastropods (mostly potamidids) on the tidal flat. (C) Dead shell accumulation at the beach. (D) Overview of the restricted embayment (right of the boy). (E) Death assemblage in the restricted embayment along with a few live individuals.

Table 2.1. Details of samples used for the analyses. The sampling sites are marked in Fig 1. G=Gastropod; B= Bivalve. Sites with less than 25 dead specimens are marked with an asterisk and are excluded from further analyses.

Environment	Site name	Collection season	Abundance at site		Pooled abundance		Richness						Measured specimens				Size range (log2(size))	
							Site specific		Pooled		Shared		All		Shared			
			Live	Dead	Live	Dead	Live	Dead	Live	Dead	Live	Dead	Live	Dead	Live	Dead	Live	Dead
Beach	B1	October, 15	0	55	0	314 (B=251, G=63)	0	8	0	32 (B=24, G=8)	0	4 (B=3, G=1)	0	243	0	27	0	2.03-6.05
	B2	October, 15	0	99			0	19										
	B3	October, 15	0	117			0	10										
	B4*	September, 16	0	4			0	3										
	B5	September, 16	0	39			0	23										
Tidal flat	T1	September, 16	113	124	1330 (B=1044, G=286)	10592 (B=10485, G=107)	5	21	9 (B=2, G=7)	25 (B=17, G=8)	7 (B=2, G=5)		117	406	114	123	2.59-5.83	1.8-6.16
	T2	July, 16	1118	2900			7	11										
	T3	October, 15	28	74			3	13										
	T4	October, 15	36	27			2	2										
	T5	October, 15	1	4210			1	7										
	T6	October, 15	10	706			3	5										
	T7	October, 15	9	989			3	6										
	T8	October, 15	15	1445			2	11										
Restricted	R1	October, 15	11	331	790 (B=227, G=567)	6966 (B=6925, G=36)	1	6	5 (B=4, G=1)	25 (B=18, G=7)	3 (B=1, G=2)	8 (B=3, G=5)	39	186	38	87	2.53-5.07	1.9-5.67
	R2	October, 15	4	27			1	7										
	R3	October, 15	313	74			1	13										
	R4	October, 15	200	4126			1	10										
	R5	July, 16	262	2408			4	11										
Estuary	E1	October, 15	0	648	0	8773 (B=8765, G=8)	0	12	0	21 (B=16, G=5)	0	2 (B=2, G=0)	0	84	0	20	0	2.23-5.79
	E2	October, 15	0	3179			0	9										
	E3	July, 16	0	4946			0	8										

2.3 RESULTS

2.3.1 Overall Richness and Composition:

A total of 24,438 mollusk specimens were collected, representing 15 species of gastropods and 49 species of bivalves (Table 2.1). Out of the total, 91% of the shells belong to the DA, representing 47 species and the remaining 9% belong to the LA, representing 12 species. Only nine species were found in both live and dead assemblages. DA showed higher species richness than LA in all the habitats. In all of the habitats, *Timoclea imbricata* demonstrated the highest abundance in both LA and DA (Fig. 2.3). *Nassarius jacksonianus*, *Paratectonatica tigrina*, and *Pirenella cingulata* were the other three most abundant species found in the LA. Among the six most common species in DAs, *Mactra luzonica, Sunetta vaginalis,* and *Donax lubricus* were not found in the live assemblage. *Tanea lineata* and *Meretrix* (cf.) *lamarckii* were the only two species that were exclusively found in the LA.

2.3.2 Fidelity of Richness:

Species relative abundances in LAs and DAs are not correlated for the overall data (Spearman correlation, rho = -0.02, p = 0.84) (Fig. 2.4B); there are four tidal flat sites, however, that demonstrate significant correlation (Table 2.2). The F1 index values show a range between 50–100% for tidal flat and 25–100% for the restricted embayment (mean for all sites = 47.34%) indicating that most species found in LAs are also found in DAs (Fig. 2.5A). The F2 index values ranged between 9–50% for the tidal flat and 7–14% for the restricted embayment (mean for all sites = 15.31%) (Fig. 2.5B), implying that species found exclusively in DAs by far outnumber the species which are found live.

Comparison of PIE of DAs and LAs show that DAs have lower evenness (Fig. 2.6A). Restricted embayment sites show a similar evenness between DAs and LAs. LAs show higher evenness compared to DAs in sites from the tidal flat. The dispersion of PIE values in DAs was relatively narrow as most of the sites (except T3, T4, and R5) have values smaller than 0.2, whereas it was more heterogeneous in LAs (0.1 to 0.8). Taphonomic fidelity of evenness and richness was measured as cross-plots of live-dead differences in evenness versus richness (ΔPIE vs ΔS) (Fig. 2.6B). Most of the tidal flat sites show negative ΔPIE values with considerable variation in ΔS values (0.19 to 0.84). Restricted embayment sites mostly show zero PIE (except R5) and fall on the boundary between the upper and lower right quadrant with higher ΔS values (0.78 to 1.11). The tidal flat sites are scattered within

three quadrants with no significant correlation between them (r = -0.11, p = 0.71). The median of Chao's Jaccard similarity indices between LA and DA are 0.005. All of the sites from the tidal flat and restricted embayment showed a taxonomic similarity (Chao's Jaccard index) < 0.5 and most sites from the tidal flat and only one site from restricted embayment show positive correlations in species rank order abundance (Spearman's rho), thus occupying the lower right corner of the Chao's Jaccard-Spearman cross plot (Fig. 2.7). However, only a few tidal flat sites show significant rank-order correlation (Table 2.2).

2.3.3 Compositional Partitioning:

The NMDS shows a separation of DAs from LAs (Fig. 2.8A). The LAs showed clear clustering of assemblages from different habitats; the tidal flat and restricted embayment sites segregated into two different groups (Fig. 2.8B). The DAs, however, do not show any such habitat-specific cluster (Fig. 2.8C, 2.8D).

2.3.4 Nature of Size Distributions and Modeling Within-Habitat Mixing :

The SFD of all habitats has a comparable range, except for the beach that showed a higher size range (Fig. 2.9). The size distribution for the simulated DA is significantly different from that of the observed DAs for all habitats (p value << 0.05) (Fig. 2.10A–2.10D). The beach shows the largest difference (Fig. 2.10A) and the tidal flat shows the smallest difference (Fig. 2.10B). Re-running the simulation using the energy-specific size cut-off for each habitat did not produce any significant change (Fig. 2.10E, 2.10F). The size distribution of the beach and the tidal flat is completely unaffected by the velocity filter because the characteristic velocity is higher than the required velocity to transport even the biggest shells. The restricted embayment and the estuarine habitat show a change in the magnitude of difference after applying the cut-off, which is not statistically significant. Other variants of the model (i.e., with only the shared species, using different equations for bivalves and gastropods) did not produce any significant change (See Appendix Figure 2.S2).

2.3.5 *Regional Nature of Storms and the Distribution of Shells*

Chandipur has been affected quite frequently by tropical cyclones in last 40 years (1977 to 2017); a total of three very severe cyclonic storms (VSCS) and 13 cyclonic storms (CS) affected the coast between 1980 to 2010 (Fig. 11) and the majority of the cyclones originated above 15°N (Fig. 2.12A, 2.12B). The published literature on reported occurrence

data of bivalve species shows a drop in compositional similarity (Bray-Curtis index) below 15°N when compared to the Chandipur bivalve assemblage (Fig. 2.12C).

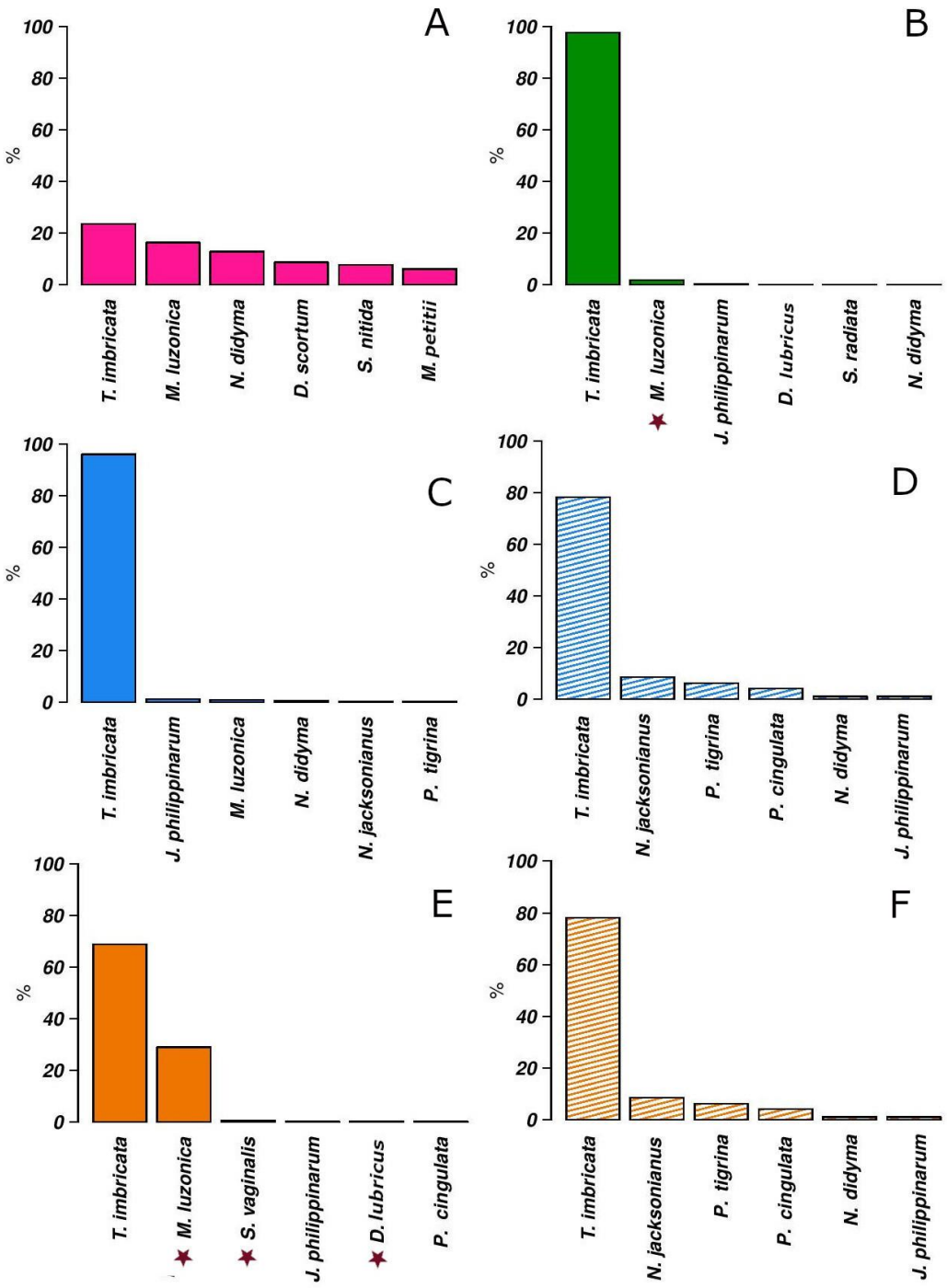

Figure 2.3. The proportion of the six most abundant species for various habitats. DAs: (A) Beach. (B) Estuary. (C) Tidal flat. (E) Restricted embayment. LAs: (D) Tidal flat. (F) Restricted embayment. Stars indicate those species that are exclusive to DAs.

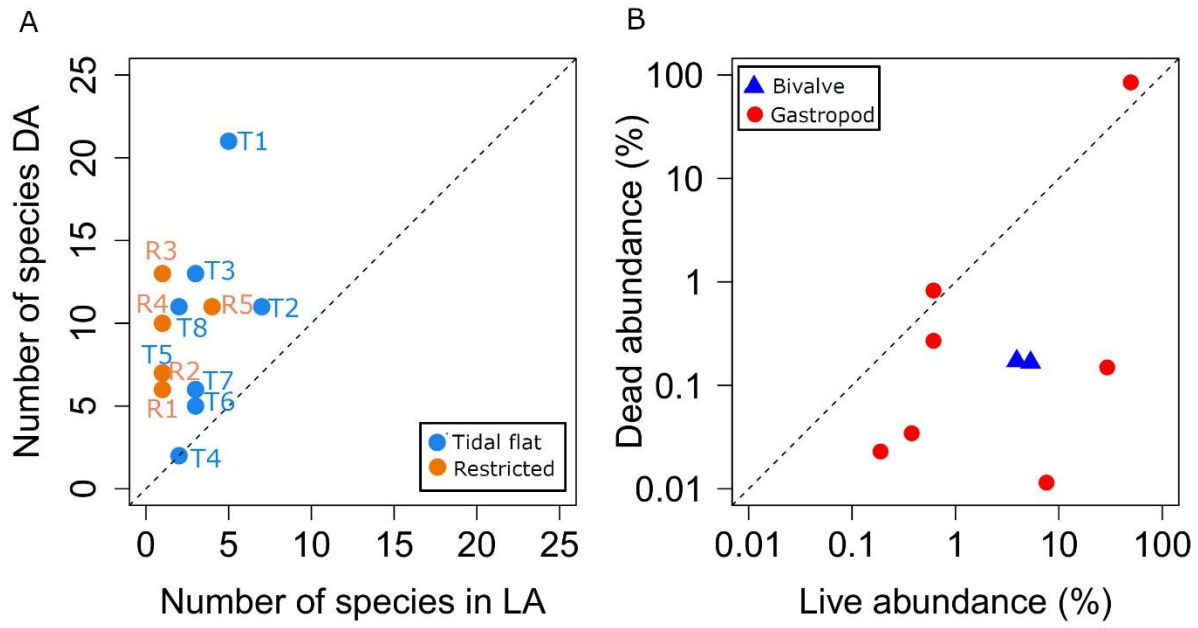

Figure 2.4. Comparison of species richness of LAs and DAs. (A) Bivariate plot showing species richness in LAs vs DAs of different sampling sites across Chandipur. (B) Bivariate plot of species relative abundance in DAs and LAs.

Table 2.2. Results of Spearman rank order correlation between LA and DAs for sampling sites within tidal flat and restricted environment. Statistically significant values are marked in bold.

Habitat	Site names	Spearman's rho	p value
Tidal flat	T1	-0.09	0.49
	T2	0.50	**0.00**
	T3	0.40	**0.00**
	T4	-0.07	0.63
	T5	0.05	0.69
	T6	0.54	**0.00**
	T7	0.37	**0.00**
	T8	0.22	0.10
Restricted	R1	-0.07	0.63
	R2	-0.05	0.71
	R3	0.22	0.11
	R4	-0.11	0.42
	R5	-0.09	0.49

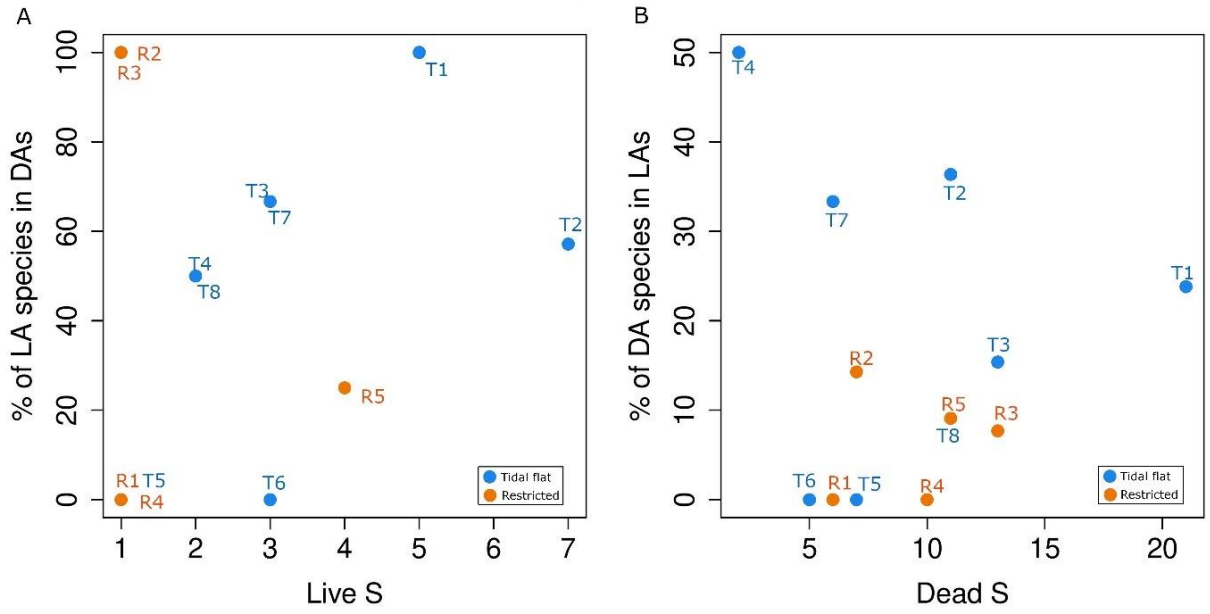

Figure 2.5. Live-dead fidelity. (A) Bivariate plot showing percentage of species found in LAs that are also found in DAs (F1 index) vs. number of species in LAs. (B) Bivariate plot showing percentage of species found in DAs that are also found in LAs (F2 index) vs. number of species in DAs.

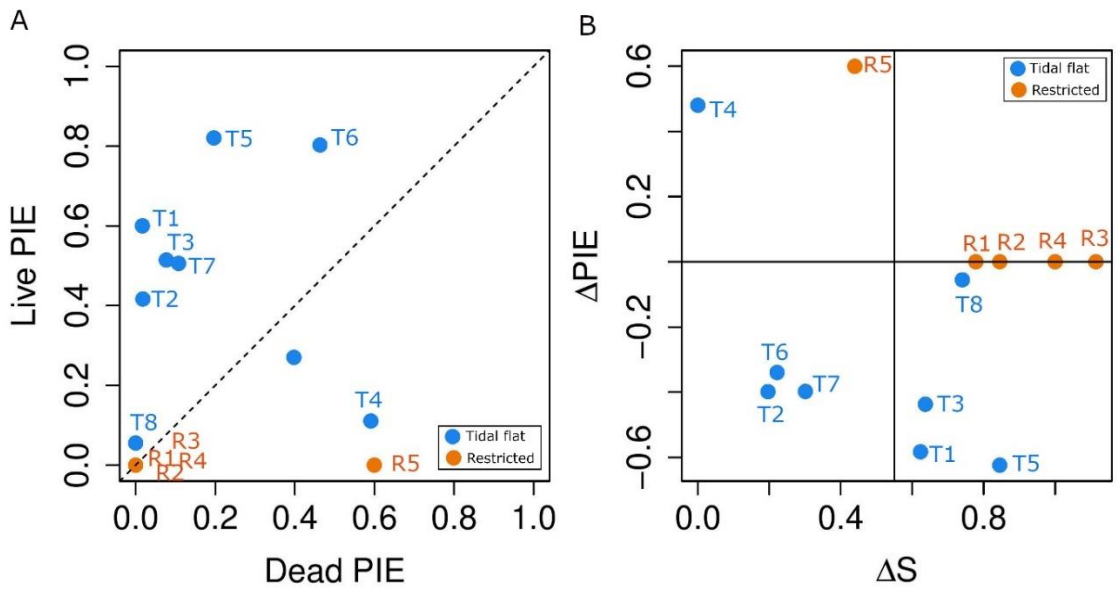

Figure 2.6. Fidelity between LAs and DAs. (A) Cross-plot of evenness (Probability of Interspecific Encounter PIE) of LAs and DAs (rho: 0.494; p: 0.08). (B) Cross-plot of differences in evenness (ΔPIE) and species richness (ΔS) between DAs and LAs at different sampling sites (rho: 0.046; p: 0.88).

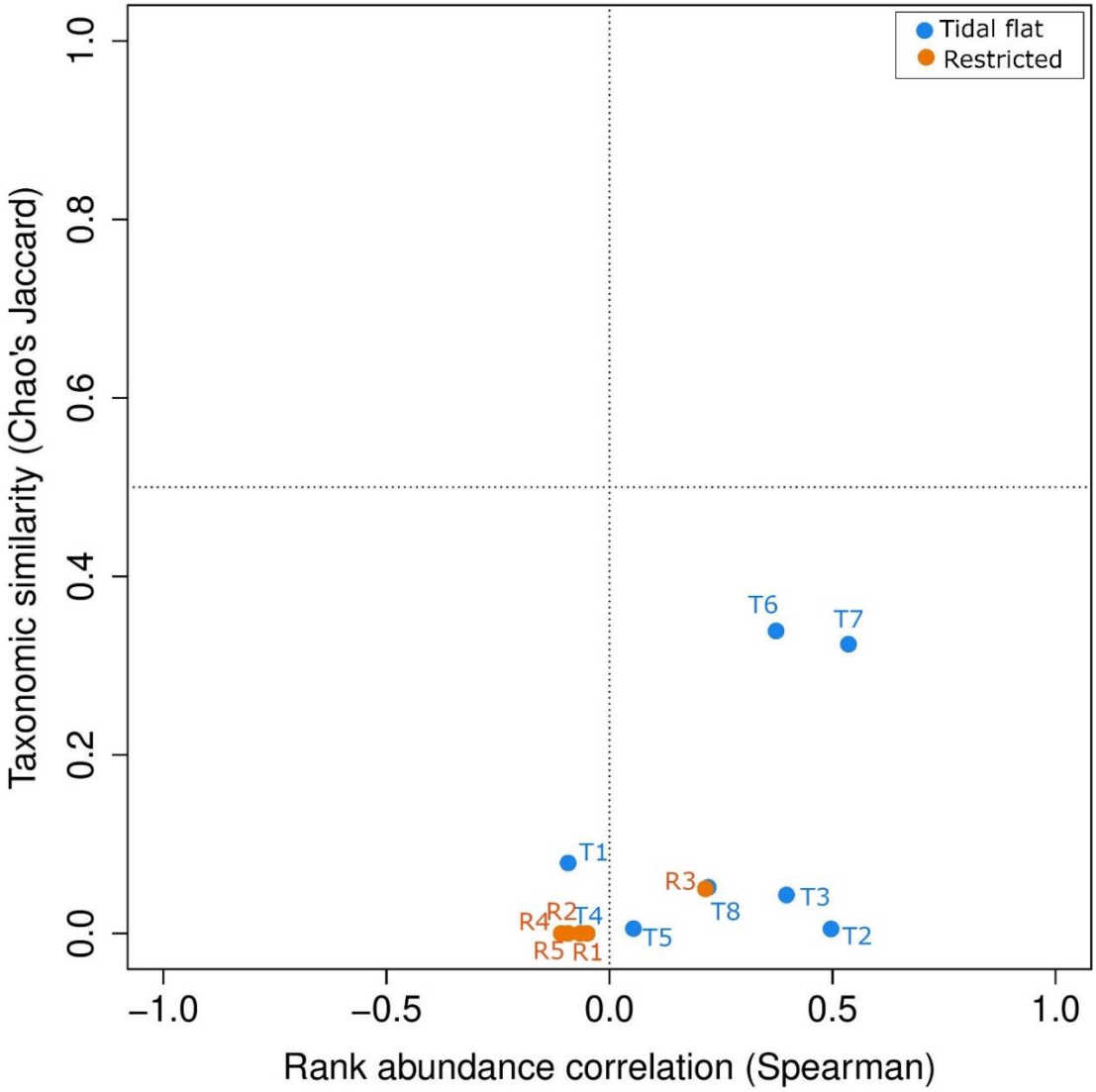

Figure 2.7. Live–dead taxonomic agreement (Chao's Jaccard similarity index) plotted against live–dead rank-order correlation (Spearman rho) across different sampling sites from Chandipur. Sites located in the upper right quadrant have the highest live-dead agreement and sites in the lower left quadrant have the lowest live-dead agreement.

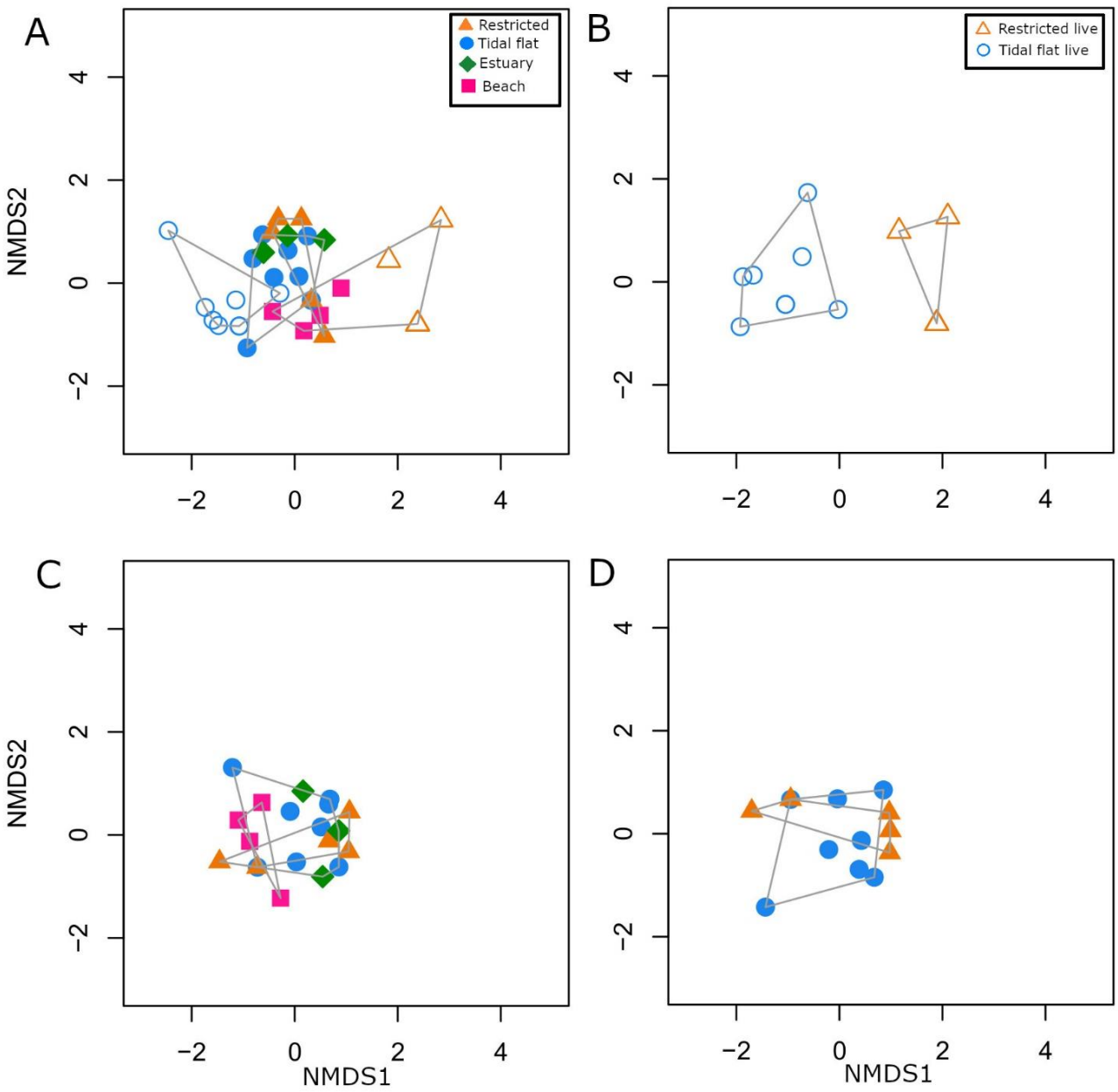

Figure 2.8. Non-metric multidimensional scaling for species abundances. (A) Pooled LAs and DAs of all sites (Stress = 0.13). B) Only LAs (Stress = 0.003). (C) DAs with all habitats (Stress = 0.16), (D) DAs from habitats with live specimens (Stress = 0.12). The closed symbols represent DAs and the open symbols represent LAs.

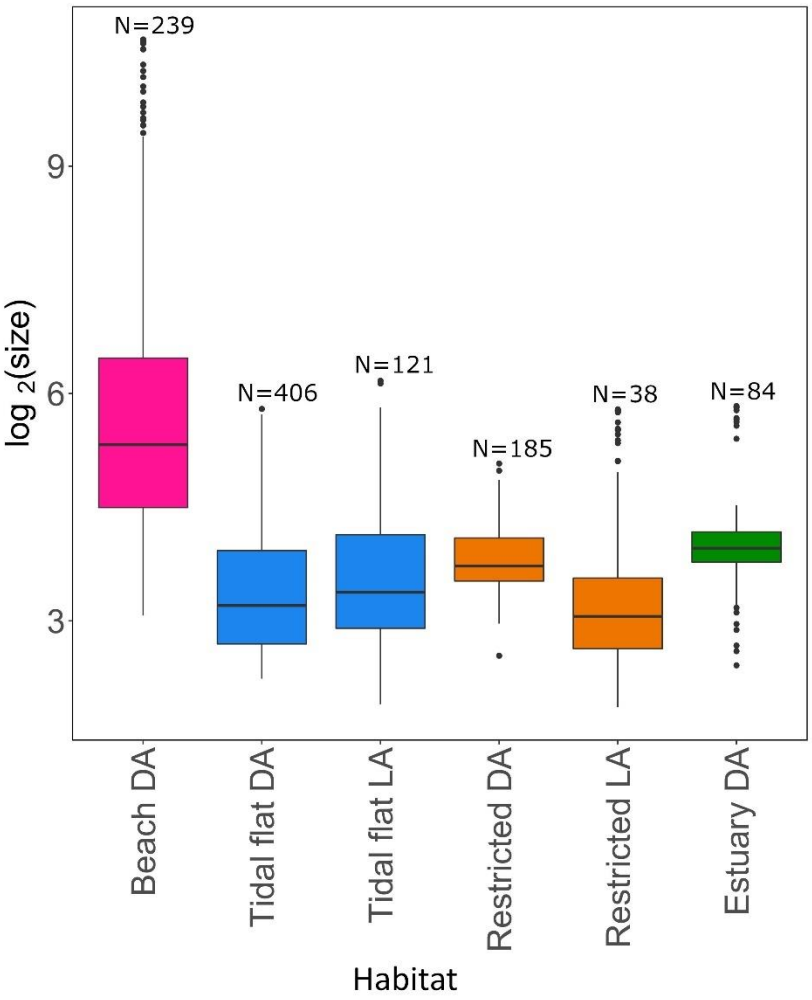

Figure 2.9. Box plots of size ranges of individuals (log_2 geometric mean of shell size) from LAs and DAs of all the habitats. Key: N = sample sizes; filled circles = outliers of the data; horizontal line inside box = median; lower and upper box boundaries = the first and third quartiles, respectively; and the lower and upper whiskers = the lowest and the highest observations of 1.5 times the Inter Quartile Range.

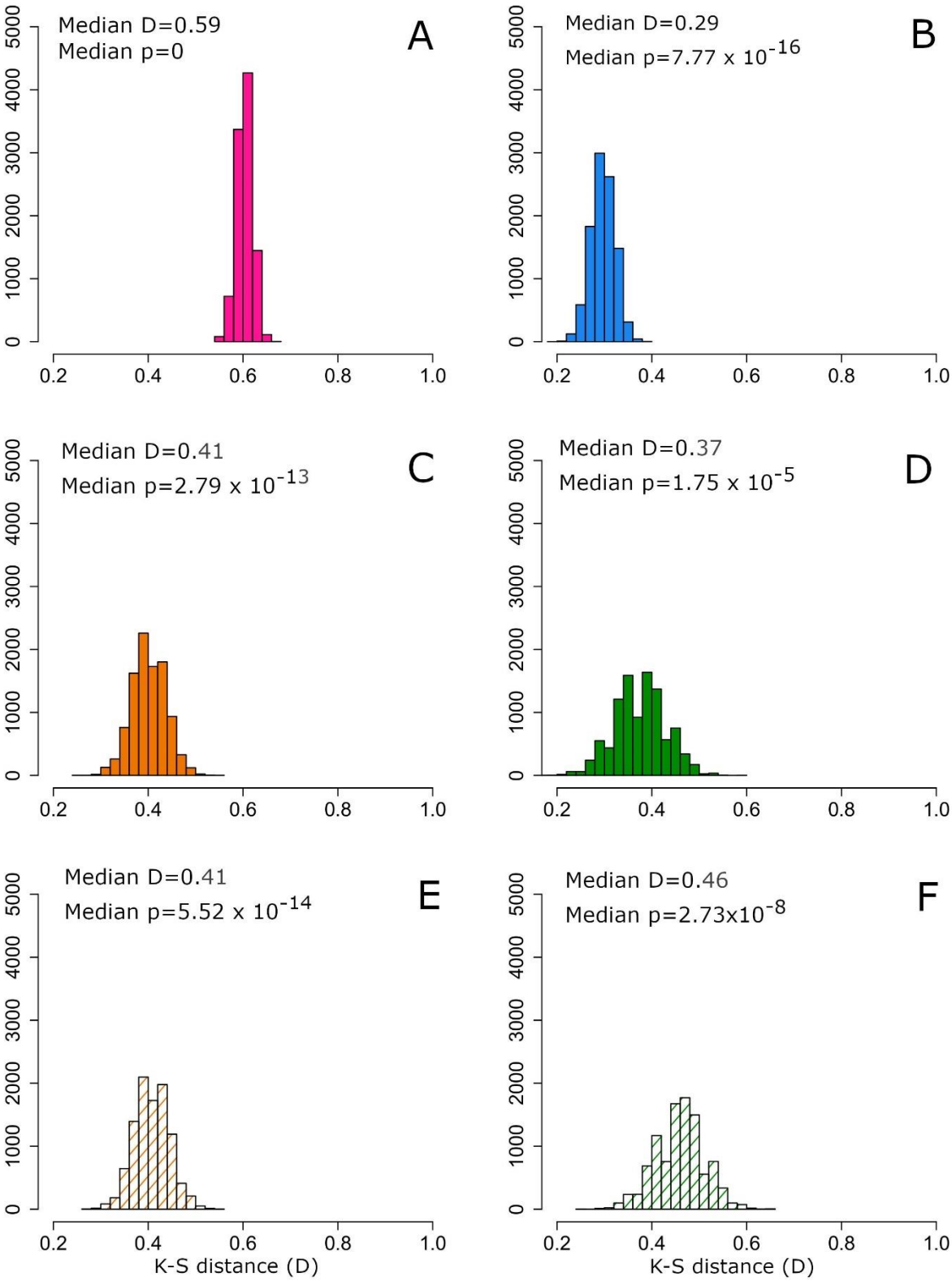

Figure 2.10. Histograms of D-values from the K-S test between simulated and observed dead size frequency distributions. (A) Beach. (B) Tidal flat. (C) Restricted embayment. (D) Estuary. (E) Restricted embayment (with size filter). (F) Estuary (with size filter).

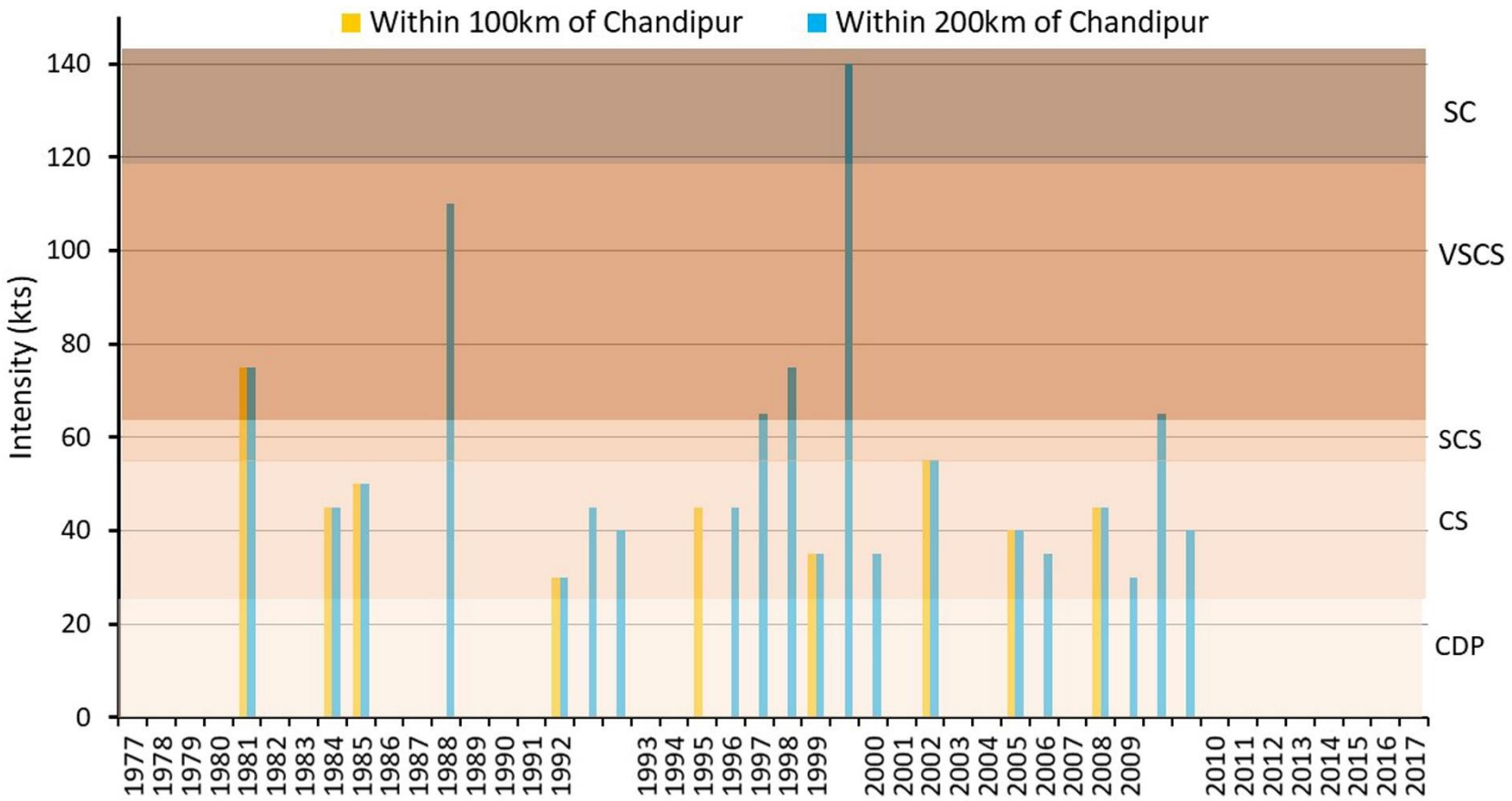

Figure 2.11. Bar diagram of intensity of cyclones from 1977 to 2017 within 100 km (yellow) and 200 km (blue) radius of Chandipur. Each bar corresponds to the occurrence of one cyclone that has affected region. The different categories of cyclones are shown in different shades of orange: SC = Super Cyclone; VSCS = Very Severe Cyclonic Storm; SCS = Severe Cyclonic Storm; CS = Cyclonic Storm; CDP = Cyclonic Depression during monsoon.

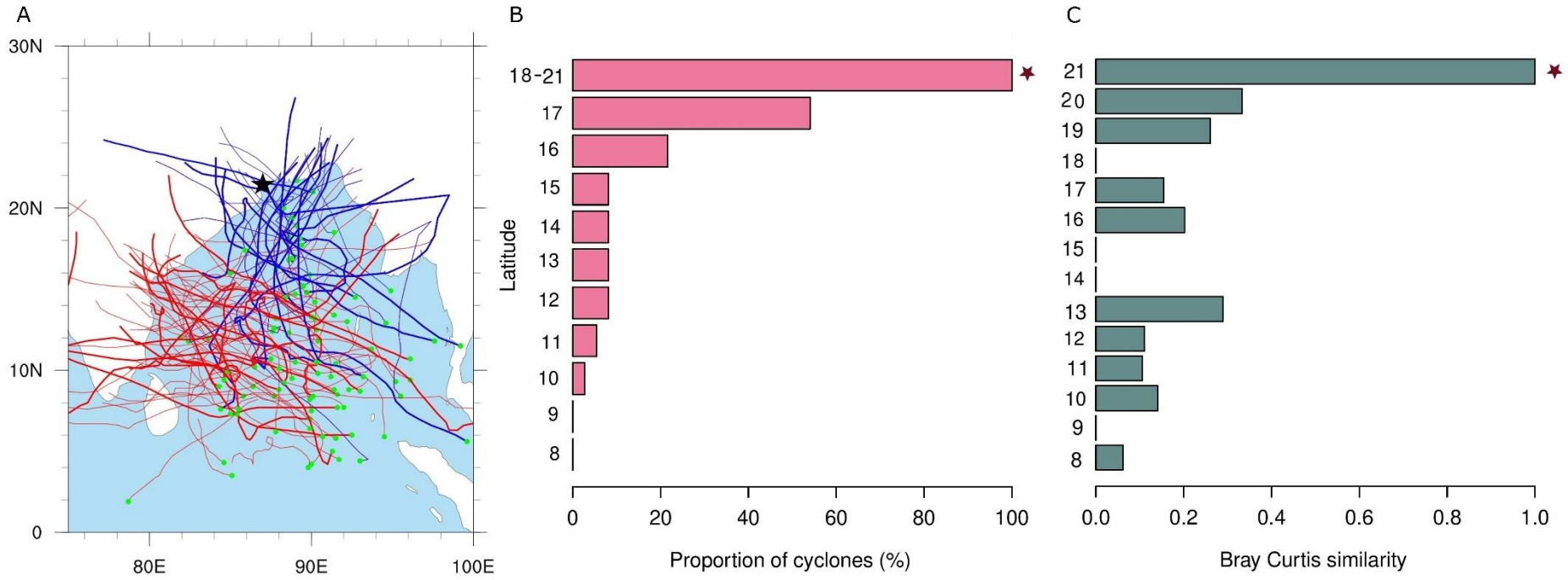

Figure 2.12. Cyclones at the eastern coast of India. A) Tracks of cyclones passing through the eastern coast of India from years 1977–2014 which are within a radius of 3° from Chandipur (blue) and those below 3° radius marked in red. Cyclones with higher intensity (> 60 knots) have bolder lines. (B) Plot showing the cyclones affecting regions within 3° latitudes of Chandipur (denoted by a star). The bars indicate the proportion of the total number of cyclones originating in each latitudinal bin that eventually affected Chandipur. (C) Bar plot showing compositional similarity of the bivalve assemblage of Chandipur (denoted by a star) with other latitudinal bins in the east coast based on published data. Occurrence based Bray-Curtis similarity index is used. A few latitudes were excluded due to insufficient data.

2.4 DISCUSSION

2.4.1 Degree of Live-Dead Fidelity:

Our study shows that DAs are about four times richer than LAs at both site-specific analyses as well as in pooled assemblages (Fig. 2.4A). These results are in agreement with the expectation of high D-L mismatch in siliciclastic environments due to the high window of time-averaging leading to high D/L ratios (Kidwell and Bosence 1991; Flessa and Kowalewski 1994; Kidwell and Flessa 1995; Kowalewski et al. 2000; Kidwell 2002, 2008; Tomašových and Kidwell 2009*a*, 2010; Tomaŝovỳch and Kidwell 2011; Kidwell 2013; Korpanty and Kelley 2014). The high D/L ratio that we observed is significantly higher than the highest ratios provided by the study on 11 datasets from primarily siliciclastic soft sediment settings in temperate environments (Tomašových and Kidwell 2009*a*). These ratios are considerably higher than those reported by Weber and Zuschin (2013) for an inner and outer tidal flat in a siliciclastic, temperate environment in the Adriatic Sea (range 1.06–2.77). The high D/L ratio observed in our study can also be attributed to the high patchiness of LAs, when sites having fewer species in the LA are compared to their respective, more homogenized DAs (García-Ramos et al. 2016). LAs in our study are depicting the environmental partitioning within habitats as expected and are likely to represent the diversity of the living community accurately (Bouchet et al. 2002; Kidwell 2002; Warwick and Light 2002; Warwick and Turk 2002; Zuschin and Oliver 2005; Albano and Sabelli 2011; Kidwell and Tomasovych 2013; García-Ramos et al. 2016; Bürkli and Wilson 2017). The lower richness in LA might be due to under-sampling (Lockwood and Chastant 2006) and the richness in DA can be increased owing to time averaging (Olszewski and Kidwell 2007) and spatial mixing between contiguous areas (Fürsich 1978).

Comparing LD fidelity in the tidal flat and restricted embayment, we observed that the percentage of dead species found in live assemblages (F2) is lower than that of living species found in death assemblages (F1). Studies have yielded values around 62–88% for F1, and 63–94% for F2 in marine settings (Kidwell and Bosence 1991; Zuschin et al. 2000; Kidwell 2002; Kowalewski et al. 2003; Zuschin and Oliver 2003; Lockwood and Chastant 2006). Previously reported values of F1 (75–100%) and F2 (12.5–100%) from an estuarine-lagoonal setting (Ritter and Erthal 2013) is comparable to the observed values of the restricted embayment in our study (Fig. 2.5A, 2.5B). It is important to note, however, that the F indices do not consider sample size discrepancies between live and dead assemblages (Lockwood and Chastant 2006; Tomašových and Kidwell 2009*a*) and may have limited interpretive value for the present scenario where the sample size of LAs and DAs differ substantially.

Unlike other studies that document good within-habitat correlation in tidal flat and associated sub-littoral soft bottom habitats (Kidwell 2001; Weber and Zuschin 2013; Zuschin and Ebner 2015), we found a lack of strong rank-order correlation for the tidal flat and for the restricted embayment except for a few sites in the tidal flat (Table 2.2). In the Chao's Jaccard-Spearman plot, sites in the upper-right and lower-left quadrants represent the highest and lowest L-D agreement respectively (Kidwell 2007). Most of the tidal flat sites fall in the lower right-hand corner with very low similarities and positive rank order correlation indicating poor L-D agreement (Fig. 2.7). In the ΔS-ΔPIE plot, $\Delta S > 0$ and $\Delta PIE > 0$ indicates that the DAs represent higher diversity and evenness respectively when compared to that of the LAs (Olszewski and Kidwell 2007; Kidwell 2008). Both tidal flat and the restricted embayment are characterized by a positive ΔS with substantial site-specific variation (Fig. 2.6B). Although the richness is generally higher in DAs, there is a high degree of variation across sites in terms of alpha diversity. The tidal flat with a negative ΔPIE indicates a higher evenness for LAs in contrast to the restricted embayment with a nearly equal evenness between LA and DA (Fig. 2.6B). The ΔPIE value of the tidal flat is consistent with the processes that bring more short-term or rare species in the live assemblage and increase the evenness in LA (Olszewski and Kidwell 2007; Kidwell 2008).

Our sampling protocol may have contributed to the observed fidelity of LA and DA. A multi-year replicate sampling is ideal to determine fidelity as species composition and abundance can vary seasonally or may differ between subsequent years (Kidwell and Bosence 1991; Kidwell and Flessa 1995; Kidwell 2001; Kidwell et al. 2001; Lockwood and Chastant 2006). It is not possible to rule out the contribution of such variations in shaping the L/D fidelity using our sampling protocol. Apart from the sampling protocol, mismatches between LA and DA of an area can also be caused by (1) time averaging (Olszewski and Kidwell 2007; Tomašových and Kidwell 2009*a*); (2) lower sedimentation rates leading to longer exposure of shells to degradation (Smith and Nelson 2003; Kosnik et al. 2009; Powell et al. 2011); and (3) shell mixing due to post-mortem transportation (Zenetos 1990; Parsons and Brett 1991; Callender et al. 1992). However, it is important to note that these three factors are not mutually exclusive and can work together in conjunction to create patterns. A high window of time averaging can lead to high D/L ratios because of higher rates of post-mortem transport and lower sedimentation rates (Kidwell 2002; Finnegan and Droser 2008; García-Ramos et al. 2016). The poor rank-order correlation between LAs and DAs often indicates that a redistribution of shelly remains in shallow sublittoral or intertidal environment at local-scale (within-habitat mixing) or large-scale (out-of-habitat mixing) due to lower sedimentation rate or higher energy conditions (e.g Miller et al. 1988; Kidwell 2008; Poirier et al. 2010; Albano and Sabelli 2011). Although we do not have measurements of the

sedimentation rate at Chandipur, its location within the Ganges-Brahmaputra River system points to a high sedimentation rate of the basin. The linear sedimentation rate (LSR) varies from a moderate (0.15mm/y) to high (3.86 mm/y) value in the nearby area of the present study (18°59.1020″ N, 85°41.1669″ E) in the western Bay of Bengal (Da Silva et al. 2017). High sedimentation rates might increase fidelity in embayments such as lagoons and estuaries because the re-equilibration rate between DAs and LAs positively correlates with sedimentation rates (Kidwell 2007; Ritter and Erthal 2013). The DAs, however, can acquire higher richness than LAs if the rate of shell input is higher than the rates of shell destruction and sedimentation (Ritter and Erthal 2013). Therefore, the high degree of L/D mismatch of the pooled data along with habitat specific data from the estuary and from the restricted embayment of Chandipur might be a result of processes such as increased shell input and consequently mixing of shells by lateral transport.

2.4.2 Fidelity of Composition:

A comparison of overall compositional fidelity between LA and DA shows the dissimilarity of the most common species in DA and LAs. Except for Timoclea imbricata which is the most abundant species in all habitats, the most common species in LAs (Nassarius jacksonianus, Paratectonatica tigrina, and Pirenella cingulata) are not the most common species in DAs, indicating a distinct compositional difference (Fig. 2.3A–2.3F). Although some of the common species in DAs are found in LAs (such as Mactra luzonica, Sunetta vaginalis, and Donax lubricus), many are absent in LAs. Moreover, LAs show a clear habitat partitioning in ordination space (Fig. 2.8B). The restricted embayment is compositionally different from the tidal flat in LAs which is not observed for DAs. The adjacent sampling sites in LAs show a tendency to cluster closer together which can be due to the patchy occurrence of LAs causing spatial autocorrelation (Tomašových and Kidwell 2009*b*; Weber and Zuschin 2013). Some sights from the restricted habitat might appear to show higher variability than other habitats that might be a caused by the artificial clustering due to presence of excess zeros in the dataset of habitats which causes them to cluster together.DAs do not preserve the compositional fidelity of the LA and cannot be reliably used to define different habitats/environments unlike our live assemblage (Tomašových and Kidwell 2009*b*; Weber and Zuschin 2013; Zuschin and Ebner 2015). Time averaging in death assemblages of beaches, tidal flats, and near shore subtidal habitats with low-moderate sedimentation rates can range up to thousands of years (Kidwell 1998). The lack of environmental partitioning and presence of a homogeneous character of DAs across habitats can therefore be the result of multiple mechanisms such as high sedimentation rate along with differential preservation of shells or addition of dead

shells from other habitats through post-mortem mixing (Flessa and Kowalewski 1994; Ritter and Erthal2013).

2.4.3 Role of Lateral Transport:

Post-mortem transportation has been considered to be one of the most important agents that leads to lower fidelity between living and death assemblages (Kidwell and Bosence 1991; Kidwell 2008). Marine death assemblages are often the product of post-mortem lateral shell transport and the two important factors which influence the transport of DA's are time and energy of the related habitat. The shells can either be transported within a small spatial scale within habitats, or they can be transported by higher energy conditions at a larger spatial scale (Kidwell and Bosence 1991). The energy of the habitat plays a major role in transporting the shells within/out of the habitat (Tomasovych 2004). Previous studies have observed that in narrow shelves the out-of habitat transportation is often species/size-specific; only a subset is transported rather than the whole assemblage (Donovan 2002; Kidwell 2008). Shell transport in wide, gently sloping shelves brought by catastrophic events such as storms or turbidity current, however, often transport the whole assemblage without significant sorting (Dominici and Zuschin 2005). Apart from influencing the species composition, transportation can also change the fidelity by influencing SFD. Tomašových (2004) observed a changing SFD fidelity between LA and DA along a bathymetric gradient (Tomasovych 2004) (Fig. 2.4). The cause of the difference has been related to water energy level, substrate type, and/or net rate of sedimentation. For example, the mixed-bottom habitats with primarily unconsolidated sediment and characterized by high rate of sedimentation demonstrate higher SFD fidelity in comparison to those of hard-gravelly habitats. Among the habitats with similar sedimentological characteristics, the SFD fidelity increases with decreasing energy. All the habitats in our study belong to unconsolidated mixed-bottom habitats of similar depth and are likely to demonstrate similar SFD fidelity unless influenced by differential energy conditions. Apart from the physical factors, there could be biological factors that may contribute to the difference in SFD between LAs and DAs. While SFDs in LAs reflect the size/age structure of the standing population at the time of sampling, SFDs in DAs correspond to the sizes at death and so depend on aspects of population dynamics (Tomasovych 2004). Although it is not possible to completely rule out the influence of these factors, it is important to note that the LAs in the present study comprise multiple samplings done over different months and hence, are more likely to represent a general pattern of the population instead of a snapshot. SFDs of LAs and DAs can differ because of size-specific mortality rates (Cummins et al. 1986). Although generally considered to have a skewed distribution, SFDs of most live assemblages are characterized by a juvenile peak. A prominent lack of such peak

in the shallowest habitats are often attributed to higher intensity of predation and competition (Cummins et al. 1986; Collins 1991; Tomasovych 2004). At the Chandipur intertidal zone a very high degree of predation has been documented (Chattopadhyay et al. 2014; Pahari et al. 2016) and hence, it is not unusual to find no juvenile peak in the live assemblage. Evidences of small-scale transportation from within habitats to the beach has been reported in foraminiferal preys drilled by gastropods from Chandipur (Mondal and Sarkar, 2021).

It is recognized that when the DA is formed by accumulation of successive, non-contemporaneous populations (Walker and Bambach 1971), its SFD is cumulative and therefore composed of many distinct cohorts. In our simulation, we used observed cohorts of the LA to simulate a cumulative SFD of the DA and the simulated DAs are significantly different from the observed DAs (Fig. 2.10A–2.10D; See Appendix for Supplementary Figure 2.S2A–2.S2D). Therefore, the size distribution of locality-specific DAs cannot be produced entirely by small-scale within-habitat mixing of LAs. A simulation with energy-specific size cut off does not change the scenario (Fig. 2.10E, 2.10F; See Appendix for Supplementary Figure 2.S2E, 2.S2F). This points to the limited influence of within-habitat transfer at small spatial scales to develop SFD of DAs. This suggests that the SFD of DAs are probably developed as a result of larger-scale transportation processes by high-energy events such as tropical cyclones.

2.4.4 Role of Storm Surges and Tropical Cyclones:

The incidence of tropical cyclones is very common over the Bay of Bengal, which experiences approximately six tropical cyclones annually with increasing intensity (Mohapatra and Mohanty 2004; Balaguru et al. 2014; Patra et al. 2016). Storm processes exert a major control over the benthic community development and also influence the preservation of benthic assemblages in the fossil record. The rapid deposition of mud leads to excellent preservation of communities and also accumulation of skeletal material. Actualistic studies documented that the storm events control the bathymetric limits of benthic communities by substrate modification and episodic physical disturbance (Miller et al. 1988). The coast of Odisha, in particular, is prone to tropical cyclones and has experienced 128 tropical cyclones in the last 109 years (Mohanty et al. 2004). The cyclone record of Chandipur shows a similar record. Chandipur has been affected quite frequently by tropical cyclones over the last 40 years (Fig. 2.11). Such storms generally transport large amounts of sediments eventually settling into graded sand and silt tempestite beds in the submarine canyons, which correlate well with the cyclone timings in the past (Kuehl et al. 1989; Kudrass et al. 1998; Michels et al. 1998). Coastal lands with gentle land slope suffer greater land loss from inundation during storm surges and Chandipur, characterized by less than 0.2 ° slope, has a high risk of

flooding and storm surge (Kumar et al. 2010; Mukhopadhyay et al. 2016). The high frequency of cyclonic storms and the gentle slope of Chandipur makes it quite vulnerable to storm-induced sediment transport.

The exact spatial extent of the "out-of-habitat" transport of an area is always difficult to determine. However, the trajectory of frequently appearing cyclones in the studied region points to large-scale transportation and mixing. The tracks show that cyclones passing through the Chandipur region move NW before entering the land. However, the majority of the cyclones originated above 15°N and never travel over the southern coast before reaching Chandipur. This indicates a limitation of mixing within a zone above 15°N (Fig. 2.12A). This is also evident from the fact that the majority of the cyclones that affect the studied region originates above 15°N (Fig. 2.12B), indicating that large-scale mixing would be prevalent within the northern latitudinal bins (16–21°N). Reported occurrence data of bivalve species from all latitudinal bins along the eastern coast of India (Sarkar et al. 2019) also shows a drop in compositional similarity (Bray-Curtis) below 15°N when compared to the Chandipur bivalve assemblage (Fig. 2.12C). Many of the reported occurrences are based on shell concentrations and not on live assemblage (Apte 1998; Rao 2017). The region shows a considerable degree of environmentally heterogeneity with a wide variety of habitats ranging from sandy and rocky substrate beaches, estuaries with muddy substrates, reef associated rocky and sandy beaches. The high environmental heterogeneity along with the high frequency of cyclones affecting indicates that the high degree of similarity within latitudinal bins above 15°N may have been due to the large-scale mixing caused by tropical cyclones along these latitudes. The similarity fades south of 15°N probably indicating a different set of mixing controlled by the southern cyclones.

2.4.5 Implication for the Past Record:

Live-dead bias can be strong in areas characterized by narrow shelves, high sediment input, and episodic occurrence of high pulse-type energy as evidenced by the high L/D mismatch found in our study. The results of the present study also demonstrate the low probability of preserving habitat-specific biotic assemblages even within a small spatial extent. In the absence of distinct taphonomic grades among the preserved specimens, it would even be difficult to recognize the degree of mixing in a fossilized assemblage. Apart from the fossilized deposit, the nature of poor spatial fidelity would also affect interpretation of regional events from historic records that heavily depend on time-averaged samples of the shallow subsurface (Tomašových et al. 2018; Gallmetzer et al. 2019; Tomašovỳch et al. 2019). The high LD mismatch due to transportation in our study indicates that the time-averaged samples retrieved from a specific location may not record local

events exclusively; instead it may be affected by assemblages transported from considerable distance. Spatial change in the sedimentological character without any change in fauna, especially along a depth gradient may point to possible mixing.

Sea-level fluctuations in the past have been detected by relative taphonomic trends using the variation in net rate and episodicity of sedimentation with distance from land and water depth (Kidwell and Bosence 1991; Brett and Baird 1993, 1997; Brett 1995, 1998). However, sea-level changes are often associated with climatic fluctuations. Any change in the climatic pattern will influence the frequency of storms (Ali 1996, 1999; Dettinger 2011; Lin et al. 2012; Mendelsohn et al. 2012) and hence would control the out-of-habitat transport and subsequent mixing. Size and shape sorting of shells along with sedimentological features such as channel structures, graded bedding, and erosional bases reflect the transport history and also affect the diversity of shelly assemblages in allochthonous beds. However, comparisons between storm deposits should be dealt with great caution as diversities are strongly governed by transport intensities, which are difficult to predict (Westrop 1986; Zuschin et al. 2005). In the absence of these obvious field signatures of transportation as observed in Chandipur, it would be difficult to recognize these storm events in the fossil assemblage. Therefore, depending on which geological period we are looking at, the extent of out-of-habitat transportation may be different. Because of the temporal variation of such climatic phenomena, they may even influence the spatial fidelity of the fossil record through time.

2.5 CONCLUSION

The extent of out-of-habitat transportation is understudied in areas of shallow shelf, frequented by high-energy events such as tropical cyclones. The present study demonstrates a high-degree of L/D mismatch from such an area indicating a high degree of post-mortem transport and mixing. Although a detailed multi-year sampling is required to establish the true variability of LAs, a SFD based modeling helps to understand the effect of lateral mixing in shaping the L/D fidelity. The model, based on the size distribution of live and dead assemblage, shows the low probability of creating the death assemblage by “within-habitat” mixing of live communities and implies the possible role of “out-of-habitat” mixing. The cyclone record of Chandipur shows a high frequency of cyclones that originate above 15°N and moves northward. The fact that there is high compositional similarity of species within the latitudinal extent of 15° to 21°N probably points to a high degree of lateral transport and mixing of shells within the latitudinal bins in the north of 15°N. These findings highlight the importance of out-of-habitat transport in shaping the regional distribution of marine fossil assemblages, especially in storm dominated siliciclastic settings. In

addition, factors such as sedimentation rate, time-averaging, and slope would contribute in creating patterns. The regional pattern of shell distribution, therefore, will be influenced by a combination of these factors and may differ significantly across storm-dominated settings.

CHAPTER 3

Controls of spatial resolution and environmental variables on observed beta diversity of molluscan assemblage at a regional scale

Controls of spatial resolution and environmental variables on observed beta diversity of molluscan assemblage at a regional scale

ABSTRACT

Beta diversity, which quantifies the compositional variation among communities, is one of the fundamental partitions of biodiversity and is associated with abiotic and biotic drivers. Unveiling these drivers is essential for understanding various ecological processes in the past and recent faunal communities. Although the quantification of beta diversity measures has improved over the years, the potential dependence of beta diversity on methodological choices is relatively understudied. Here, we investigate the effect of the variable scale of sampling on different measures of beta diversity at a regional scale. The west coast of India, bordering the eastern margin of the Arabian sea, presents a coastal stretch of approximately 6100km from 8–21◦N. We used marine bivalve distribution data, consisting of live occurrence data from literature reports and abundance data from death assemblages collected from localities representing latitude bins. We tested if variable sampling scales explain the observed variation in beta diversity due to differences in bin sizes and unequal coastline length. We developed a null model to generate a beta diversity pattern with an increase in the spatial scale of sampling by progressively increasing the grid size along the 14 latitude bins. Our null model demonstrates that for both the live and dead datasets, the total beta diversity measured by Bray-Curtis, Whittaker, and Sorenson indices decreases with increasing sampling scale. The species replacement (turnover) evaluated by the Simpson index decreases, and the species loss (nestedness) measured by the Sorenson index increases with increasing sampling scale. A comparison between the simulated and observed beta diversity distribution using the K-S test demonstrated that the observed pattern of beta diversity is significantly different from the pattern generated from the null model in both live and death assemblages. Our findings imply that sampling alone does not create this region's spatial variation in beta diversity. The results show that environmental parameters such as salinity, productivity, and cyclones significantly shape the regional beta diversity along the west coast. Our study provides an approach for evaluating the effect of variable sampling scales on comparing regional beta diversity. It also highlights spatial standardization's importance while inferring processes driving spatial diversity changes.

Keywords: spatial fidelity, similarity indices, scale dependence, environmental variability

3.1 INTRODUCTION

Biological diversity is spatially heterogeneous across the globe, and understanding the causes of spatial variation in marine diversity is one of the primary focus of ecological and paleoecological research (Kowalewski 1996; Olszewski and Patzkowsky 2001; Kidwell and Holland 2002; Huntley and Kowalewski 2007; Melo et al. 2009; Tittensor et al. 2010; Brown 2014; Tyler and Kowalewski 2017). The measures of spatial differences in diversity have three main partitions: alpha, beta, and gamma diversity (Whittaker 1960). Alpha and gamma diversity represent diversity at the finest and largest scale of observation, respectively (Patzkowsky and Holland 2012). Beta diversity, defined as within-habitat diversity (Whittaker 1960), is used to quantify the spatial variation in community composition among localities (Harrison et al. 1992; Gray 2000; Anderson et al. 2011). Evaluating within-habitat differences in the composition helps understand different aspects of ecosystem functioning (Legendre 2014), including drivers of community assembly, and are considered essential for conservation-based studies (Purvis and Hector 2000; Cleary 2003; Tuomisto et al. 2003; Baselga 2010).

However, beta diversity is a derived quantity unlike the directly measurable alpha and gamma diversities. One can measure beta diversity in numerous ways without any consensus on which measure is suitable for a particular ecological question, making it a complex metric to interpret (Whittaker 1960; Anderson et al. 2006, 2011; Baselga 2010; Beck et al. 2013; Barwell et al. 2015). Beta diversity can be partitioned into two major components: turnover and nestedness (Harrison et al. 1992; Baselga 2007, 2010; Anderson et al. 2011). Turnover can be explained as the replacement of some species by others between assemblages along a gradient due to environment sorting and/or historical constraints such as dispersal barriers due to geographic isolation (Qian et al. 2005; Leprieur et al. 2011). In contrast, nestedness reflects a spatial pattern where assemblages with lower species richness are subsets of those sites with higher species richness, resulting from selective extinction or colonization (Wright and Reeves 1992; Ulrich and Gotelli 2007). These components are not mutually exclusive, and the resulting assemblages can be a mix of both components. Exploring these components across a gradient can reveal the role of different processes in shaping the patterns of assemblage composition along that gradient, which will, in turn, help in designing strategies for protecting the diversity of a landscape (Leprieur et al. 2011; Qian et al. 2020).

The patterns and processes influencing beta diversity have been an area of considerable research interest. The model organisms in studies of beta diversity are dominated by terrestrial

communities such as plants (Fournier and Loreau, 2001; Kraft et al., 2011; Qian et al., 2005; Qian and Ricklefs, 2007; Qian and Xiao, 2012; Wagner et al., 2000), insects (Fleishman et al. 2003; Gering et al. 2003; Summerville et al. 2003; Lindo and N. Winchester 2008), birds (Fleishman et al. 2003; Jankowski et al. 2009), mammals (Gabriel et al. 2006; Soininen et al. 2007; Melo et al. 2009; Svenning et al. 2011; Peixoto et al. 2017) and freshwater fauna (Stendera and Johnson 2005). In contrast, the marine communities are relatively poorly studied except for reefal communities such as fishes and benthic invertebrates (Hewitt et al. 2005; Harborne et al. 2006; Josefson 2009; Belley and Snelgrove 2016; Roden et al. 2020; Souza et al. 2021). Large-scale patterns in beta diversity is linked to latitudinal and altitudinal gradients (Soininen et al. 2007; Jankowski et al. 2009; Kraft et al. 2011). A combination of abiotic factors (such as temperature, habitat heterogeneity, biogeographic isolation events) and biotic factors (such as dispersal limitation, competitive exclusion) are attributed as important drivers of taxonomic and phylogenetic beta diversity in both terrestrial and marine realm (Becking et al. 2006; Qian and Ricklefs 2007; Arias-González et al. 2008; Leprieur et al. 2011; Baselga et al. 2012; Segre et al. 2014; Hattab et al. 2015; Klompmaker and Finnegan 2018; Fluck et al. 2020; Qian et al. 2020; Maxwell et al. 2022).

Identifying the drivers of beta diversity is highly dependent on the spatial scale and resolution of the study (Mac Arthur and Wilson 1967; Hewitt et al. 2005; Tokeshi 2009). The factors that will determine variability in composition at a small spatial scale (site-scale or point-based studies) will differ from the determinant processes at larger scales. Typically, beta diversity increases rapidly at local scales as new sampling units are incorporated due to high variation in stochastic species occupancy patterns among sites (Rosenzweig 1995; Barton et al. 2013). At regional scales, beta diversity increases more slowly as fewer new species are encountered between sites than local ones. At larger scales, beta diversity increases as new species are encountered between sites across biogeographic regions with different geological and evolutionary histories. Consequently, similar patterns of beta diversity observed at different scales may not imply causative similarities (Whittaker et al. 2001; Hortal et al. 2010). Conceptually, beta diversity should increase with increasing spatial scale of individual units of observation (grid size) considering all individual units of observation (Barton et al. 2013). However, the choice of grid sizes for sampling, even within a constant extent of the study area, significantly affects the variability in species composition (Steinbauer et al. 2012). Barton et al (2013) proposed that a ‘sliding window’ perspective, in which both grid size and extent vary, would be an informative way to understand compositional variation across scales. Uncertainties produced due to unequal sampling and variable geographic configuration further complicate the comparison of measured beta diversity (Womack et al. 2020). Despite acknowledging the potential scale dependence, only a few studies attempted spatial scaling

of beta diversity (Kraft et al. 2011; Barton et al. 2013; Womack et al. 2020). Moreover, the patterns of beta diversity and the sensitivity to sampling can differ among time-averaged death assemblages (DA) and live assemblages (LA) residing in various environments (Tyler and Kowalewski 2017). Understanding the effect of increasing grid size of sampling, implying increasing sample size per bin within a constant extent on observed beta diversity of both live and death assemblages, will provide a unique insight into the spatial patterns of beta diversity.

The diverse ecosystem of tropical shallow marine environments is characterized by many co-existing species within habitats and high rates of species turnover between habitats (Gray 2000). Although these are important factors impacting beta diversity (Segre et al. 2014; Klompmaker and Finnegan 2018), only a handful of studies explored the regional patterns along tropical shallow marine environments. Using the marine bivalve distribution over a regional stretch of the environmentally heterogeneous coastline of India, we evaluated the beta diversity and its dependence on the scale of study. Specifically, we tried to address the following questions:

i. Can the beta diversity variation be explained by the unequal grid size of sampling for LA and DA?
ii. What is the effect of the choice of beta diversity index on the observed pattern?
iii. If variations due to unequal sampling are minimal, which environmental parameter explains the observed beta diversity pattern?

3.2 MATERIALS AND METHODS

3.2.1 Locality and sampling:

The study was conducted along the west coast of India. The west coast of India, bordering the eastern Arabian Sea, represents a latitudinal spread of 14° (8–23°N) spanning approximately 6100km from Kanyakumari in the south to Koteshwar in the north. The coast is characterized by a high degree of environmental heterogeneity consisting of coral reefs, lagoons, seagrass habitats, and sandy beaches. The northern part of the Arabian sea has low siliciclastic input and high productivity associated with upwelling during winter cooling. The southern region has a well-developed reefal system with moderate variation in salinity (Parulekar and Wagh 1975; Slater 1984; Madhupratap et al. 1996; Levin et al. 2000; Sarkar et al. 2019).

For collecting time-averaged death assemblage, 25 sampling sites representing 14 latitudinal bins were selected (Fig 3.1). Each bin is represented by at least one sampling locality, with a

minimum of a five km gap between two consecutive localities within a bin. All visible molluscan specimens were collected from a traverse of ~1 km along the sea shore from each locality. We repeated this process twice for each sampling site. The sampling was done over five and a half years from July 2010 to December 2015 in both post and pre-monsoon. Each latitudinal bin was represented by a minimum of 200 individuals of bivalve. The bivalve specimens from death assemblage (DA) was identified using published work by Rao (2017) and the World Register of Marine Species (WoRMS Editorial Board, 2020) (for details, see Chattopadhyay et al. 2021). For constructing live assemblage (LA) dataset, the occurrence data on marine bivalves was obtained from a marine biodiversity database reported from various published literature, maintained by the Bioinformatics Centre, National Institute of Oceanography, Goa, India (for details, see Sarkar et al., 2019). The database provided the scientific name of the bivalves, taxonomic details, feeding habits, habitat, size, and location. We often used Google Earth, supplementing location data to acquire the correct latitude and longitude.

3.2.2 Oceanographic variables:

We retrieved data on oceanographic variables (productivity, sea surface temperature, and salinity) from Ocean Productivity database. The diversity of shallow marine fauna is also known to depend on the habitat area (Smith and Benson 2013); therefore, we use shelf area and coastline length as a proxy for the habitat area. The coastal length and shelf width data are obtained from GEBCO Compilation Group (2020). Because high-energy storm events affect the distribution of molluscan death assemblages (Bhattacherjee et al. 2021), we included cyclone frequency data for our analyses. We used the global-tropical-extratropical cyclone climatic atlas from the United States Navy National Climate Data Center cyclone records. The processing details of cyclone data are discussed in Bhattacherjee et al. (2021).

3.2.3 Diversity estimates:

Taxonomic beta diversity can be measured in several ways. According to the concept of additive partitioning (Lande 1996), the gamma diversity (γ) in an area with multiple samples equals the sum of the average diversity within each of the samples (α) and among the samples (β); therefore $\gamma = \alpha + \beta$, and β is given by $\gamma - \alpha$ (Crist et al. 2003). We report results using both classical additive metrics and pairwise metrics. Classical additive metrics are derived directly from the relationship between alpha diversity and gamma diversity, such as the Whittaker index (Lande 1996). The pairwise metric is based on the similarity between a pair of sites, or an average of all

pairs and quantifies turnover (Anderson et al. 2011). The pairwise metrics used are Sørensen (Sørensen,1948), the Nestedness component of Sørensen, Simpson (Simpson 1943) and Bray-Curtis (Pairwise proportional dissimilarity) (Bray and Curtis 1957; Koleff et al. 2003; Anderson et al. 2006) indices. Sørensen dissimilarity measures the compositional dissimilarity component arising from species replacement and species loss (nestedness). The component of dissimilarity caused by species replacement is explained by the Simpson dissimilarity (Simpson 1943). The nested component of Sørensen can be calculated by subtracting the Simpson dissimilarity from the Sørensen dissimilarity measure (Baselga 2010). The presence-absence version of the Bray-Curtis indices or pairwise proportional dissimilarity (PPD) is relatively insensitive to variable sample sizes (Wolda 1981; Ferrier et al. 2007).

All calculations were performed on both datasets (LA and DA). The abundance data is transformed to presence-absence data prior to the measurement of beta diversity. Classical beta diversity measures like Whittaker's beta diversity are calculated in R using the "betadiver" function from the package Vegan, and pairwise measures are calculated using the "beta.pair" function from the package betapart (Baselga and Orme 2012).

3.2.4 Null model:

The null hypothesis states that the variation in beta diversity along the coast is explained by unequal sampling due to differences in bin sizes and unequal coastline length. To test it, we designed a null model following a resampling technique with increasing grid size (Ulrich and Gotelli 2007; Astorga et al. 2014; Loiseau et al. 2017). We created two variations of the model: 1) Combined bin method and 2) Individual bin method (Fig 3.2). These variations allow prediction of the pattern of beta diversity with increasing grid size and spatial extent of observation.

In both variations, we randomly choose two latitude bins between 8 to 21, 8 being the southernmost bin and 21 being the northernmost bin. Each of these bins is of unequal sizes spanning variable coastline lengths. We consider each of these bins as grid or individual units of observation. Therefore, bin sizes or coastline length is considered as our study's measure of sampling scale. In the "Combined bin method," we incrementally increase the grid size from the smaller latitude bin towards the larger bin by adding one bin in each step. The remaining latitudinal bins at that step are also clubbed together into a single unit. At each step, the beta diversity is calculated between that grid and the other unit containing the rest of the latitude bins combined. The grid size from the smaller bin is increased at each step until it reaches the bin prior to that iteration's maximum latitude bin value. This process is repeated for 50 iterations (Fig. 3.2). The beta diversity is calculated at each step of every iteration.

In the “Individual bin method,” we increase the grid size at each step from the smaller latitude bin by adding one bin. In contrast to the "Combined bin method," multiple latitude bins are clubbed together as one single unit, here, we consider the remaining latitudinal bins as individual units; the beta diversity at each step is calculated between that grid with the other individual latitude bins. The remaining steps within the first iteration are common to the "Combined bin method" and are followed in the same sequence as explained previously (Fig. 3.2).

To evaluate the effect of choice of the beta diversity measure, we used various beta diversity measures such as Whittaker (β_{whit}), Bray Curtis (β_{ppd}), Simpson (β_{sim}), Sorenson (β_{sor}) and nestedness component of Sorenson (β_{sne}). Spearman rank-order coefficient is used to measure the correlation of beta diversity values (β_{Null}) of each index with varying bin sizes and coastline length. The model was used for the LA and DA datasets, and the results are compared.

To check the effect of unequal grid sizes on the observed beta diversity distribution we checked whether β_{Obs} (β_{Obs_LA} and β_{Obs_DA}) could be generated from the distribution of null model values β_{Null} (β_{Null_LA} and β_{Null_DA}). A resampling method (described in Bhattacherjee et al, 2021) was performed to simulate a distribution of β values ($\beta_{simulated}$) by randomly sampling from the distribution of null model values (β_{Null}). We resampled 14 values with replacement corresponding to 14 latitude bins from the distribution of β_{Null} to generate a simulated distribution ($\beta_{simulated}$). We calculated the K-S distance between the distribution of simulated β values ($\beta_{simulated}$) and observed β values (β_{Obs_LA} and β_{Obs_DA}) using the ks.test () function in R. We repeated this step 10,000 times to get Bootstrap densities of K-S distances and p-values. This process is performed for all the β diversity indices. If β_{Obs} can be generated from β_{Null} then the K-S test will generate p values >0.005, implying the scale-dependent sampling strategy can create the observed difference in beta diversity. We can reject the null hypothesis if $p<0.005$. A statistically significant difference between β_{Obs} and $\beta_{simulated}$ indicates that β_{Obs} cannot be generated from the distribution of β_{Null}. Such a result would imply that methodological issues such as sampling strategy alone and probably demonstrating the natural variation cannot explain the variation in beta diversity.

3.2.5 Statistical analyses:

We used the Spearman rank-order correlation test to evaluate the relationship between β diversity and physical factors (such as latitude, coastline length, and other environmental variables). We used Bray-Curtis (PPD) dissimilarity for evaluating the correlation of β_{obs} with environmental variables. We also used multiple generalized linear models (GLMs) to analyze the effect of environmental variables by taking all parameters simultaneously and evaluating their contributions to the total variation in diversity (Quinn and Keough 2002). To assess the change in species

composition with environmental variables, a canonical correspondence analysis (CCA) and Redundancy Analysis (RDA) were conducted (Ter Braak 1986). CCA uses a site-by-species matrix and a site-by-environment matrix to extract orthogonal ordination axes that represent linear combinations of environmental variables. RDA is a canonical extension of principal component analysis (PCA), where ordination vectors are constrained by multiple regression to be linear combinations of the original explanatory variables (Legendre and Legendre 1998).

All statistical tests were performed in R version 4.2.0 (R Core Development Team, 2012).

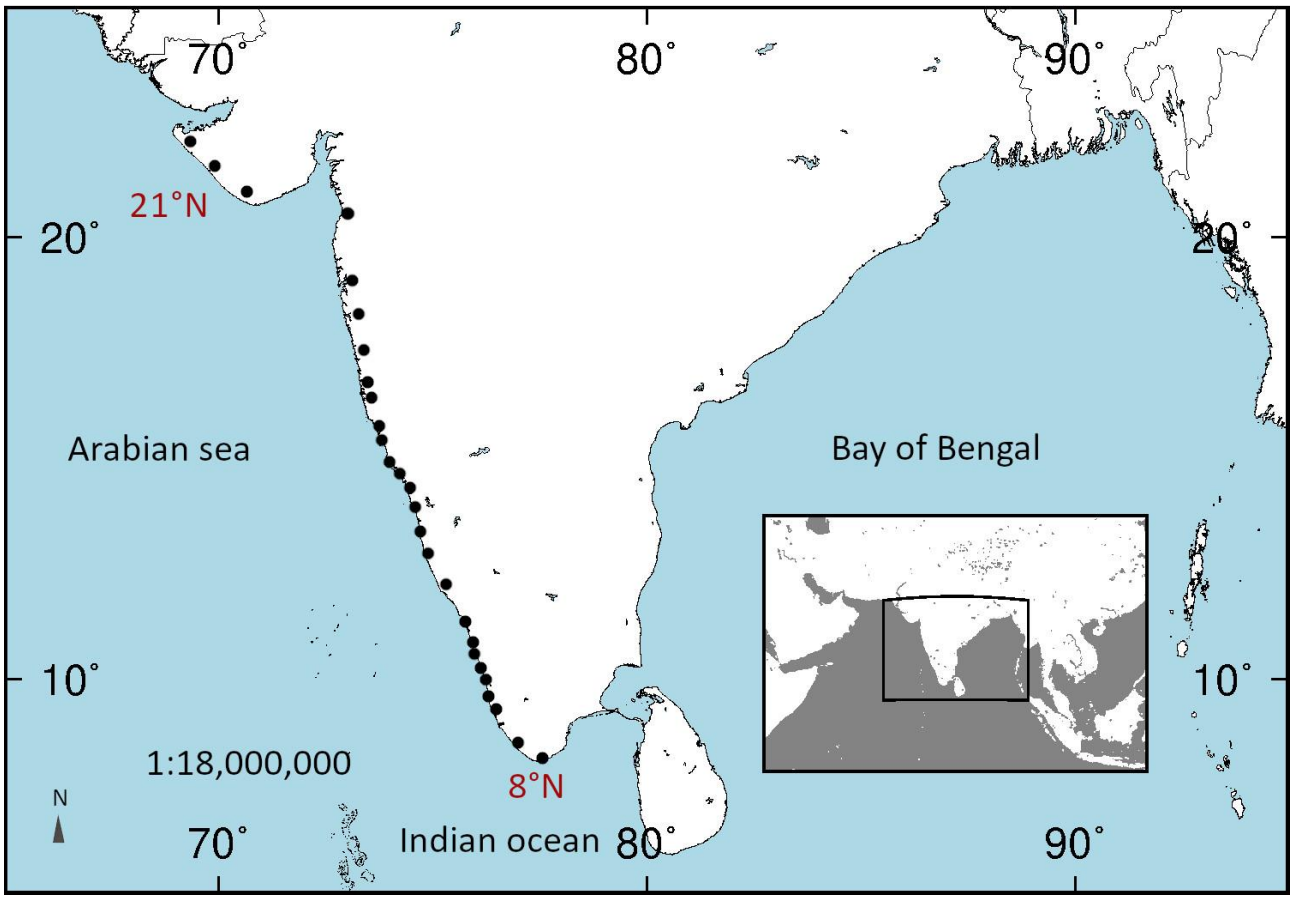

Figure 3.1: Map of India showing the sampling locations for collection of death assemblages.

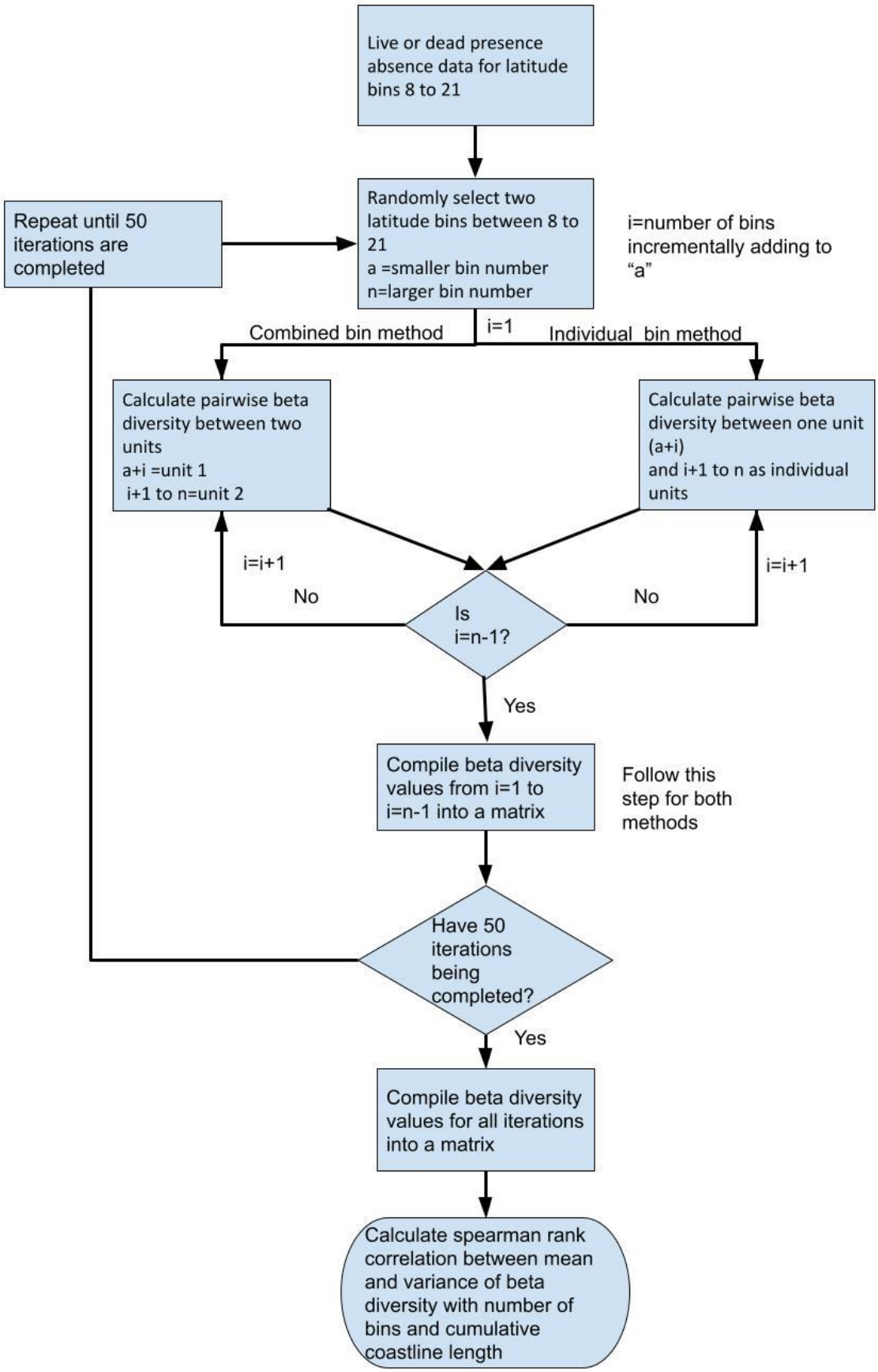

Figure 3.2: Flowchart describing the general framework for the null model

3. 3 RESULTS

The DA consists of 13757 bivalve specimens collected from 25 localities over 14 latitude bins representing 167 species from 28 families. The LA consists of 177 species representing 37 families. Mean beta diversity values in LA vary from 0.156 for β_{obs_sne} to 0.864 for β_{obs_ppd} (Table 3.1). Mean beta diversity values in DA vary from 0.151 for β_{obs_sne} to 0.851 for β_{obs_ppd} (Table 3.1).

3.3.1 Predicted effect of sampling and choice of index on beta diversity:

In the live assemblages (LA), the null model-generated beta diversity values did not show any consistent pattern, and the correlation was dependent on the unit of spatial resolution (bins and coastline length) and the method used (Table 3.2). Bray-Curtis dissimilarity (β_{ppd}), although not significantly correlated with coastline length, was negatively correlated with some bins in the individual bin method. However, the negative correlation with coastline length is significant in the combined bin method (Fig 3.3A, 3.S1A). The total dissimilarity component is negatively correlated with coastline length. While the Simpson index (β_{sim}) values show a negative correlation with both coastline length and the number of bins in the individual bin method (Fig 3.3F, 3.S1F), the nestedness component of Sorenson (β_{sne}) is positively correlated. In the combined bin method, however, β_{sne} is negatively correlated with the number of bins (Fig 3.3J, 3.S1J).

In the DA's, beta diversity of all indices from the null model was negatively correlated with the number of bins and coastline length in the combined bin method, except β_{sim} where the correlation wasn't significant with coastline length (Fig 3.4, 3.S1; Table 3.3). Only Bray-Curtis (β_{ppd}) was positively correlated with coastline length and the number of bins for both methods (Fig 3.4A-B, 3.S2A-B). Whittaker's beta diversity (β_{whit}) is negatively correlated with coastline length and the number of bins combined bin method and only with bins in the individual bin method (Fig 3.4C, 3.S2C-D). The Simpson index (β_{sim}) demonstrates a consistent negative correlation with coastline length in the individual bin method and the number of bins in both methods (Fig 3.4E, 3.S2E-F). Sorenson (β_{sor}) shows a similar pattern to β_{sim} being negatively correlated with coastline length in the combined bin method and with the number of bins in both methods (Fig 3.4G, 3.S2G, 3.S2H). The variance in β_{sim} and β_{sor} is also negatively correlated with the number of bins in both methods and coastline length in the combined bin method (Fig 3.4E, 3.4G, 3.S2E-H; Table 3.3). On the other hand, the nestedness component of Sorenson (β_{sne}) shows a positive correlation with coastline length in the individual bin method and a negative correlation in the combined bin method (Fig 3.4I-J, 3.S2I). All the correlations mentioned before were significant, if not mentioned otherwise (Table 3.3).

3.3.2 *Effect of sampling scale and choice of index on observed beta diversity pattern:*

The observed variation pattern of beta diversity along the west coast also shows no significant correlation with coastline length in LA and DA (Fig 3.5). The distribution of β_{obs} is significantly different from β_{Null} in the K-S test for all beta diversity indices except the nestedness component of Sorenson (β_{sne}) in the combined bin method (Fig 3.6). In the individual bin method, the difference is significant for β_{sor} distribution in live assemblages and β_{ppd} in live assemblages (Fig 3.6 D, N). β_{Null} and β_{obs} in the nestedness component of Sorenson (β_{sne}) are never significantly different in either of the methods (Fig 3.6Q-T). Most of the results for total dissimilarity indices β_{sor} and β_{ppd} are significant (Fig 3.6 A, C-D, M-O), which implies that they are sensitive proxies that can be used to evaluate methodological influence. Since β_{ppd} shows a consistent pattern, it is a good index for determining the effect of the sampling scale.

3.3.3 *Overlapping and non-overlapping patterns in LA and DA:*

For LA and DA, beta diversity patterns from the null model were different, particularly when the combined bin method was used. While LA did not show a significant correlation with the number of bins in β_{ppd} β_{whit} β_{sim}, DAs were strongly negatively correlated for all indices (Table 3.2-3.3). The patterns in LA were less consistent than the patterns observed in the DA. β_{ppd} shows a significant positive correlation with the number of bins in individual bin method, for the LA and DA (Fig 3.S1B, 3.S2B). The turnover component (β_{sim}) shows a negative correlation with coastline length and the number of bins in the individual bin method for both datasets (Fig 3.3F,3.4F, 3.S1F, 3.S2F; Table 3.2-3.3). On the other hand, the nestedness component (β_{sne}) positively correlated with coastline length in the individual bin method and negatively correlated with the number of bins in the combined bin method in both LA and DA (Fig 3.3J, 3.4J, 3.S1I, 3.S2I). Overall, both LAs and DAs showed a decreasing pattern in the total dissimilarity components and turnover components with an increase in sampling scale, except for the nestedness component, which showed an increasing pattern. B_{Null_LA} and β_{Null_DA} produced by both the LA and DA datasets were significantly different from the β_{obs_LA} and β_{obs_DA} of respective LA and DA datasets in the combined bin method. In the individual bin method, however, β_{Null} and β_{obs} difference were not significant for most indices in both LA and DA except for β_{sor} in LA and β_{ppd} in DA, which were significantly different. Except for two instances (Fig 3.6B-D, 3.6N-P), LA and DA behaved the same for all treatments (index, type of null model). This implies that the sensitivity to the sampling scale is similar for both live assemblages and time-averaged death assemblages.

3.3.4 *Effect of environmental variables on beta diversity:*

Because of the robustness of β_{ppd} (Fig 3.6), we selected this index to evaluate the influence of the environmental variables on beta diversity. Only oxygen concentration shows a significant negative correlation with Bray-Curtis dissimilarity (β_{ppd}) in LAs (Fig 3.7M).

Salinity (range) significantly correlates with other environmental variables (Table 3.4). After excluding salinity (range) based on autocorrelation, none of the explanatory variables show a significant effect on the beta diversity in single and multiple or single GLM for LA and DA (Table 3.5).

In Canonical correspondence analysis (CCA), 58% variation in species composition in LAs was explained by the environmental variables of salinity mean, productivity mean, productivity range, temperature mean, shelf area, oxygen concentration, and cyclones (Fig 3.8A). Of the three ordination axes, axis 1 explained 12% of the total variation in the dataset, and 42% of the variation was explained by all three axes. The same combination of variables was able to explain 6.3% of the total variation in species composition in DAs (Figure 3.8B). In DAs, out of the three ordination axes, axis 1 explained 17% of the total variation in the dataset, and 43.5% of the variation was explained by all three axes.

About 50% of the constrained variation in species distribution in LAs is explained by a combination of productivity (range), salinity (mean), temperature (mean), and cyclones using RDA on presence-absence species data (Adjusted R^2=23.7%) (Fig 3.8C). With a forward selection, only salinity (mean and range) was a significant predictor (p=0.03). The same set of variables, along with shelf area, was able to explain about 53% of the variation in species distribution in DAs (Adjusted R^2=23.7%) (Fig 3.8D). Forward selection to choose a model with fewer variables, however, stopped because of the limited explanatory power of fewer environmental variables.

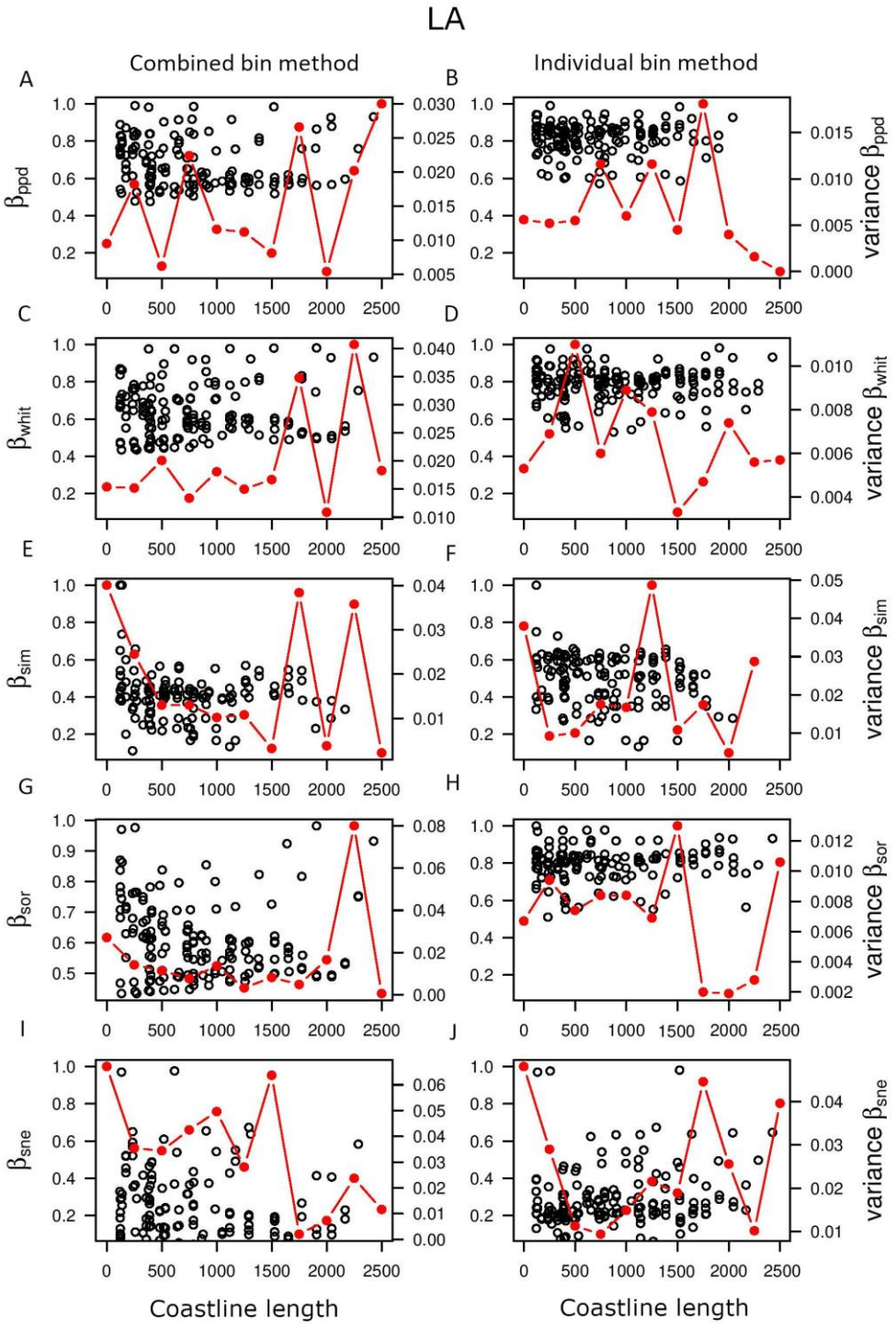

Figure 3.3: Null model predicted mean (black circles) and variance of beta diversity (red dash) with coastline length based on LA data. The left column represents "combined bin method" and the right column represents "individual bin method". The indices of beta diversity used here include Bray-Curtis (β_{ppd}) (A-B), Whittaker index (β_{whit}) (C-D), Simpson index (β_{sim}) (E-F), Sorenson index (β_{sor}) (G-H), Nestedness component of Sorenson (β_{sne}) (I-J).

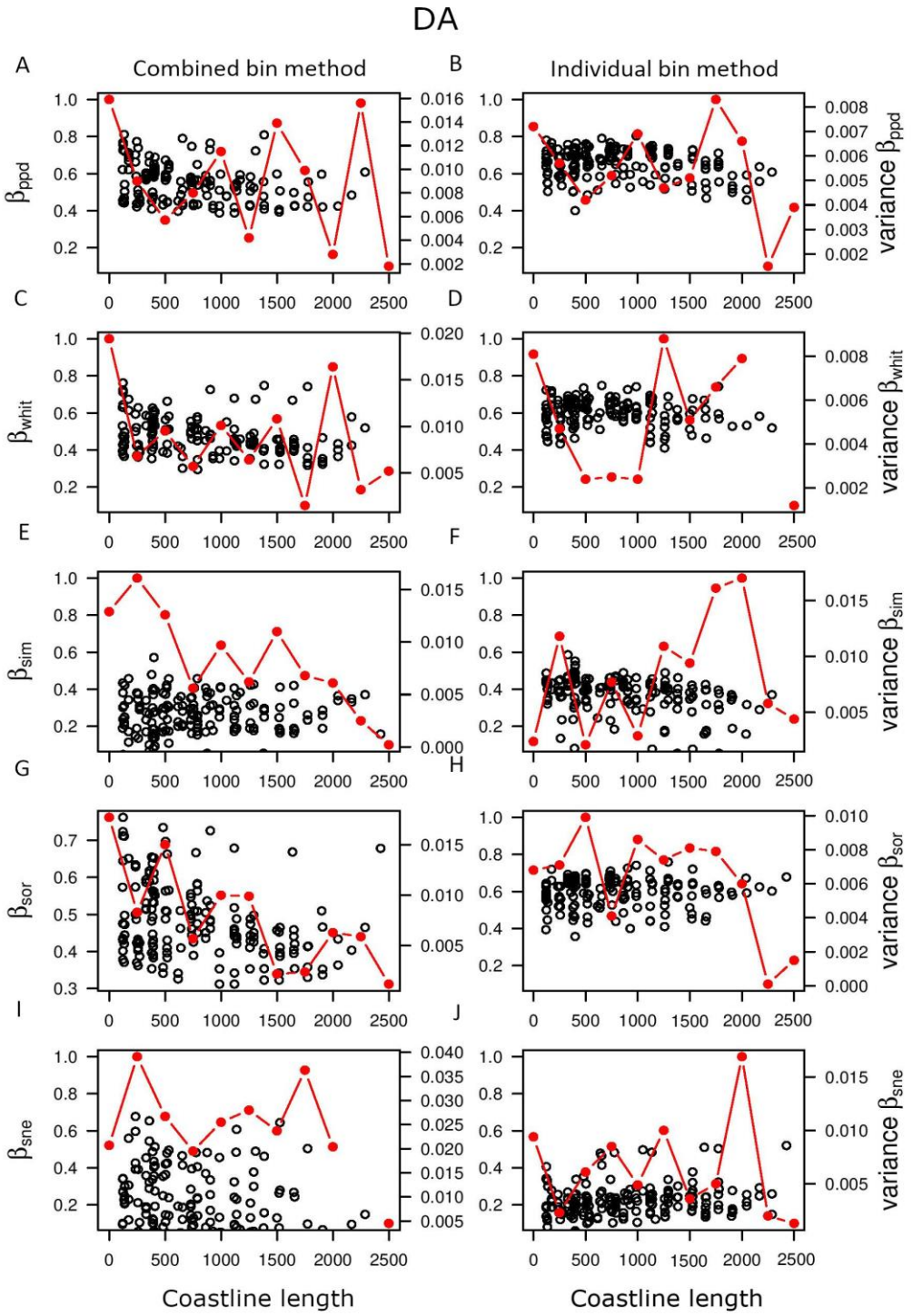

Figure 3.4: Null model predicted mean (black circles) and variance of beta diversity (red dash) with coastline length based on DA data. The left column represents "combined bin method" and the right column represents "individual bin method". The indices of beta diversity used here include Bray-Curtis (β_{ppd}) (A-B), Whittaker index (β_{whit}) (C-D), Simpson index (β_{sim}) (E-F), Sorenson index (β_{sor}) (G-H), Nestedness component of Sorenson (β_{sne}) (I-J).

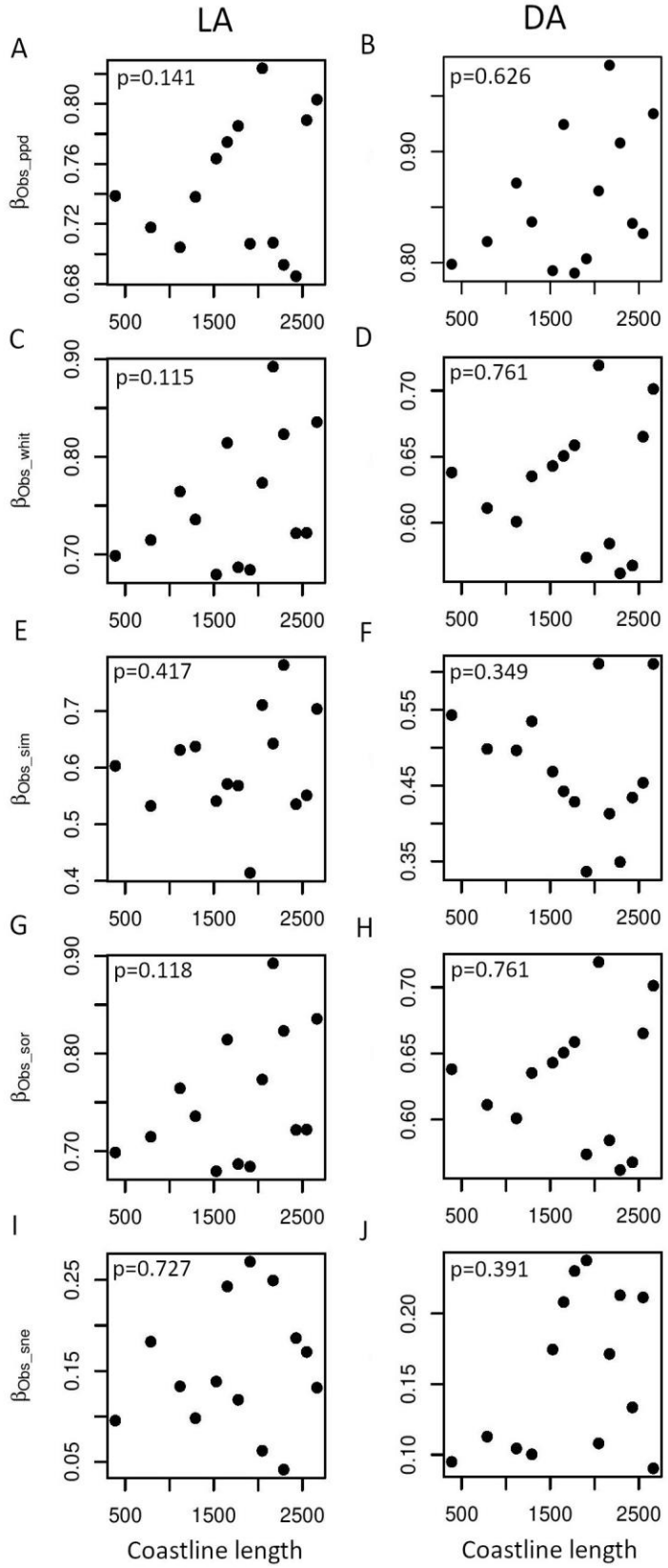

Figure 3.5: Relationship between observed mean beta diversity and coastline length. The left column represents LA and the right column represents DA. The indices of beta diversity used here include Bray-Curtis (β_{ppd}) (A-B), Whittaker index (β_{whit}) (C-D), Simpson index (β_{sim}) (E-F), Sorenson index (β_{sor}) (G-H), Nestedness component of Sorenson (β_{sne}) (I-J).

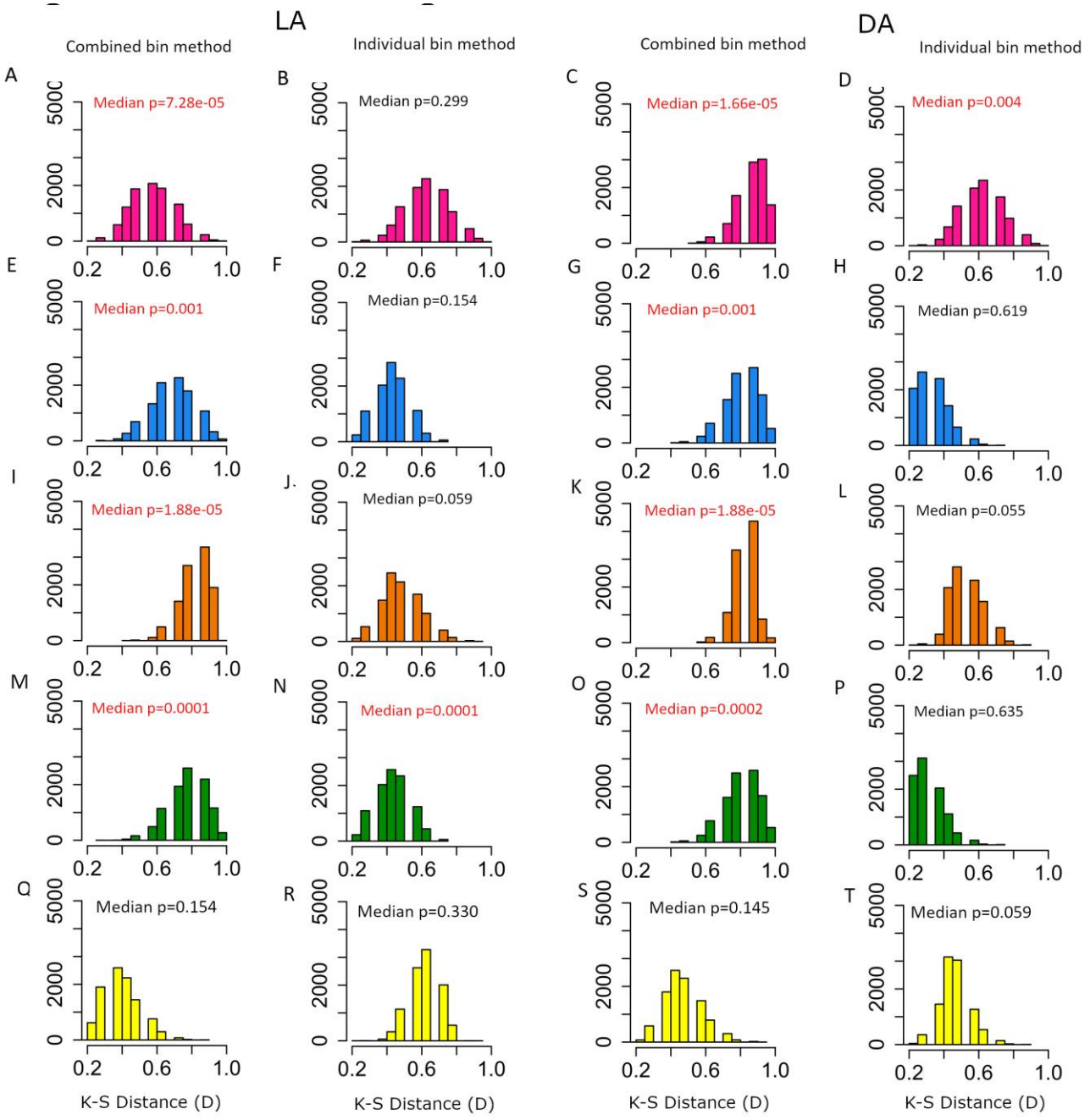

Figure 3.6: Histograms of D-values produced by K-S test between simulated (combined and individual method) and observed beta diversity distributions. The first two columns represent LA and the right two columns represent DA. The indices of beta diversity used here include Bray-Curtis (β_{ppd}) (A-D), Whittaker index (β_{whit}) (E-H), Simpson index (β_{sim}) (I-L), Sorenson index (β_{sor}) (M-P), Nestedness component of Sorenson (β_{sne}) (Q-T). The significant p-values are marked in red.

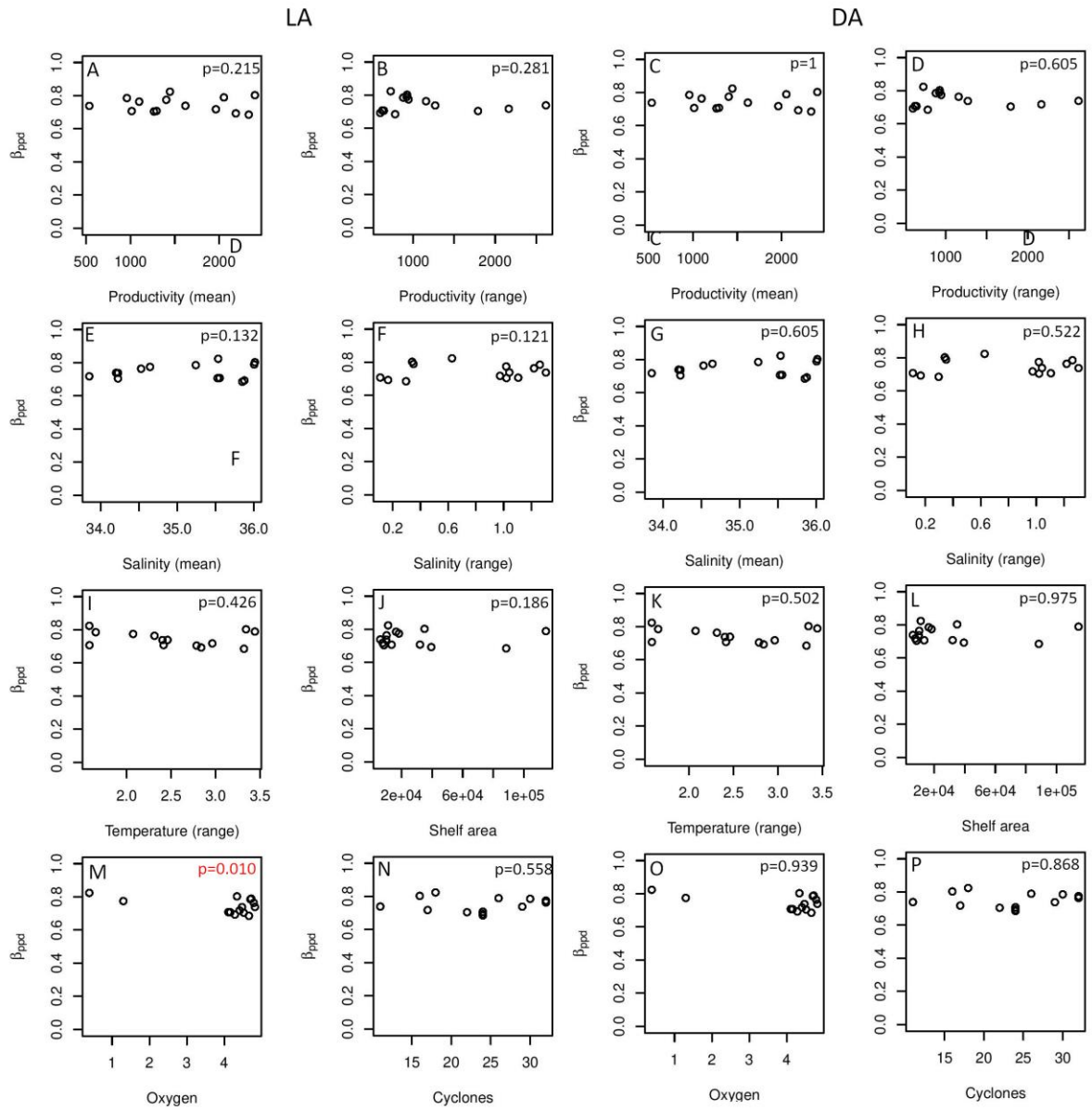

Figure 3.7: Relationship between β_{ppd} and different oceanographic parameters. The first two columns represent LA and the right two columns represent DA.

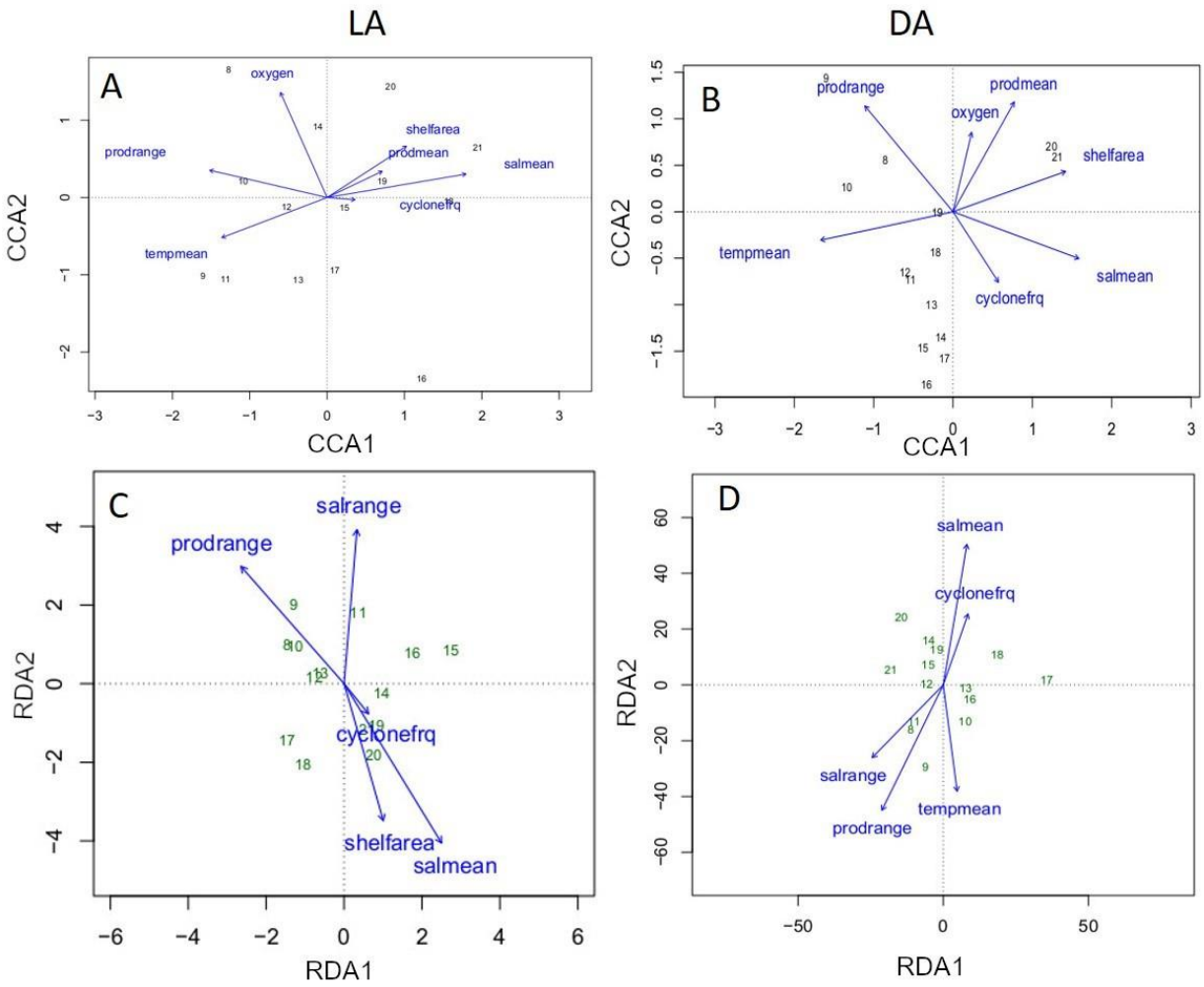

Figure 3.8: Biplots showing the relationship between β_{ppd} and environmental parameters using canonical correspondence analysis (CCA) (A-B) and redundancy analysis (RDA) (C-D). The left column represents LA and the right column represents DA.

Table 3.1. Mean of observed beta diversity values of different indices from LA and DA.

β diversity index	**LA**	**DA**
Bray-Curtis (β_{obs_ppd})	0.851	0.864
Whittaker (β_{obs_whit})	0.753	0.629
Simpson (β_{obs_simp})	0.602	0.473
Sorenson (β_{obs_sor})	0.753	0.629
Nestedness component of Sorenson (β_{obs_sne})	0.151	0.156

Table 3.2. Results of Spearman rank correlation test between beta diversity and spatial scale of sampling (grain size) for LA. The statistically significant results are marked in bold.

	LA															
	Number of bins								Coastline length							
	Combined bin method				Individual bin method				Combined bin method				Individual bin method			
	Mean		Variance		Mean		Variance		Mean		Variance		Mean		Variance	
Index	p	rho	p	rho	p	rho	p	rho	p	rho	p	rho	p	rho	p	rho
βppd	0.636	-0.032	**0.000**	**0.335**	**0.034**	**0.148**	0.087	-0.545	**0.004**	**-0.191**	0.341	0.382	0.296	0.074	0.141	-0.473
βwhit	0.496	-0.046	0.503	0.227	0.388	0.056	0.354	-0.293	0.106	-0.109	0.356	0.309	0.975	-0.002	0.451	-0.254
βsim	0.519	0.047	0.232	-0.418	**0.000**	**-0.339**	0.880	0.066	0.735	-0.024	0.145	-0.469	**0.000**	**-0.277**	0.945	0.030
βsor	**0.012**	**-0.169**	0.968	-0.018	0.085	0.118	0.457	-0.237	0.053	-0.131	0.451	-0.254	0.321	0.068	0.654	-0.150
βsne	**0.056**	**-0.139**	0.299	-0.345	**0.000**	**0.471**	0.225	-0.400	0.252	-0.084	**0.021**	**-0.700**	**0.000**	**0.335**	0.946	-0.027

Table 3.3. Results of Spearman rank correlation test between beta diversity and spatial scale of sampling (grain size) for DA. The statistically significant results are marked in bold.

	DA															
	Number of bins								Coastline length							
	Combined bin method				Individual bin method				Combined bin method				Individual bin method			
	Mean		Variance		Mean		Variance		Mean		Variance		Mean		Variance	
Metric	p	rho	p	rho	p	rho	p	rho	p	rho	p	rho	p	rho	p	rho
βppd	**0.000**	**0.315**	0.758	-0.115	**0.001**	**0.221**	0.095	-0.563	**0.000**	**0.292**	0.341	-0.318	**0.001**	**0.227**	0.236	-0.391
βwhit	**0.000**	**-0.436**	0.967	0.018	**0.002**	**-0.214**	0.707	-0.139	**0.000**	**-0.353**	0.145	-0.472	0.752	0.220	0.802	-0.091
βsim	**0.045**	**-0.141**	**0.001**	**-0.872**	**0.000**	**-0.474**	0.100	-0.527	0.072	-0.126	**0.004**	**-0.809**	**0.000**	**-0.263**	0.327	0.327
βsor	**0.000**	**-0.428**	0.427	-0.284	**0.000**	**-0.271**	**0.033**	**-0.654**	**0.000**	**-0.327**	**0.016**	**-0.718**	0.658	0.029	0.192	-0.427
βsne	**0.000**	**-0.354**	0.743	0.133	0.097	0.119	0.503	0.227	**0.001**	**-0.222**	0.349	-0.333	**0.022**	**0.163**	0.313	-0.336

Table 3.4. Results of multiple and single GLM analyses to assess contribution of environmental variables in determining observed Bray-Curtis dissimilarity (β_{obs_ppd}).

Environmental variables	LA West Coast								DA West Coast							
	Multiple GLM				Single GLM				Multiple GLM				Single GLM			
	Estimate	Std. Error	t value	Pr(>|t|)	Estimate	Std. Error	t value	Pr(>|t|)	Estimate	Std. Error	t value	Pr(>|t|)	Estimate	Std. Error	t value	Pr(>|t|)
Productivity mean	-0.0001	0.0001	-0.7246	0.5012	0.0000	0.0000	0.9590	0.3570	-0.0001	0.0000	-1.5158	0.1900	0.0000	0.0000	-0.1720	0.8660
Productivity range	0.0000	0.0001	-0.0890	0.9325	0.0000	0.0000	-1.4380	0.1760	0.0002	0.0001	2.1764	0.0815	0.0000	0.0000	-0.4580	0.6550
Salinity mean	0.1011	0.1586	0.6371	0.5521	0.0258	0.0208	1.2400	0.2390	0.0593	0.1040	0.5701	0.5933	0.0091	0.0164	0.5540	0.5900
Temperature mean	0.0797	0.2094	0.3808	0.7190	-0.0359	0.0296	-1.2120	0.2488	-0.2376	0.1373	-1.7306	0.1441	-0.0072	0.0235	-0.3060	0.7650
Temperature range	0.1654	0.1068	1.5496	0.1819	0.0184	0.0263	0.6990	0.4980	-0.0381	0.0700	-0.5440	0.6098	-0.0158	0.0197	-0.8050	0.4370
Oxygen concentration	-0.0317	0.0207	-1.5307	0.1864	-0.0152	0.0119	-1.2800	0.2250	-0.0296	0.0136	-2.1778	0.0813	-0.0156	0.0084	-1.8710	0.0859
Cyclones	0.0002	0.0071	0.0297	0.9774	-0.0004	0.0027	-0.1500	0.8830	0.0101	0.0046	2.1847	0.0806	0.0002	0.0021	0.0950	0.9260
Shelf area	0.0000	0.0000	-1.2324	0.2726	0.0000	0.0000	0.2330	0.8190	0.0000	0.0000	-1.9635	0.1068	0.0000	0.0000	-0.0700	0.9460

3.4 DISCUSSION

Abiotic and biotic drivers influence the compositional variation among communities captured by beta diversity. Unveiling these drivers of spatial heterogeneity in diversity requires us to rule out variations arising due to methodological strategies. The high marine diversity of tropical oceans, although studied in detail, their spatial structure is relatively poorly known. The west coast of India, bordering the eastern Arabian Sea, represents a tropical marine realm with a latitudinal spread of 14° (8–23°N) and has high degree of environmental heterogeneity. The alpha diversity of the coastal and shelf region of the Arabian sea has been relatively well studied (Jayaraj et al. 2008; Joydas and Damodaran 2009, 2014). In contrast, this region's beta diversity of macrobenthic species has been largely unexplored (Sarkar et al. 2019; Sivadas et al. 2020, 2021). Our study attempts to develop a methodological framework to assess how beta diversity is influenced by methodological strategies such as spatial scale and diversity index. It also attempts to identify the oceanographic drivers shaping the distribution by using the regional distribution of LA and DA from a tropical coast with high environmental heterogeneity.

3.4.1 Effect of sampling scale:

Coastline length is an important predictor of the biodiversity of recent marine ecosystems (Tittensor et al. 2010). A longer coastline offers higher availability of essential habitat features that positively influence both abundance and richness of coastal species (Rosenzweig 1995). However, variable coastline lengths of each latitude bin might lead to uneven sampling from different spatial bins resulting in increased beta diversity. Alpha diversity also increases quickly with increasing scale at smaller spatial scales due to high variation in stochastic species occupancy patterns among sampling units and variation in species responses to habitat heterogeneity (Rosenzweig 1995; Whittaker et al. 2001). At intermediate or regional scales, diversity increase with scale is slower because of the limited addition of new species relative to the regional pool. This pattern is also applicable to beta diversity, wherein dissimilarity is higher at the smallest and biggest spatial scales but lower at the intermediate scale (when based on a “sliding window” with varying grid size and extent) (Barton et al. 2013).

The null model provides a ‘sliding window’ perspective wherein the spatial grid size increases incrementally within a constant spatial extent. According to the results of our null model, the consistent pattern observed in beta diversity across LAs and DAs was a decreasing trend or negative correlation with an increasing sampling scale (Table 3.2, 3.3). This decreasing pattern contradicts the general theory of increasing beta diversity with increasing grid sizes within a

constant extent (Barton et al. 2013; Womack et al. 2020). Harborne et al. (2006) observed a positive correlation of beta diversity with environmental conditions within a specific spatial scale across a tropical seascape, supporting the importance of multiple scale- studies over single-scale studies for generalizing ecological patterns (Levin 1992). However, the observed pattern in beta diversity from mollusc LA and DAs from the west coast does not significantly correlate with increasing coastline length. The null-model-generated distribution of beta diversity in this study provides an opportunity to evaluate the effect of scale on regional beta diversity quantitatively. Our study also demonstrated that slight changes in the null model design might result in differing conclusion of the scale sensitivity. Between the two variations of the null model, the combined bin method appeared more robust in identifying beta diversity variations developed due to non-methodological processes. This affirms that data categorization decisions can influence the observed beta diversity patterns at regional scales.

3.4.2 Effect of choice of index:

Unlike the overall diversity measures (alpha and gamma diversities) beta diversity cannot be measured directly. Because it is a derived quantity, the choice of measure is often debated as there is no general consensus on the suitability of a measure for addressing particular ecological question (Whittaker 1960; Anderson et al. 2006, 2011; Baselga 2010; Beck et al. 2013; Barwell et al. 2015). Moreover, the very concept of beta diversity is scale dependent and hence, the individual measures may differ in their sensitivity of the scale dependence. Our study shows that different measures of beta diversity may have a varying degree of sensitivity to spatial scale of sampling. Multisite pairwise measures of beta diversity (β_{ppd}, β_{sor}, β_{whit}) shows a general negative correlation with increasing sampling scale represented by number of bins/coastline length, contrary to the a priori expectation of increasing beta diversity with increasing scale (Barton et al. 2013). Partitioning beta diversity into nestedness and species replacement components facilitates a greater understanding of patterns in beta diversity. However, we find a difference in their scale sensitivity implying a potential problem in interpreting observed patterns in beta diversity. In our study, the turnover component (β_{sim}) decreases with increasing sampling scale whereas the nestedness component (β_{sne}) increases, although in some of the analyses the nestedness component also decreases with increasing scale from the null model. Species replacement component or turnover component is the dominant component of variation in compositional dissimilarity and it is supposed to increase with increasing spatial scale, while the nestedness component decreases with increasing scale (Baselga 2007; Womack et al. 2020). The patterns of these components are logical consequences of the effect of environmental or ecological conditions that are operating at different scales. However, these

studies have been performed at global scale where the role of dispersal limitation of species is higher and geographical differences in environmental conditions will also increase, which will likely increase the beta diversity. Our study has been performed at an intermediate scale in tropics, with a latitudinal range of 14 where such large scale geographical and dispersal limitation are less likely to occur. While comparing the simulated and observed pattern in beta diversity, the nestedness component (β_{sne}) did not show significant difference between observed and simulated patterns in any of the results, indicating that this index is not a reliable index in this context, as it cannot tell apart the methodological influence from the biological influence. Whereas, in total dissimilarity indices like β_{sor} and β_{ppd} , the simulated and observed distribution are significantly different in most results. This implies that they are sensitive proxies that can be used to evaluate methodological influence. Therefore, we used β_{ppd} in our subsequent analyses for determining the contribution of environment.

3.4.3 Patterns observed in LA and DA:

Death assemblages showed a consistent pattern of negative correlation of beta diversity with increasing sampling scale from the null with the exception of nestedness component which showed a positive correlation with sampling scale. The live assemblages were also negatively correlated with sampling scale except β_{sne} , however the correlation was significant in only very few analyses and indices. The observed beta diversity pattern in both DA and LA was not significantly correlated with coastline length and both showed the same signal of being significantly different from the predicted beta diversity pattern generated from the null model. In comparison of observed and simulated beta diversity, LA and DA behaved the same for all treatments (index, type of null model) except for two instances. This implies that the sensitivity to sampling scale is similar for both datasets. This means that in contrary to the previous observation that time averaging generally reduces the beta diversity in an assemblage (Tomašových and Kidwell 2009), our study demonstrated that time-averaged death assemblages and fossils are no worse than the LA when it comes to beta diversity scaling. Therefore, death assemblages preserve the biological signal that is observed in the live assemblages as observed in other marine assemblages (Tyler and Kowalewski 2017). Time averaging and post-mortem mixing did not change the spatial fidelity in beta diversity pattern at a regional scale study such as this one.

3.4.4 Role of environmental factors:

Environmental processes are commonly known to explain beta diversity at regional scales and lower latitudes (Qian and Ricklefs 2007). Studies showing substantial effect of environmental

as opposed to spatial variables on community similarity have been reported from tropical forests and marine macrofauna in European marine sediments (Condit et al. 2002; Duivenvoorden et al. 2002; Ellingsen 2002; Ellingsen and Gray 2002; Cleary et al. 2004). The eastern Arabian sea's environmental variables significantly influence beta diversity. Salinity is one of the primary structuring factors for macrobenthic species turnover at a regional scale, as observed in the estuarine species in the northern Baltic sea, where beta diversity changed at the same rate as the change in salinity between regions (Bleich et al. 2011; Josefson and Göke 2013). There is a significant variation in salinity in the southern part of the west coast because of the influence of rainfall in summer monsoons and the mixing of Bay of Bengal waters during winter. This salinity variation is likely to affect marine benthos on the west coast. In our study, salinity played a decisive role in determining the variability of the species composition in both the northern and southern parts of the west coast based on the results of CCA and RDA.

Productivity also plays an important role in shaping up the diversity profile along a coastal region (Sarkar et al. 2019). Benthic marine communities showed a higher response than pelagic communities since physical mixing plays a significant role in the homogenization of species composition (Zinger et al. 2011). However, our study does not show any significant correlation between beta diversity and productivity. The productivity range plays a significant in controlling the variability of composition in both LA and DA, as observed by the proximity of southern latitudinal bins to the productivity range in RDA. This relationship develops because the west coast experiences increase productivity due to upwelling processes with the onset of the summer monsoon (June- September) (Madhupratap et al. 1996). During winter months, there is a rise in productivity in the surface layer, mainly in the northeastern Arabian sea, whereas the southern part has low productivity (Kumar and Prasad 1996; Madhupratap et al. 1996). The difference between summer and winter productivity is, therefore, higher in the southern Arabian sea, resulting in a higher productivity range in the south.

Shelf area had a significant effect on the LAs but not DAs, which is likely attributable to the fact that LAs have habitat-specific patchy occurrences. In contrast, DAs are more prone to post-mortem mixing. A greater shelf area indicates gentler slopes which cause lower rates of mixing, whereas a lower shelf area means a steeper slope causing higher rates of post-mortem transportation (Kidwell and Bosence 1991; Donovan 2002).

Our RDA plot (Fig 3.8C, 3.8D) shows a higher effect of cyclones on the species composition of the northern part of the west coast in both LA and DA, as illustrated by the

proximity of northern latitudinal bins to the frequency of cyclones. There has been an increase in the intensity of pre-monsoon tropical cyclones over the Arabian Sea during recent years owing to an increase in the heat content in the ocean (Rajeevan et al. 2013) (Fig 3.S3). The cyclone tracks from the western Arabian sea move northwesterly from 14°N to 17°N and gradually weaken towards the north (Subrahmanyam et al. 2002). These cyclones thereby follow a northwesterly track impacting the northern part of the west coast more significantly. Such cyclones can impact the beta diversity of shallow marine benthos due to species loss due to storms, as documented at a tidal flat in Brazil (Corte et al. 2017).

The results of this study suggest that substantial variation in beta diversity can arise from methodological artifacts like uneven sampling and spatial resolution. Unless such variation is identified and accounted for, the actual spatial pattern of biodiversity will remain obscured, and it will not be possible to identify the environmental drivers influencing the ecological processes.

3.5 CONCLUSION

In conclusion, the present study analyzed the effect of the sampling scale on the beta diversity at a regional scale using live and dead bivalve assemblages along the west coast of India. The beta diversity pattern generated from the null model provides a reference to assess the effect of sampling scale on regional beta diversity pattern and its sensitivity on the choice of beta diversity index. Our analyses show that the observed beta diversity distribution on the west coast cannot be explained by the null model alone, implying uneven sampling to be a minor factor in shaping the beta diversity pattern. Among the environmental variables, salinity and productivity are significant variables explaining the beta diversity of this region. Consistent patterns were obtained for live and dead datasets indicating that at the regional scale, spatial and compositional fidelity has not changed significantly despite time averaging and post-mortem transportation events affecting the death assemblages. However, the consistency in this study should not be generalized to imply that live and death assemblages can always be considered congruent at regional scales, and evaluation of live-dead fidelity should not be overlooked even at regional scales. A possible caveat of our study is the lack of detailed information on seasonal variation of the live assemblages as we had to mostly rely on snapshots of community data from literature. As we covered data from a large region, we believe these caveats would not distort our findings.

CHAPTER 4

Community evenness and sample size affect estimates of predation intensity and prey selection: A model-based validation

Community evenness and sample size affect estimates of predation intensity and prey selection: A model-based validation

ABSTRACT

Predation estimates inferred from the preserved records of predation traces are essential in evaluating the evolutionary effect of ecological interactions. It is, however, crucial to establish how sampling intensity and community composition of an assemblage influence the reliability of these measures.

Using a resampling technique, we evaluated the effect of sampling intensity and a community's evenness on the inferred predation estimates. We theoretically simulated model communities representing different levels of evenness, predation intensity, and predatory behavior (selective, non-selective). We calculated the total predation intensity and the number of prey species for each community. We then resampled each community without replacement and noted variations in the inferred measure from the accurate measure as the sampling intensity increased. Our results demonstrate that the evenness of a community does not influence the inferred predation intensity for non-selective predation. However, communities with highly selective predation are sensitive to evenness and sampling intensity; inferred predation intensity of these assemblages can substantially differ from the actual value. The inferred number of prey species is also influenced by the community's original evenness, predation selectivity, and predation intensity. When predation is selective, sampling intensity heavily influences communities with low evenness and low predation intensity; inferred predation intensity is underrepresented at smaller sample size. For communities of low evenness and predation intensity where rare species are attacked preferentially, the inferred prey richness differs significantly at a small sample size.

We proposed a post-facto standardization method for comparing predation estimates of discrete communities that differ in the sample size. We validated its utility using the published predation data of the Plio-Pleistocene molluscan fossil assemblage. The present approach attempts to provide critical insight into the reliability of predation estimates and may help in comparing predation patterns across time and space. There might be a number of factors including preservation bias and time-averaging that may impact the final predation signature of an assemblage. It warrants for a future direction of research to develop a comprehensive framework of post-hoc standardization of assemblages with differing predation style and preservation history.

4.1 INTRODUCTION

The role of predation in shaping the marine ecosystems through time has been a common theme of study (Vermeij 1977; Vermeij et al. 1981; Signor and Brett 1984; Langerhans 2007; Stanley 2008; Barnes et al. 2010; Gorzelak et al. 2012; Kotta et al. 2018; Petsios et al. 2021). The relationship between the prey and predator is complex in theoretical terms posing a challenge in predicting the evolutionary outcome of predation (DeAngelis et al. 1975; Berryman 1992; Haque 2012; Abrams 2015). For evaluating the evolutionary effects of predation, researchers rely on the deep time record of predation (Kitchell and Kitchell 1980; Vermeij et al. 1981; Kelley and Hansen 1993; Vermeij 1993; McNamara 1994; Kowalewski et al. 2005; Huntley and Kowalewski 2007; Baumiller et al. 2010; Klompmaker et al. 2017; Bicknell and Paterson 2018). The accurate estimation of predation measures is, therefore, of primary importance to studies of predator-prey systems.

For establishing predation events and inferring predation intensities, ecological studies use direct observations or indirect measures such as compositional characterization of digested food and fecal matter (Nilsen et al. 2012; Pringle et al. 2019). Although it is possible to recover direct observational evidence of predation events in past ecosystems by studying "caught-in-the-act" occurrences (Ehret et al. 2009; Ebert et al. 2015), paleoecological studies primarily rely on preserved predation traces, such as drill holes and repair scars (DeAngelis et al. 1985; Kelley and Hansen 1993; Dietl and Alexander 2000; Dietl et al. 2004; Alexander and Dietl 2005; Klompmaker and Kelley 2015). Based on the neontological experiments and field observations, complete drill holes and repair scars are interpreted as a successful attack by carnivorous gastropod (Carriker 1951; Kitchell et al. 1981; Kowalewski 2004; Hutchings and Herbert 2013; Chattopadhyay et al. 2014*a*; Mondal et al. 2014) and an unsuccessful predation attempt by durophagous predator respectively (Carriker 1951; Blundon and Kennedy 1982; Dietl and Alexander 2009). These traces recording the predation attempts on the prey's hard shells, are some of the best quantifiable proxies for inferring predation from the fossil record (for review see (Alexander and Dietl 2003; Kelley and Hansen 2003; Klompmaker et al. 2019)). The frequency of repair scar (RF) and complete drill holes (DF) are used for evaluating various aspects of predation in deep time, including predation intensity and prey selection (Kitchell et al. 1981; Kelley and Hansen 1993; Kowalewski et al. 1998; Dietl 2003; Kase and Ishikawa 2003; Chattopadhyay and Baumiller 2010; Chattopadhyay and Dutta 2013; Tyler et al. 2013).

Inferences about interactions from predation traces have their limitations. The implicit assumption for such interpretation is that other processes do not alter the quantitative data provided by predation traces. It is recognized, however, that biases introduced through taphonomy may influence the biological reliability of these measures affecting overall frequency of traces, site stereotypy, prey selection, and size selection (Roy et al. 1994; Nebelsick 1999; Zuschin et al. 2003; Kosloski 2011; Gorzelak et al. 2013; Chattopadhyay et al. 2014*b*; Chojnacki and Leighton 2014; Sime and Kelley 2016; Dyer et al. 2018; Pruden et al. 2018; Smith et al. 2019; Salamon et al. 2020). Apart from taphonomy, methods of collection and subsequent analyses may also influence the interpretation of predation patterns. In contrast to bulk collection, targeted sampling of specific size class or taxon impacts inferred predation intensities (Kowalewski and Hoffmeister 2003; Kosloski et al. 2008; Ottens et al. 2012; Hattori et al. 2014; Chattopadhyay et al. 2016; Hausmann et al. 2018). Theoretical investigations also demonstrated the effect of sample size on inferred predation intensity (Smith et al. 2018, 2022). Analytical techniques to evaluate and compare predation measures across groups often impact the inferences (Kowalewski 2002; Leighton 2002; Grey et al. 2006; Stafford and Leighton 2011; Dietl and Kosloski 2013; Smith et al. 2018; Budd and Mann 2019).

Aspects of a specific community, such as evenness, selectivity of predation, and sampling intensity may influence predation inferences drawn at the community level, such as predation intensity, prey selection. Such influences are crucial for studies that attempt to combine predation data from discrete samples and reconstruct temporal/spatial changes in predation patterns. Using theoretical simulation based on a resampling technique, we develop a methodological framework to understand the effect of community evenness, sampling intensity, and the nature of predation selectivity on inferred predation estimates. We attempt to estimate these effects on the inferred predation intensity and the number of prey species. The inferred number of prey species provides an insight about the choice of prey by the predator. We also propose a method of post-facto standardization and validate our approach using predation data from four Plio-Pleistocene fossil assemblages of Florida.

4.2 MATERIALS AND METHODS

We created several hypothetical live assemblages of molluscs that are attacked by a specific group of predator with differing probabilities. We use a resampling method to compare the predation patterns inferred from these assemblages. We assumed that all individuals are finally

represented in the death assemblage, each predation attempt leaves a distinct mark on the prey, and all predators demonstrate the same prey-selection behavior in specific situations. We acknowledge that some of the specific values of predation intensity, and predation selectivity might be rare to observe in nature. Our attempt, however, is to design and test a general framework applicable to a large spectrum of community structures with varying evenness and predation patterns, even if some end-member scenarios do not have a natural representation. It is also true that predation patterns observed in fossil assemblages may differ from that of the death assemblage due to taphonomic factors which has not been considered in the present study.

4.2.1 Model assemblages:

We created 30 hypothetical model assemblages, each with 30 species and 3000 individuals with varying evenness, predation intensity, and prey preferences (Table 4.1). Each model assemblage had a unique combination of evenness, predation intensity, and prey preference. To evaluate evenness, we used Pielou's evenness index which is one of the commonly used measures of evenness. We calculated the evenness of an assemblage (E_T) as

$$E_T = H/\ln(S_T)$$

Where,

H = Shannon's diversity index

S_T = Total number of species in the assemblage

The evenness in these models ranged from a theoretical minimum of 0.1 to a theoretical maximum of 1. Model assemblages with maximum evenness of one had 100 individuals for 30 species. Assemblages with intermediate evenness of 0.6 had five common species with 500 individuals each and 25 rare species with 20 individuals each (Table 4.1). Assemblages with low evenness of 0.4 had 910 individuals in each of the three common species and ten individuals in each of the 27 rare species. For assemblages with a very low evenness of 0.1, there is only one common species with 2710 individuals, and the remaining 29 rare species consists of 10 individuals each. The specific values of evenness and the species richness are comparable to the observed values from molluscan live assemblages (Olszewski and Kidwell 2007).

We calculated the predation intensity at the level of the assemblage (PI_T) as well as for prey species (PI_{prey}). The total number of prey species is S_{prey}. PI_T is calculated as

$$PI_T = N_P/N$$

Where,

N_P = Number of individuals with predation mark

N = Total number of individuals in the assemblage

PI_{prey} denotes predation intensity in the species that have been attacked. The predation intensity of the total assemblage (PI_T) was categorized into three levels: low (0.2), medium (0.5), and high (0.8) (Table 4.1). A certain number of individuals from specific species would be considered prey with predation marks as dictated by the (PI_T). The prey-preference of the predator can either be non-selective or selective. For the sake of simplicity, here we have expressed the selectivity in terms of the relative abundance of species. In the case of non-selective predation (Case 1), all species have an equal probability of being attacked irrespective of their abundance (Fig 4.1). Selective predation represents assemblages where prey species have an unequal chance of being attacked. In model assemblages with selective predation, we constructed three cases; the predator can attack the common species (Case 2), the rare species (Case 3), or a mix of common and rare species (Case 4) (Fig 4.1).

For all models, the probability of an attack is determined by the PI_T which can be 0.2, 0.5 or 0.8. For selective predation, only certain species are available as prey and we assign the probability of attack as 0 to the rest of the species. In the case of selective predation on abundant species with low predation intensity, for instance, the probability of an attack is assigned as 0.2 for all the individuals of common species and 0.0 for all the individuals of rare species. Selective predation has not been considered for assemblages with maximum evenness because the probability of attack is assigned to be equal for all species in our designed model.

4.2.2 Simulation design:

We performed a simulation to evaluate the effect of sample size on inferred predation intensity ($PI_{T.inf}$) and the number of prey species ($S_{prey.inf}$) for all the model assemblages. In the simulation, 100 individuals were drawn randomly from a model assemblage. The number of attacked individuals (N_P) and the number of prey species (S_{prey}) represented by the attacked individuals were counted in those 100 individuals. Inferred predation intensity ($PI_{T.inf}$) for the drawn sample is calculated as a ratio of the number of attacked individuals and the total number of individuals (i.e., 100 in the first draw). We kept the step size as 100 to gain an accurate representation of predation intensity and to avoid the issues related to insufficient sample size (Kosloski et al. 2008; Dietl and Kosloski 2013; Smith et al. 2022). The exact process is repeated 30 times without replacement until all the individuals from the

assemblage are sampled. Following the principles of rarefaction analysis that are known to be useful when attempting to standardize sampling effort, we chose to use subsampling without replacement (Kowalewski and Novack-Gottshall 2010). This entire process was iterated 1000 times. The mean and standard deviation are calculated for inferred predation intensity ($PI_{T.inf}$) and prey species richness ($S_{prey.inf}$) over 1000 iterations for a specific model assemblage. Difference of predation intensity ($Diff_{PI}$) is calculated as the difference between PI_T and $PI_{T.inf}$ for an assemblage. Similarly, the difference between S_{prey} and $S_{prey.inf}$ is taken as the difference of prey species richness ($Diff_S$). The same technique is applied to all the model assemblages.

4.2.3 Simulated time-averaged assemblage:

We created a time-averaged assemblage by random selection of three model assemblages. Using the simulation design described before, we calculated $PI_{T.inf}$ and $S_{prey.inf}$ for the time-averaged assemblage in contrast to the individual model assemblages.

4.2.4 Predation dataset:

We used published data on predation records of molluscs from four Pleistocene localities in Florida (Chattopadhyay and Baumiller 2010) for validating the proposed technique. The goal is to quantitatively evaluate if we can compare the predation estimates of discrete communities characterized by different evenness, predation style and sample size. The dataset consists of abundance, drilling frequency, and repair scar frequency of 14 molluscan species. We drew samples without replacement from each locality with increasing sample size. The sample size for each draw was a hundred until the last draw; in the last draw, where the remaining sample size is less than 200, all are drawn. For Punta Gorda (total=2418 individuals), 100 individuals were drawn 23 times, and 118 individuals were drawn for the last (24^{th}) draw. A similar procedure is followed for Miami Canal (total = 4794 individuals), Mc Queens pit (total=659 individuals), and Chiquita (total=894 individuals).

We used a sampling standardization protocol to compare these assemblages and assess the sensitivity of the inferred predation intensity ($PI_{T.inf}$) and inferred prey-species richness ($S_{prey.inf}$) on sampling intensity. The sample size of Mc Queens pit (659) is considered as a reference as it has the smallest sample size among all four locations. The distribution of inferred predation intensity (PI_T) is compared for all assemblages at a sample size of 500 by a pairwise comparison using Kolmogorov-Smirnov (K-S) tests. If the pairwise

K-S test shows significant differences between all pairs of assemblages, then the variation between assemblages is not caused by sampling and community evenness. If two assemblages show non-significant difference in pairwise K-S test, then small sample size might be influencing inferred predation intensity and prey richness. Hence, a larger sample size is considered as a new reference, and the pairwise comparison using K-S test is repeated again for those pairs of assemblage. The same process is repeated till the maximum number of assemblage pairs show significant differences. Following a similar protocol, the distribution of inferred prey-species richness ($S_{prey.inf}$) is also compared.

All simulations and statistical analyses were performed in R (version 4.2.0) (R Core Development Team, 2012).

Table 4.1. A summary of the model assemblages used for this study with varying evenness, predation intensity and predator preference.

Evenness	Structure	PI_T for Case 1 (Preys of all species are attacked with a probability of 0.2, 0.5 and 0.8 for low, medium and high $PI_{prey,}$ respectively)			PI_T for Case 2 (Preys of only common species are attacked with a probability of 0.2, 0.5 and 0.8 for low, medium and high PI_{prey} respectively)			PI_T for Case 3 (Preys of only rare species are attacked with a probability of 0.2, 0.5 and 0.8 for low, medium and high PI_{prey} respectively)			PI_T for Case 4 (Preys of one rare and one common species are attacked with a probability of 0.2, 0.5 and 0.8 for low, medium and high PI_{prey} respectively)		
		Low	Medium	High	Low	Medium	High	Low	Medium	High	Low	Medium	High
$E_T = 0.2$	$N_{(S=1:29)} = 10$, $N_{(S=30)} = 2710$ [1*2710 + 29*10] = 3000	0.2	0.5	0.8	0.18	0.45	0.72	0.02	0.05	0.08	0.18	0.45	0.73
$E_T = 0.5$	$N_{(S=1:3)} = 910$, $N_{(S=4:30)} = 10$ [3*910 + 27*10] = 3000	0.2	0.5	0.8	0.18	0.46	0.73	0.02	0.05	0.07	0.06	0.15	0.24
$E_T = 0.7$	$N_{(S=1:5)} = 500$, $N_{(S=6:30)} = 20$ [5*500 + 25*20] = 3000	0.2	0.5	0.8	0.17	0.42	0.67	0.03	0.08	0.13	0.03	0.09	0.14
$E_T = 1$	$N_{(S=1:30)} = 100$ [30*100] = 3000	0.2	0.5	0.8	NA	NA	NA	NA	NA	NA	NA	NA	NA

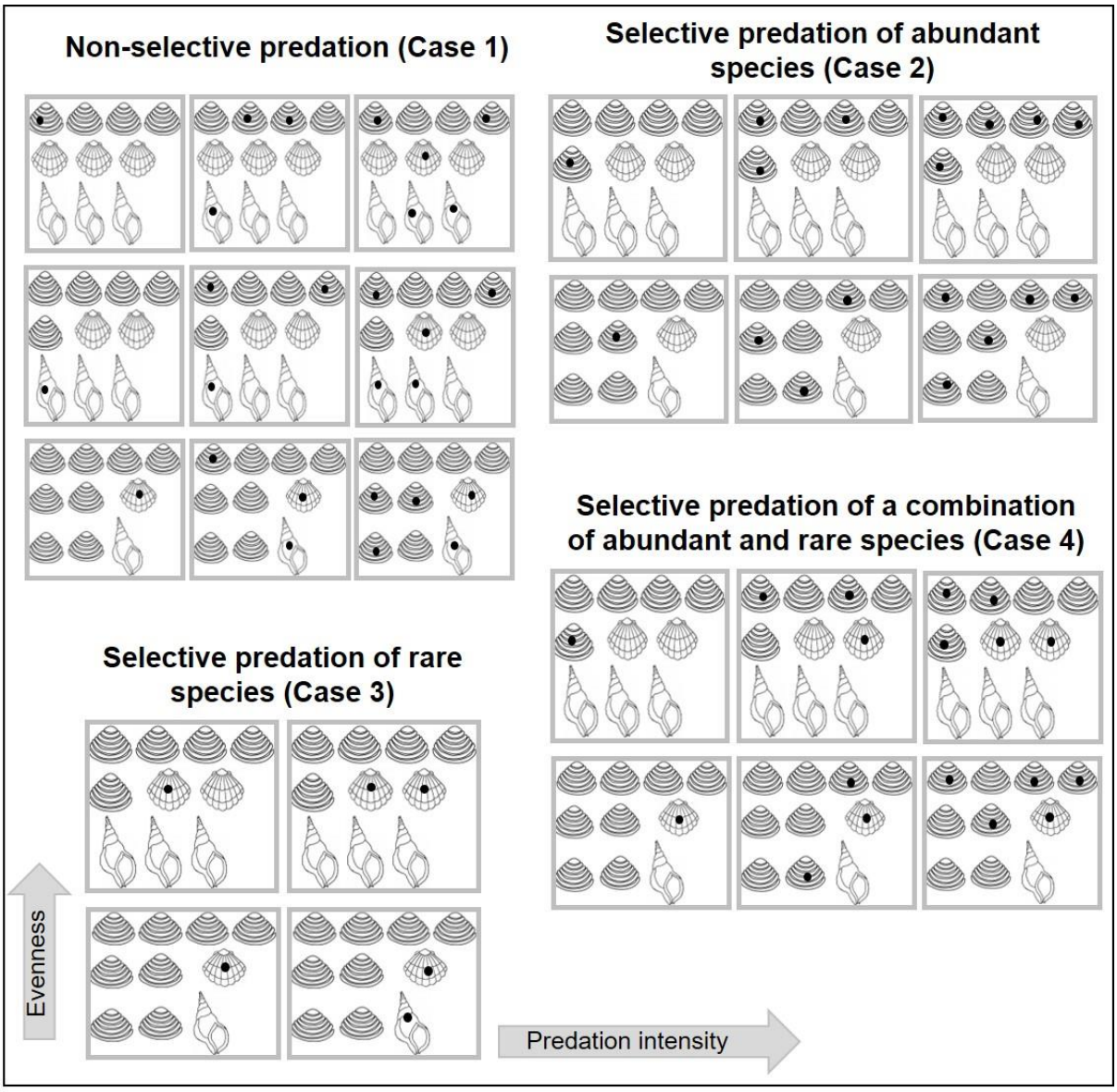

Figure 4.1. An illustrative diagram of model assemblages with varying degrees of evenness, predation intensity, and predation style (selective and non-selective). Mollusc drawings are from publicdomainpictures.net with subsequent modifications.

4.3 RESULTS

4.3.1 Inferred predation intensity:

The inferred predation intensity ($PI_{T.inf}$) may vary substantially from the actual value of overall predation intensity (PI_T) and predation intensity of prey groups (PI_{prey}), especially at smaller sample sizes (Fig 4.2). For non-selective predation (Case 1), $Diff_{PI}$ is affected by the sample size, although not by evenness. At a smaller sample size, the difference is higher ($Diff_{PI}$=0.04) implying a lower $PI_{T.inf}$ than the actual value of PI_T. $PI_{T.inf}$ converges to PI_T with increasing sample size (Fig 4.3, Table 4.5).

Evenness influences inferred predation intensity ($PI_{T.inf}$) when the predation is non-selective (Case 2-4) (Fig 4.3). When the common species are preferentially attacked (Case 2), $Diff_{PI}$ is low (mean = -0.0003, standard deviation = 0.0124) for communities with lower evenness (E_T=0.2) and low original predation intensity (PI_T =0.2) implying good correspondence between $PI_{T.inf}$ and PI_T (Fig 4.3.2, Table 4.5). Communities with higher evenness (E_T>0.2) showed high $Diff_{PI}$ (Table 5) even at a higher sample size implying that $PI_{T.inf}$ will be different from PI_T (Fig 4.3.2). Except for one specific model assemblage (E_T=0.5, PI_T =0.2), all assemblages show a lower $PI_{T.inf}$ in comparison to original PI_T (Table 4.5).

When rare species are attacked (Case 3), the $Diff_{PI}$ vary depending on the combination of evenness and predation intensity. The $Diff_{PI}$ is positive for all communities with low evenness (E_T=0.2) irrespective of the predation intensity (Fig 4.3.3.A-4.3.3.C, Table 4.5) implying a lower value of $PI_{T.inf}$ compared to PI_T. Communities with high evenness (E_T=0.7) showed negative $Diff_{PI}$, implying a higher $PI_{T.inf}$ compared to PI_T (Fig 4.3.3.G-4.3.3.I). The $Diff_{PI}$ value in communities with medium evenness (E_T=0.5) depends on predation intensity; in those communities, $PI_{T.inf}$ is lower compared to PI_T for low predation intensity (PI_T= 0.2) (Fig 4.3.3.D) and higher for higher predation intensities (Fig 4.3.3.E-4.3.3.F, Table 4.5). The variation in $Diff_{PI}$, however, is lower for Case 3 in comparison to comparable communities in Case 2 (Table 4.5).

When some combination of abundant and rare species is attacked (Case 4), the $Diff_{PI}$ vary depending on the combination of evenness and predation intensity (Fig 4.3.4). The $Diff_{PI}$ is negative for most of the communities with varying predation intensities irrespective of the evenness (Table 4.5) implying a higher value of $PI_{T.inf}$ compared to PI_T. Communities with high evenness (E_T=0.7) show a positive $Diff_{PI}$ for medium and high predation intensity.

4.3.2 Inferred number of prey species:

The inferred number of prey species ($S_{prey.inf}$) follows a rarefaction curve where $S_{prey.inf}$ increases with increasing sample size before plateauing and converging to the actual value of S_{prey} (Fig 4.4). The required sample size for convergence depends on evenness and selectivity of predation. In the case of non-selective predation (Case 1), the $Diff_S$ decreases exponentially with increasing sample size and then converges to zero at a range of sample sizes depending on the evenness and predation intensity (Fig 4.5.1, Table 4.6). At a given predation intensity, the convergence takes place at smaller sample size with increasing evenness. For example, at low predation intensity (PI_T=0.2), the required sample size for $Diff_S$ to converge to 0 is 3000 when evenness is low (E_T=0.2) (Fig 4.5.1.A) and 1200 when evenness is high (E_T=1) (Fig 4.5.1.J, Table 4.6).

In selective predation when common species are preyed upon (Case 2), $Diff_S$ does not reflect any sensitivity to the sample size (Fig 4.5.2). This is due to the low value of S_{prey} that converges to its actual value within the first few draws (Fig 4.5.2, Table 4.6). However, when the rare species are attacked (Case 3), $S_{prey.inf}$ is highly sensitive to the sample size because the required sample size for convergence of $Diff_S$ depends on evenness and predation intensity (Fig 4.5.3). When a specific combination of rare and abundant species is attacked (Case 4), $S_{prey.inf}$ shows an intermediate pattern where the sensitivity on sample size is lower than Case 3, yet higher than that of Case 2 (Fig 4.5.4). In general, communities with higher evenness require small sample size for convergence of $Diff_S$, implying less sensitivity of $S_{prey.inf}$ on sample size at a given predation intensity (Fig 4.5.3-4.5.4). For example, at low predation intensity (PI_T=0.2), the required sample size for $Diff_S$ to converge to 0 is 3000 when evenness is low (E_T=0.2) (Fig 4.5.3.A) and 2800 when evenness is high (E_T=0.7) (Fig 4.5.3.G, Table 4.6).

4.3.3 Inferred predation estimates for time-averaged assemblage

The predation estimates of a time-averaged assemblage can be different from those of the contributing model assemblage. In the constructed time-averaged assemblage, $PI_{T.inf}$ shows high overlap with one of the contributing model assemblage (E_T=0.7, PI_T = 0.5, Case 1) while the other two show no overlap (Fig. 4.6A). A similar pattern was found for $S_{prey.inf}$ (Fig. 4.6B).

4.3.4 Inferred predation estimates from Florida:

The assemblages from the four localities in Florida are different in terms of their evenness and sample size (Table 4.2). All the localities except Miami Canal, showed a lack of correlation between the relative abundance of the prey and prey-specific predation intensity (PI_{prey}) for drilling and durophagous predation implying non-selective predation (Table 4.3). In Miami Canal, the significant positive correlation implies that this is a case of selective predation. There is substantial overlap in inferred predation intensity ($PI_{T.inf}$) between three localities (Punta Gorda, Miami Canal, and Mc Queens pit) for both drilling and durophagy (Fig 4.7). For inferred prey species richness ($S_{prey.inf}$), the assemblages show slightly different patterns between drilling and durophagous predation. For drilling predation, all the assemblages show a substantial overlap (Fig 4.7). The durophagous predation record, however, shows a separation between communities with low evenness (Punta Gorda) and high-evenness (Mc Queens pit, Chiquita) (Fig 4.7).

The sample size-standardized resampling protocol (described before) shows a significant difference (p <0.005) in all pairwise K-S test at a reference size of 500 (Table 4.4). This implies that the difference in the inferred predation intensity ($PI_{T.inf}$) and species richness ($S_{prey.inf}$) across assemblages cannot be explained by the sampling intensity or the evenness of the assemblage.

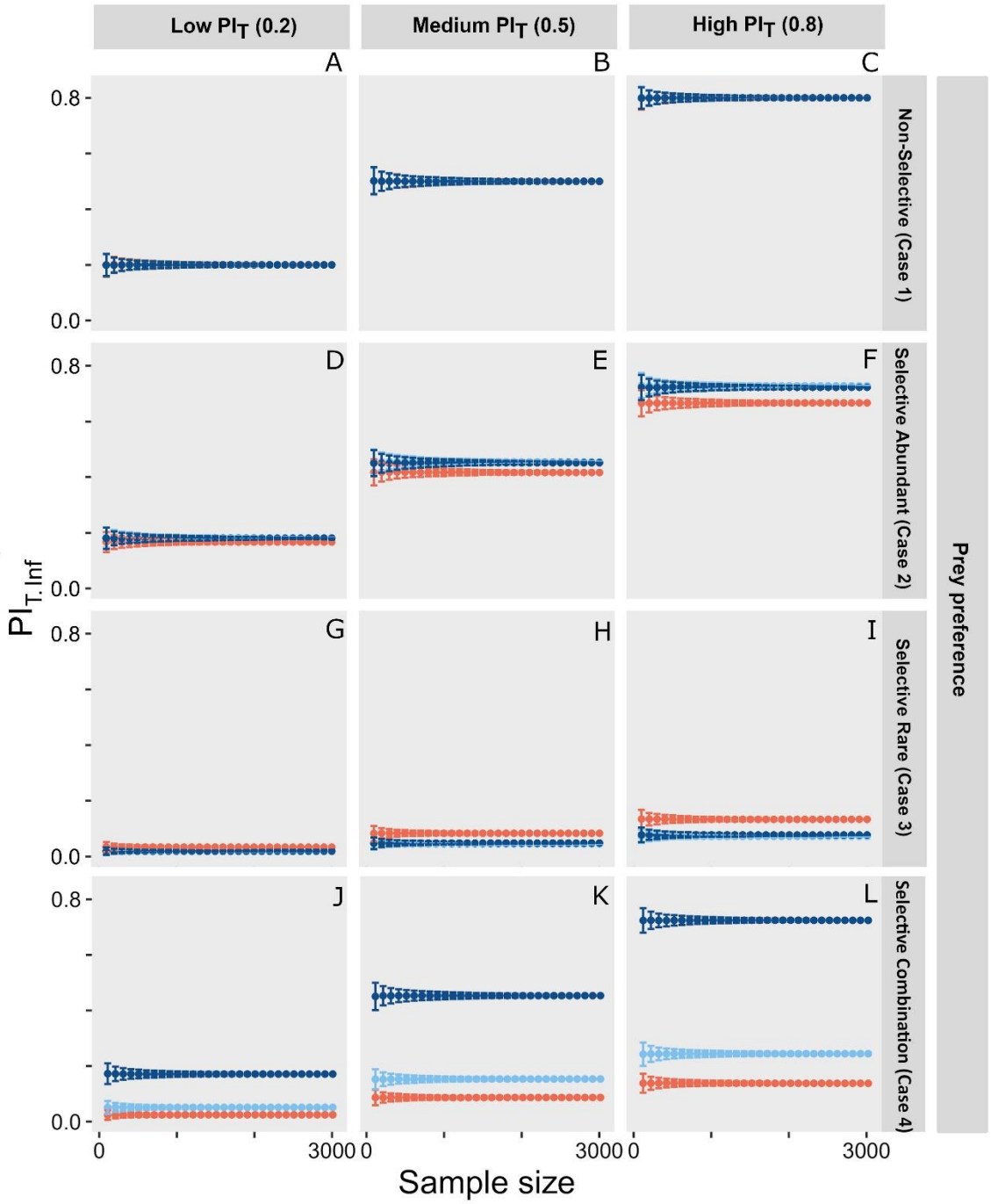

Figure 4.2. Plot showing variation in inferred predation intensity ($PI_{T.inf}$) with varying sample sizes for different model assemblages. The rows indicate the nature of the selectiveness of predation, and the columns indicate predation intensity in the original assemblage (PI_T). The warmer colors represent assemblages with higher evenness.

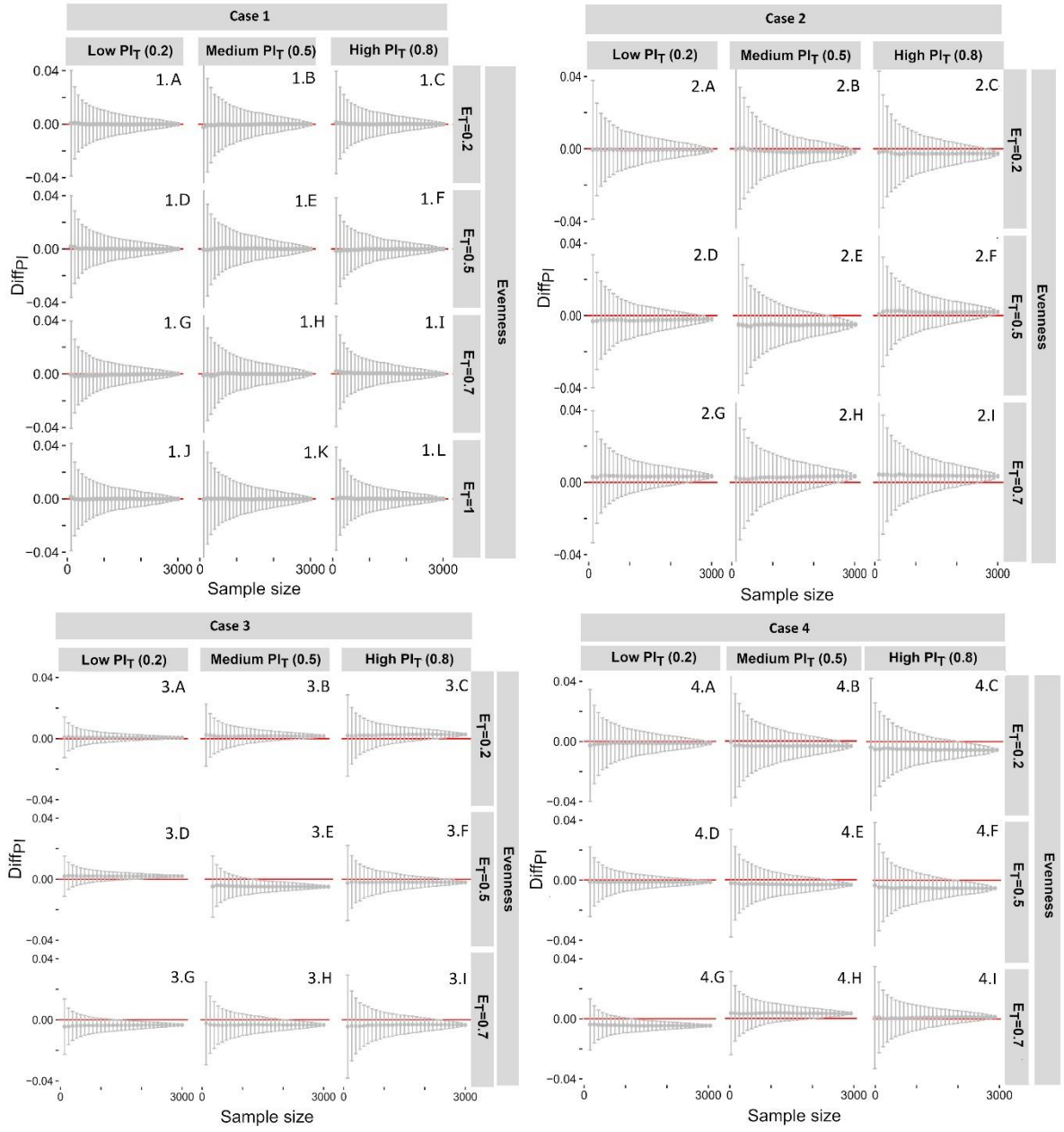

Figure 4.3. Plot showing the difference between the original (PI_T) and inferred predation intensity ($PI_{T.inf}$) at varying sample size for selective and non-selective predation (Case 1-4). The rows indicate evenness and the columns represent original predation intensity. The red line represents the zero line where overall and inferred predation intensities are the same ($PI_{T.inf}$ = PI_T). The grey dots and bars represent the mean and standard deviation of the simulated differences for specific model assemblages.

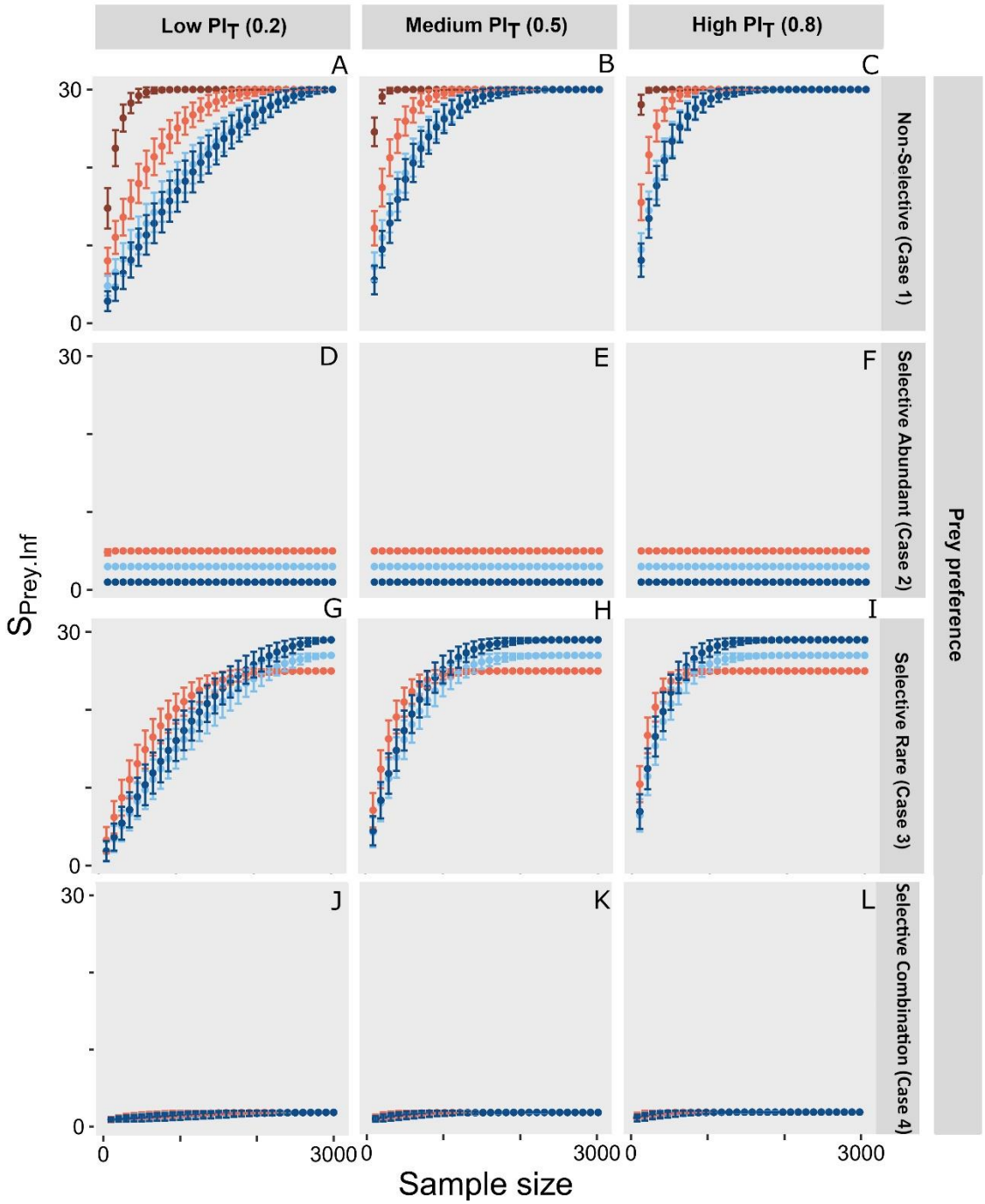

Figure 4.4. Plot showing variation in inferred prey species richness ($S_{prey.inf}$) with varying sample sizes for different model assemblages. The rows indicate the nature of the selectiveness of predation, and the columns indicate prey species richness in the original assemblage (S_{prey}). The warmer colors represent assemblages with higher evenness.

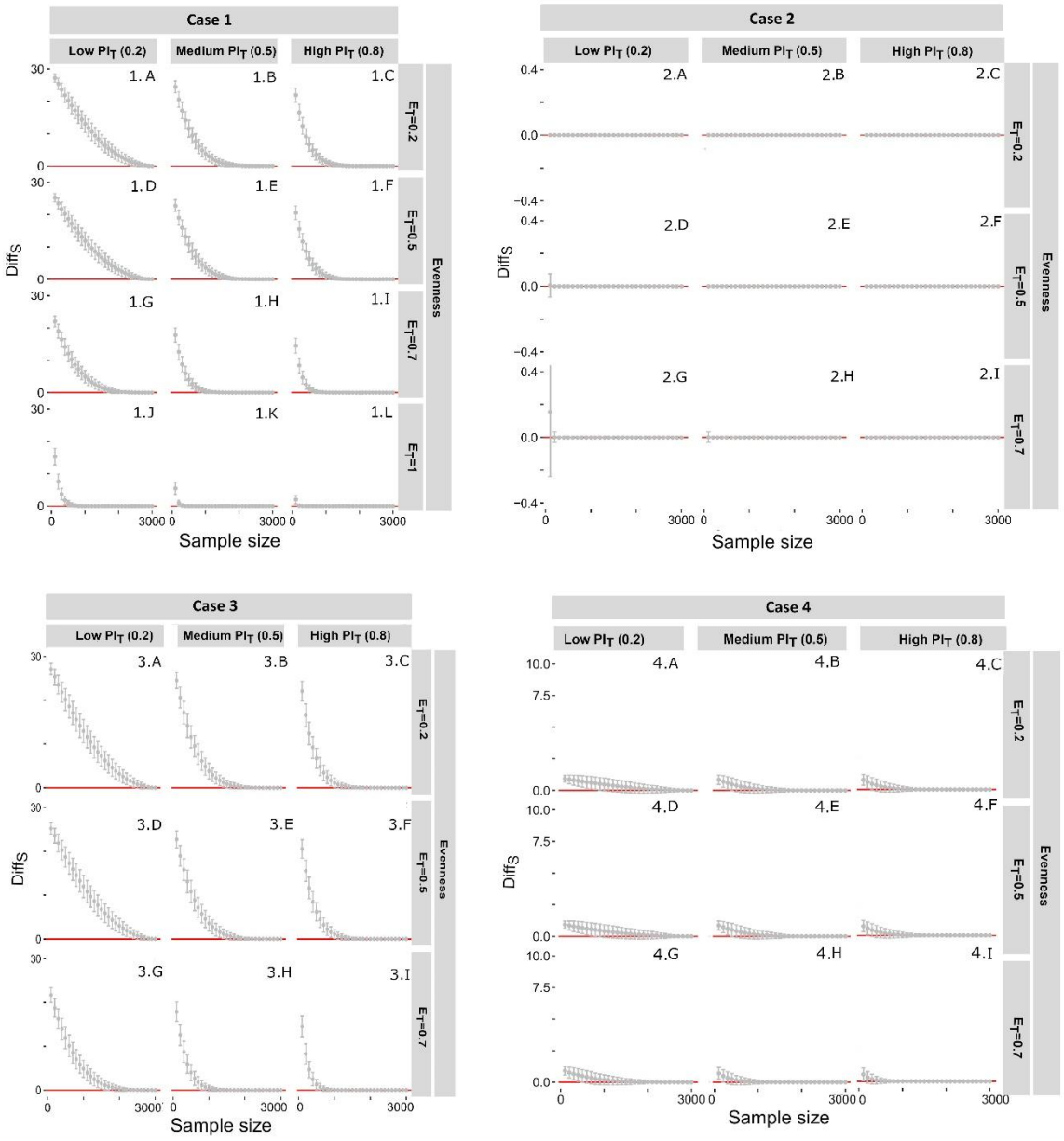

Figure 4.5. Plot showing the difference between the original (S_{prey}) and prey species richness ($S_{prey.inf}$) at varying sample size for selective and non-selective predation (Case 1-4). The rows indicate evenness and the columns represent original predation intensity. The red line represents the zero line where overall and inferred prey species richness are the same ($S_{prey.inf}$ = S_{prey}). The grey dots and bars represent the mean and standard deviation of the simulated differences for specific model assemblages.

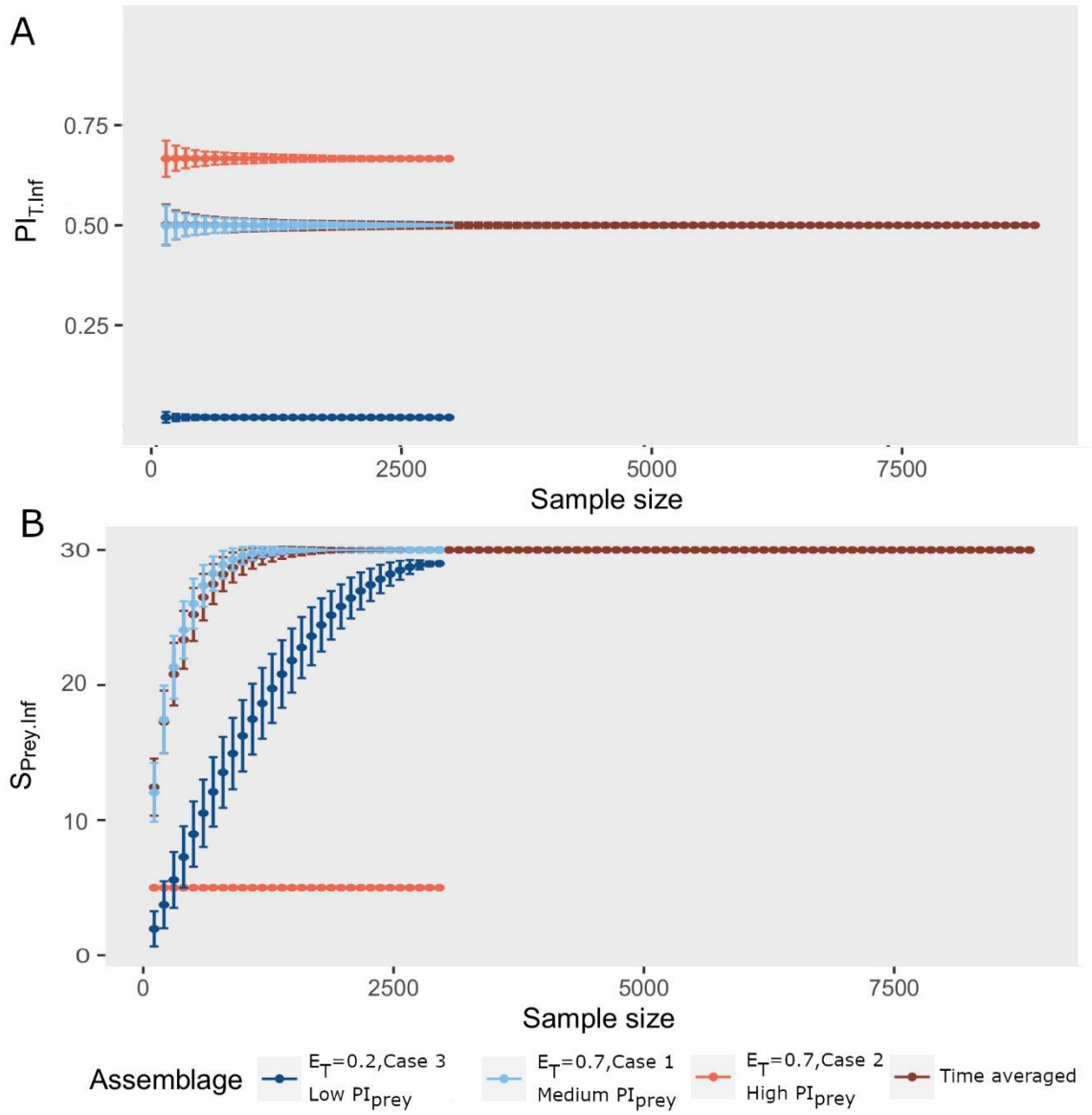

Figure 4.6. Plot showing variation in inferred predation intensity ($PI_{T.inf}$) and inferred prey species richness ($S_{prey.inf}$) with varying sample sizes for different model assemblages in contrast to a time-averaged assemblage.

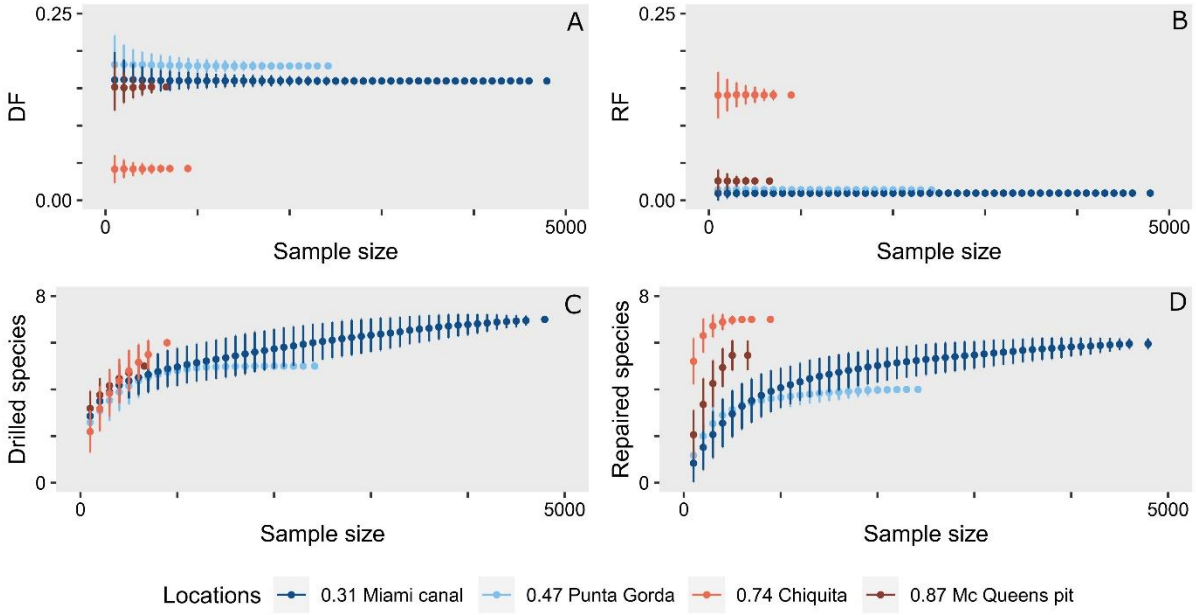

Figure 4.7. Plot showing variation in inferred estimates of drilling and durophagous predation with varying degrees of sampling for four Pleistocene molluscan assemblages of Florida with different evenness (E_T). The top row represents the sample size variation in inferred predation intensity (PI_{inf}). The bottom row shows the inferred number of prey species ($S_{prey.inf}$) with varying sample sizes. The warmer colours represent assemblages of higher evenness.

Table 4.2. A summary of the predation data from four Plio-Pleistocene fossil assemblages of Florida.

Locality	Evenness (E_T)	Sample size	S_T	Drilling frequency	$S_{prey.drill}$	Repair scar frequency	$S_{prey.repair}$
Miami Canal	0.31	4794	7	0.16	7	0.01	6
Punta Gorda	0.47	2417	5	0.18	5	0.01	4
Chiquita	0.74	894	7	0.04	6	0.14	7
McQueen's pit	0.87	657	6	0.15	5	0.03	6

Table 4.3. The result of Spearman rank order correlation test for proportional abundance and PI_{prey} for the predation estimates across four Plio-Pleistocene fossil assemblages of Florida (Chattopadhyay and Baumiller, 2010). The statistically significant ($p<0.05$) results are marked in bold.

Predation	Location	rho	p
Drilling	Punta Gorda	0.87	0.05
	McQueen's pit	0.83	0.06
	Chiquita	0.68	0.08
	Miami canal	**0.99**	**<0.001**
Durophagy	Punta Gorda	0.21	0.74
	McQueen's pit	0.46	0.35
	Chiquita	0.24	0.61
	Miami canal	**0.79**	**0.03**

Table 4.4. The test-statistic (D) of Kolmogorov–Smirnov test comparing the predation estimates across four Plio-Pleistocene fossil assemblages of Florida using sample-standardization protocol. All the results are statistically significant ($p<0.05$).

Estimate	Predation	Location	McQueen's pit	Chiquita	Miami Canal
Predation intensity	Drilling	Punta Gorda	**0.8**	**1**	**0.53**
		McQueen's pit		**0.24**	**0.31**
		Chiquita			**1**
	Durophagy	Punta Gorda	**0.9**	**1**	**0.19**
		McQueen's pit		**0.96**	**0.85**
		Chiquita			**1**
Prey species richness	Drilling	Punta Gorda	**0.38**	**0.31**	**0.13**
		McQueen's pit		**0.24**	**0.36**
		Chiquita			**0.29**
	Durophagy	Punta Gorda	**0.84**	**1**	**0.41**
		McQueen's pit		**1**	**0.95**
		Chiquita			**1**

Table 4.5. A summary of the difference in inferred predation intensity from the original value for the model assemblages. Each cell contains information about the mean value and standard deviation of DiffPI; the first two represents the sign and magnitude of the mean value. A positive mean value of DiffPI indicates a larger value of original than inferred predation intensity (PIT > PIT.inf).

Evenness	$Diff_{PI}$ for Case1			$Diff_{PI}$ for Case2			$Diff_{PI}$ for Case3			$Diff_{PI}$ for Case4		
	Low	Medium	High	Low	Medium	High	Low	Medium	High	Low	Medium	High
$E_T = 0.2$	+ve, <0.001, 0.013	+ve, <0.001, 0.016	+ve, <0.001, 0.013	-ve, <0.001, 0.012	-ve, 0.001, 0.015	-ve, 0.003, 0.014	+ve, <0.001, 0.004	+ve, 0.002, 0.006	+ve, 0.002, 0.008	-ve, 0.001, 0.0003	-ve, 0.003, 0.0004	+ve, 0.005, 0.0005
$E_T = 0.5$	+ve, <0.001, 0.013	+ve, <0.001, 0.016	+ve, <0.001, 0.013	-ve, 0.002, 0.012	+ve, 0.005, 0.015	+ve, 0.002, 0.014	+ve, 0.002, 0.004	+ve, 0.005, 0.006	-ve, 0.002, 0.008	-ve, 0.001, 0.0002	-ve, 0.003, 0.0003	-ve, 0.005, 0.0003
$E_T = 0.7$	+ve, <0.001, 0.012	-ve, <0.001, 0.015	-ve, <0.001, 0.012	+ve, 0.003, 0.012	+ve, 0.004, 0.016	+ve, 0.003, 0.016	-ve, 0.003, 0.006	-ve, 0.003, 0.009	-ve, 0.003, 0.011	-ve, 0.004, 0.00009	+ve, 0.003, 0.00016	+ve, 0.001, 0.0003
$E_T = 1$	-ve, <0.001, 0.013	+ve, <0.001, 0.015	+ve, <0.001, 0.013	NA	NA	NA	NA	NA	NA	NA	NA	NA

Table 4.6. A summary of the difference in inferred prey species richness from the original value for the model assemblages. Each cell contains the minimum sample size required for $Diff_S$ to converge to zero for each model assemblages. A smaller number indicates that the inferred prey species richness converges to the original value ($S_{prey.inf} = S_{prey}$) at smaller sample size.

Evenness	Required sample size for convergence of $Diff_S$ for Case 1			Required sample size for convergence of $Diff_S$ for Case 2			Required sample size for convergence of $Diff_S$ for Case 3			Required sample size for convergence of $Diff_S$ for Case 4		
	Low	Medium	High	Low	Medium	High	Low	Medium	High	Low	Medium	High
$E_T = 0.2$	3000	2800	2100	100	100	100	3000	2700	2200	3000	2300	2200
$E_T = 0.5$	3000	2700	2100	100	100	100	3000	2700	2200	3000	2100	1700
$E_T = 0.7$	2900	1900	1400	300	100	100	2800	1900	1400	2500	1500	1000
$E_T = 1$	1200	700	400	NA	NA	NA	NA	NA	NA	NA	NA	NA

4.4 DISCUSSION

Paleontological research on predation has expanded rapidly in scope, methods, and goals over the years. In recent years, a number of studies focused on documenting the evidence of predation from times, geographic areas and taxa that are poorly known for their predation record (Rojas et al. 2014; Randle and Sansom 2019; Bicknell and Holland 2020; Gordillo and Malvé 2021; Klompmaker and Landman 2021; Gordillo et al. 2022) and using predation records for testing evolutionary hypotheses (Klompmaker et al. 2017; Gehling and Droser 2018; Harper et al. 2018; Lerosey-Aubril and Peel 2018; Petsios et al. 2021). In contrast, a relatively small number of studies focused on the analytical methods to evaluate the reliability of predation measures in recent years (Smith et al. 2018, 2019, 2022; Budd and Mann 2019). Our model demonstrates how inferred predation intensities may vary with evenness, predation selectivity and sampling intensities. It highlighted the importance of these factors in influencing predation estimates of live and death/fossil assemblages; it also underscores why it is necessary to develop a methodological framework of sample standardization before comparing predation estimates of assemblages separated by time and space.

4.4.1 Effect on the inferred intensity:

Our simulation results show that communities' evenness does not significantly change the inferred predation intensity when random encounters between predator and prey guide predation. It is, however, uncommon to find predation events to be completely random in the natural world. Prey species are selected by predators to maximize net energy gain, within the constraints of a number of factors including reproductive demands, predator interference, predation risk, avoidance of prey, deterrents, and predator behavior (Seitz et al. 2001; Stephens and Krebs 2019). In such selective predation, the inferred predation intensity may differ significantly from the original predation intensity. Following the considerations of optimal foraging theory (Hughes 1980; Pyke 1984; Burrows and Hughes 1991; Stephens and Krebs 2019), two aspects make the predation selective. The first is the relative ease with which a predator encounters a prey. Encounter in marine ecosystem is determined by a number of things including abundance of the prey, accessibility of the prey, landscape heterogeneity, predator abundance, abundance of secondary predators, habitat type (Ryer and Olla 1995; Seitz et al. 2001; Sims et al. 2006; Casey and Chattopadhyay 2008; Martinelli et al. 2015). Keeping the other factors constant, the probability of encounter increases with the

increasing relative abundance of a prey species (Vermeij 1983; Leighton 2002; Leonard-Pingel and Jackson 2013); this decreases the foraging time and increases the net energy gain of the predator. The second aspect is the traits (morphological, ecological, behavioral) of the prey that dictate the net energy gain of the predator. The final selection by the predator is often a combination of these factors. A higher attack rate may be found in an abundant prey species due to its higher encounter rate than a rarer species. This would lead to scenarios similar to Case 2, where the inferred predation intensity of low-evenness communities would be higher than the actual predation intensity. This inflated measure results from the over-representation of common species in smaller samples that are primarily attacked.

Most often than not, the encounter frequency does not dictate the attack frequency, and the selection of prey is guided by the prey traits such as size, morphology, behavior (Kitchell et al. 1981; Palmqvist et al. 1996; Leighton 2001; Zlotnik and Ceranka 2005; Chattopadhyay and Dutta 2013; Chattopadhyay et al. 2014*a*, 2015, 2020; Martinelli et al. 2015; Chandroth and Chattopadhyay 2022). These would be similar to Case 3, where the most dominant groups are not preyed upon. The inferred predation intensity of low-evenness communities would be lower than the actual predation intensity. This apparent drop in predation intensity results from the lack of representation of rare species in smaller samples that are never attacked. It is especially problematic because this difference is substantial for all evenness. This observation is consistent with the findings by Smith et al. (2021) where they demonstrated the effects of overdispersion and zero inflation using count data of predation traces. They concluded that the major element underlying these effects was sample size. Their results support our findings that predation measures lack of reliability at small sample size.

4.4.2 Effect on inferred selectivity:

Predation is known to impact the structure of a community, including the overall richness, distribution and evenness (Schemske et al. 2009; Freestone et al. 2011, 2020). It is therefore important to evaluate the inherent dependence of the predation inferences on one aspect of community structure such as evenness before evaluating the evolutionary impact of predation on shaping the community structure in deep time. Our models demonstrate that the inferred number of prey species may depend on the evenness of the live community. Communities with low evenness differ significantly from the original prey species and yield fewer inferred prey species even when the predation is non-selective (Case 1). This may lead

to the development of an artificial selectivity, primarily driven by the preferential counting of the dominant species and not by the biological preference demonstrated by the predators. Therefore, any community with low evenness suffers from the high likelihood of underrepresenting the number of prey species. The deviation from the true prey-species richness is higher for smaller sample size and lower intensity of predation. Communities with higher predation intensity will provide the true prey-species richness at a smaller sample size than communities with lower predation intensity. Selective predation (as indicated by Case 2-4) also creates similar deviations.

The sensitivity of inferred prey species richness on sample size, evenness, and original predation selectivity makes the comparison of prey species richness in spatially or temporally distinct assemblages somewhat unreliable unless they are normalized. This is especially important when comparing predation estimates from assemblages representing different time-bins or environments likely to show varying diversity/evenness.

4.4.3 Paleontological case study:

The assemblages from the four localities of Florida have been used for interpreting the relationship between durophagy and drilling predation (Chattopadhyay and Baumiller, 2010). However, the study's conclusions did not consider sample size or evenness of the communities. The assemblages at these localities are quite different in terms of their evenness and sample size (Table 4.2). Only in Miami Canal, predatory attacks (durophagous and drilling) are guided by the relative abundance of prey species and hence deviates from non-selective predation. The sample size-standardized resampling protocol revealed a significant difference in pair-wise comparison for all inferred predation intensity and prey species richness estimates. This implies that the differences in predation measure across assemblages are largely independent of sampling intensity or the evenness of the assemblage.

It is important to recognize that a number of factors played a role in this particular case that made these assemblages less susceptible to community evenness and sampling intensity. Because three localities (Punta Gorda, Mc Queens pit, Chiquita) are showing predation pattern that is non-selective with respective relative abundance, they are less likely to be affected by sample size. Moreover, they have medium to high evenness that makes them less sensitive to sample size. Miami Canal, however, is characterized by low evenness (0.31), shows evidence of selective predation and low predation intensity (PI_T<0.2). Assemblages with these characteristics are more prone to show large difference from actual

predation measures at small sample size (Fig 4.3.2.A). Because Miami Canal has the largest sample size among the localities, makes it less likely to be affected by these factors. Hence, the observed $S_{prey.drill}$ and $S_{prey.repair}$ are least likely to be affected by these factors.

4.4.4 Proposed protocol of post-facto standardization of predation data:

We demonstrated how inferred predation estimates may be influenced by different assemblages with varying evenness and predation intensity. It is evident that such inferences are more prone to differ from the original value at small sample size. There has been a standard practice of excluding assemblages where the sample size is less than 30 (Kosloski et al. 2008) or 50 (Forcino 2011). Considering the sensitivity of the sample size also depends on the evenness and predation intensity, a static cutoff is not appropriate. Here we are proposing a resampling-based standardization protocol to identify and exclude assemblages that are not comparable. Such assemblages represent scenarios where the difference in observed predation estimates could have resulted due to small sample size. We suggest the following steps (Fig 8) to be followed for comparing predation patterns of spatially/temporally distinct assemblages to avoid misinterpretation.

1. We identify the smallest sample size among the assemblages. That sample size is considered as reference sample size (RSS).
2. Using the described protocol in the simulation model, inferred predation intensity ($PI_{T.inf}$) and inferred prey-species richness ($S_{prey.inf}$) need to be calculated at a specific step size of 100 for all assemblages. The step size of all assemblages should be equal till the last step when the remaining number of individuals in that assemblage are drawn. The step size can be lowered till 30 if the total assemblage size is small. Lowering the step size any further may create erroneous results due to smaller sample size (Kosloski et al. 2008; Dietl and Kosloski 2013; Smith et al. 2022).
3. The distribution of inferred predation intensity (PI_T) for all assemblages should be compared at RSS by a pairwise comparison using Kolmogorov-Smirnov (K-S) test. If the pair-wise comparison yields a significant difference between two assemblages, then the differences in inferred predation intensity (PI_T) cannot be explained by sample size alone and hence, likely to represent the actual variation. These pairs would be considered comparable at that RSS.

4. If assemblages show non-significant difference in pairwise K-S test, we cannot reject the possibility of small sample size influencing the inferred predation intensity and hence, should not be considered for further comparative analysis at that pre-selected RSS. If any such pair contains the assemblage with a sample size equal to RSS, then we cannot include the pair for further analysis.
5. The next step is to compare the remaining pairs with non-significant differences at a larger sample size (new RSS). The new RSS is determined by selecting the smallest sample size of the remaining assemblages and following the above protocol (2-3) we will find the assemblages that can considered comparable at the new reference sample size. The same process can be repeated to understand the sensitivity of the inferred prey-species richness ($S_{prey.inf}$) on sample size.
6. This iteration should be performed with increasing sample sizes till the maximum number of assemblage pairs show significant differences in distribution of inferred predation intensity (PI_T) and prey species richness ($S_{prey.inf}$).

The pairs that show non-significant difference even at the highest sample size, we cannot reject the influence of sampling intensity and inherent community evenness in shaping the predation measures. They should be excluded from comparative analyses of predation signals. Estimating PI_{prey} is difficult, especially for cases where rare species are attacked; excluding species without any predation trace while calculating PI_T may give us some insight.

4.4.5 Caveats and implications:

The fossil record of predation has shaped our understanding of how the nature of biotic interaction changed over time and its role as an evolutionary mechanism. Preserved traces, such as drill holes and repair scars, are some of the best quantifiable proxies of predation and they are often used to assess the evolutionary impact of predation in deep time (Vermeij et al. 1981; Alexander and Dietl 2003; Kelley and Hansen 2003). Studies aiming to evaluate the predation trend through time, however, are often forced to use predation data from discrete assemblages that differ in sample size, inherent community evenness, and the type of predation selectivity (Harper 2016). Our study demonstrates the effect of such factors on the inferred predation intensity and the recognized prey richness. Comparison between temporally separated collections, such as Paleozoic and Cenozoic predation records that are

known to be different in the sample size (and probably predatory behavior), are susceptible to such factors.

Our proposed method of post-facto standardization will be essential for such comparisons and to establish the true nature of biotic interaction through time. It is important to recognize that the proposed protocol is a preliminary attempt towards standardization, without considering a number of complexities. The simulations are primarily developed for communities that are preserving the community structure of the live communities. It is true that average evenness of molluscan time-averaged assemblage is shown to preserve the evenness of the live assemblage (Olszewski and Kidwell 2007). Other characters of the live assemblages, however, can substantially differ in death/fossil assemblage because they are typically time-averaged representing a mix of multiple generations (Kidwell et al. 1991; Kidwell and Flessa 1995; Kidwell 2007; Tomašových and Kidwell 2009; Kidwell and Tomasovych 2013; Bhattacherjee et al. 2021). In a simple hypothetical time-averaged assemblage where all the individuals of a live-assemblage are preserved, we have demonstrated that the inferred predation pattern may or may not resemble the contributing assemblage (Fig 4.6). If specific section of the live community is preferentially lost due to preservation and if the predation signature of those specimens differ from the remaining assemblage, the proposed standardization method will fail to detect that. For example, some predation attempts are size selective and larger size class often show higher predation resistance and lower predation intensity. Because, the preservation potential of smaller size class is lower than larger ones (Cooper et al. 2006), selective absence of small size class in the fossils would result in a low inferred predation intensity compared to the original value. Multiple interactions during the lifetime or after the death of the prey may change the frequency of the overall assemblage (Kosloski 2011; Gordillo and Archuby 2014). A molluscan community affected by drilling predation may also be subjected to crushing predation; because the durophags only go after the live prey (non-drilled), the relative proportion of drilled shells increase if the predators successfully destroy the shells as part of the predation process (Smith et al. 2019). Predation style and resulting predation trace also differ among predators. Two of the most common types of predations studied in the fossil, drilling and durophagy, are quite different in a number of aspects. It is possible to identify successful and unsuccessful predation by studying the completeness of the drill holes, successful attacks by durophagous predators often result in unrecognizable fragmentation (Kosloski 2011; Leighton et al. 2016; Dyer et al. 2018). Repair scars represent a failed

durophagous attack. Comparing drillhole and repair scars, therefore, are not without limitations. Our study, although attempts to recognize the possible source of analytical bias and to recognize them in the observed database, clearly glosses over the full complexities of predation style, post-mortem alteration and time-averaging. Following the direction of reconstructing fossil assemblages from live data using modeling approach (Olszewski 2004, 2012), we plan to develop more inclusive frameworks in future to address such complexities.

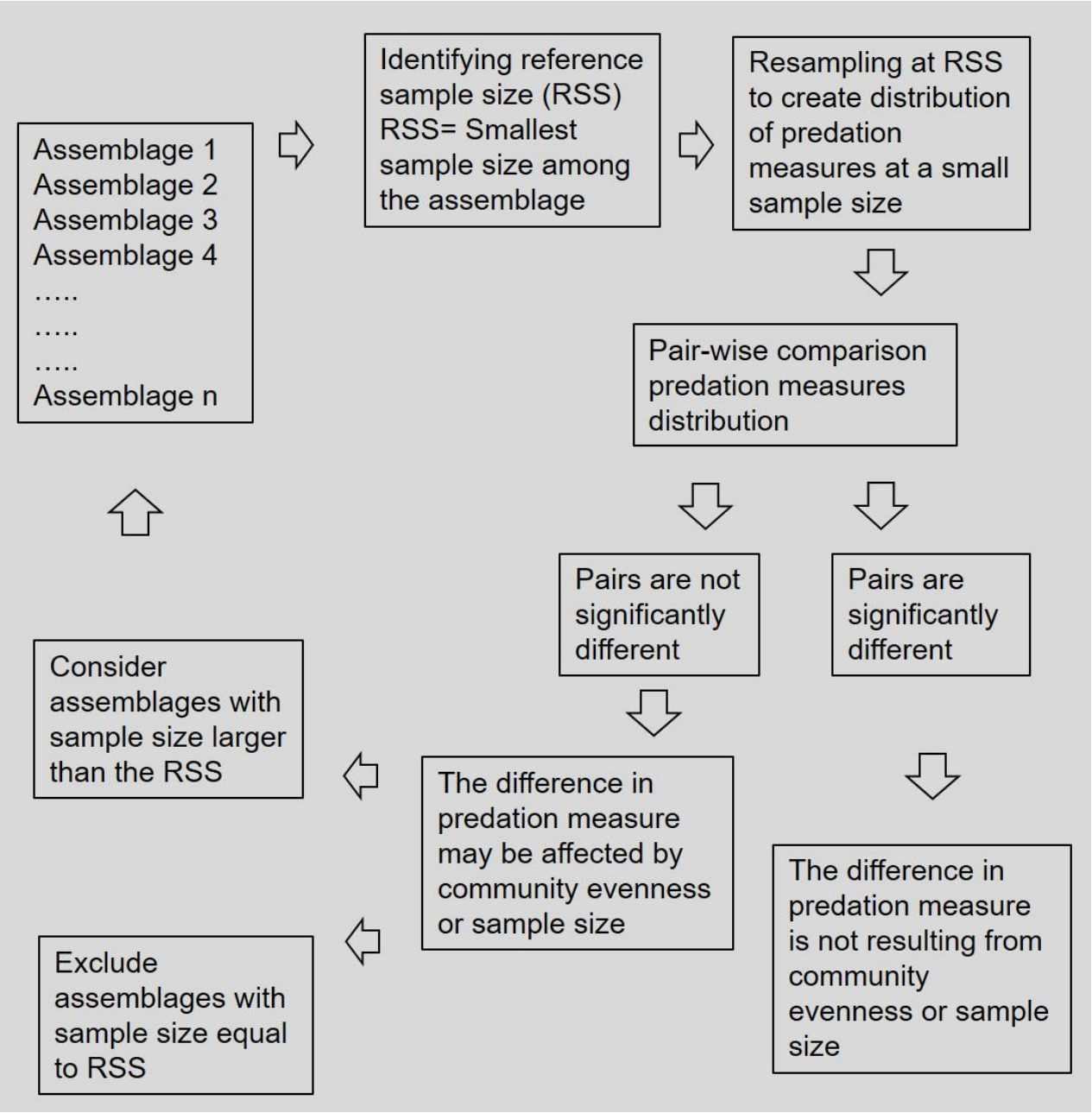

Figure 4.11. Flowchart of the general framework of proposed method of the post-hoc standardization.

4.5 CONCLUSION

The effect of community structure and sampling intensity on the inferred predation estimates is rarely explored. Using a resampling technique, our study demonstrates the impact of these aspects on the estimates of predation intensity and the number of prey species. Our results show that the communities with highly selective predation are the most sensitive to sampling intensity, and the inferred predation intensity of these assemblages can substantially deviate from the actual value. In contrast, predation intensity for non-selective predation tends to be unaffected by sampling intensity. Inferred prey-species richness is also influenced by the nature of community evenness, predation selectivity, and actual predation intensity. For non-selective predation, communities with low evenness and low predation intensity are highly sensitive to sample size. The inferred prey-species richness can be underrepresented significantly at smaller sample size. For selective predation, the sensitivity depends on the nature of selection. The inferred prey-species richness deviates significantly when rare species are attacked preferentially. Our study also provides a framework of post-facto standardization of the predation data to remove the effect of sample size/evenness during comparison. The proposed method, although simple, will provide fundamental framework for comparison of discrete assemblages as they are often characterized by a difference in sample size, evenness and predation selectivity.

CHAPTER 5

Conclusion

5.1 CONCLUSION

Marine biodiversity varies across space and through time. Identifying the drivers of such variation is crucial to understand the underlying ecological mechanism generating complex spatio-temporal distribution of marine biodiversity. The rich fossil record of marine fauna provides insight about the long-term processes shaping distributional pattern. In the context of the recent climate changes, identifying the mechanisms for ecological variation is of primary importance to quantify the processes which may potentially cause an ecosystem collapse (Jablonski 1998; Olszewski and Patzkowsky 2001; Bonelli et al. 2006; Clapham et al. 2006; Clapham and James 2008; Heim 2009). Apart from the ecological mechanisms, however, taphonomy and methodological strategies can also influence observed patterns of faunal distribution in the present and past ecosystem (Jurasinski 2007). To establish the reliability of observed faunal distribution, therefore, it is important to quantify the impact of taphonomy and various operational decisions about sampling protocols, analytical methods and data categorization before inferring any spatio-temporal patterns from fossil assemblages. Molluscan assemblages are one of the ubiquitous faunal assemblages found in the shallow marine region. They have been used extensively for large-scale quantitative paleoecological studies. They also have a remarkably documented fossil record because of their taphonomically durable shells. In this thesis, I assessed the role of taphonomy and sampling on various paleobiological inferences using marine molluscan assemblages.

It is generally assumed that the role out-of-habitat post-mortem transportation events in ordinary level bottom sublittoral environments with gentle slopes is insignificant, and they mostly experience within-habitat transportation. The results of our study on the live-dead fidelity and size frequency distribution (SFD) of the molluscan fauna from a shallow marine siliciclastic setting with a narrow shelf, high sedimentation rate and frequented by episodically high-energy events (Chapter 2) reject the assumption. The results demonstrate that the LA and DA are poorly correlated and the DA did not show the environmental partitioning observed in the LA. Since the entrainment velocity of the shell depends on shell size, I constructed a numerical simulation of the shell SFD for death assemblages (DAs) from live assemblages (LAs) and compared it with the observed SFD of the DAs. The results of the SFD based simulation as well as the high L-D mismatch indicate that DA in such areas are not produced by within-habitat mixing and are receiving shells via regional transport facilitated by tropical cyclones. The specific field locality in the east coast of India, is

frequently affected by cyclones originating above 15°N, causing a high degree of out-of-habitat transport and mixing of shells between 15°N to 21°N. This study provides a method to use SFD to recognize out-of-habitat transport using LA and DA. The high likelihood of out-of-habitat transport of molluscan assemblage in storm-dominated environment also provide a taphonomic caution while reconstructing paleoecology based on environmental distinct fossil assemblages.

Beta diversity, or within-habitat diversity is a measure of spatial distribution and heterogeneity of the fauna. It is highly dependent on the spatial scale and resolution of the study. Using a probabilistic model, I evaluated the effect of unequal spatial scales of sampling on beta diversity at a regional scale (Chapter 3) using LA and DA along the west coast of India. The results of this model provided an expected beta diversity pattern if unequal grid sizes of sampling had caused the variation. The observed variation in beta diversity in this study was different from the expected pattern produced by the null model, indicating that sampling scale alone cannot generate the beta diversity pattern of this region. Environmental parameters such as salinity, productivity, and cyclones were found to play a significant role in shaping the beta diversity. The model-based comparison would be useful to evaluate the beta diversity of fossil assemblages across different spatial scale. The observed consistency of the results between LA and DA indicate that DA record reliable spatial and compositional fidelity at regional scale. This confirms that molluscan fossil assemblages representing time-averaged DAs are a close approximation of regional distribution of the living community of the past with limited effect from time averaging and post-mortem transportation.

Apart from faunal composition, different sampling strategies may also impact inferences of other important paleoecological processes such as biotic interactions. Predation is an important evolutionary driver and predation estimates play an important role in evaluating the evolutionary effect of ecological interactions. Predation estimates are generally based on the assumption that these are not influenced by methodological artefacts. Using a resampling technique, I evaluated the effect of sampling intensity and the prey community's evenness on the inferred predation intensity and prey species richness (Chapter 4). The results demonstrate that the inferred predation intensity is not influenced by the evenness of a community when the predation is non-selective. However, the inferred predation intensity is sensitive to evenness and sampling intensity and can substantially deviate from the actual

value when the predation is highly-selective. When rare species are preferentially attacked, inferred predation intensity and inferred prey species richness is underrepresented at smaller sample size as sampling intensity heavily influences communities with low evenness and low predation intensity. Additionally, I also proposed a post-facto standardization method for comparing predation estimates of discrete communities that differ in the sample size. The utility of this method was tested using the published predation data of the Plio-Pleistocene molluscan fossil assemblage. The method will be helpful in comparing predation patterns across collections varying in sampling intensity and community composition. This study also provide critical insights into the biological reliability of predation estimates compiled across time and space.

Using a combination of field observation and quantitative modelling, this thesis demonstrates the importance of taphonomy and methodological nuances on the inferences from mollascan assemblages representing recent and past ecosystem. The methods developed as part of this work provides a way to recognize such issues and recommends methods to rectify them before making important paleoecological inferences from the fossil record.

APPENDIX

Supplementary materials

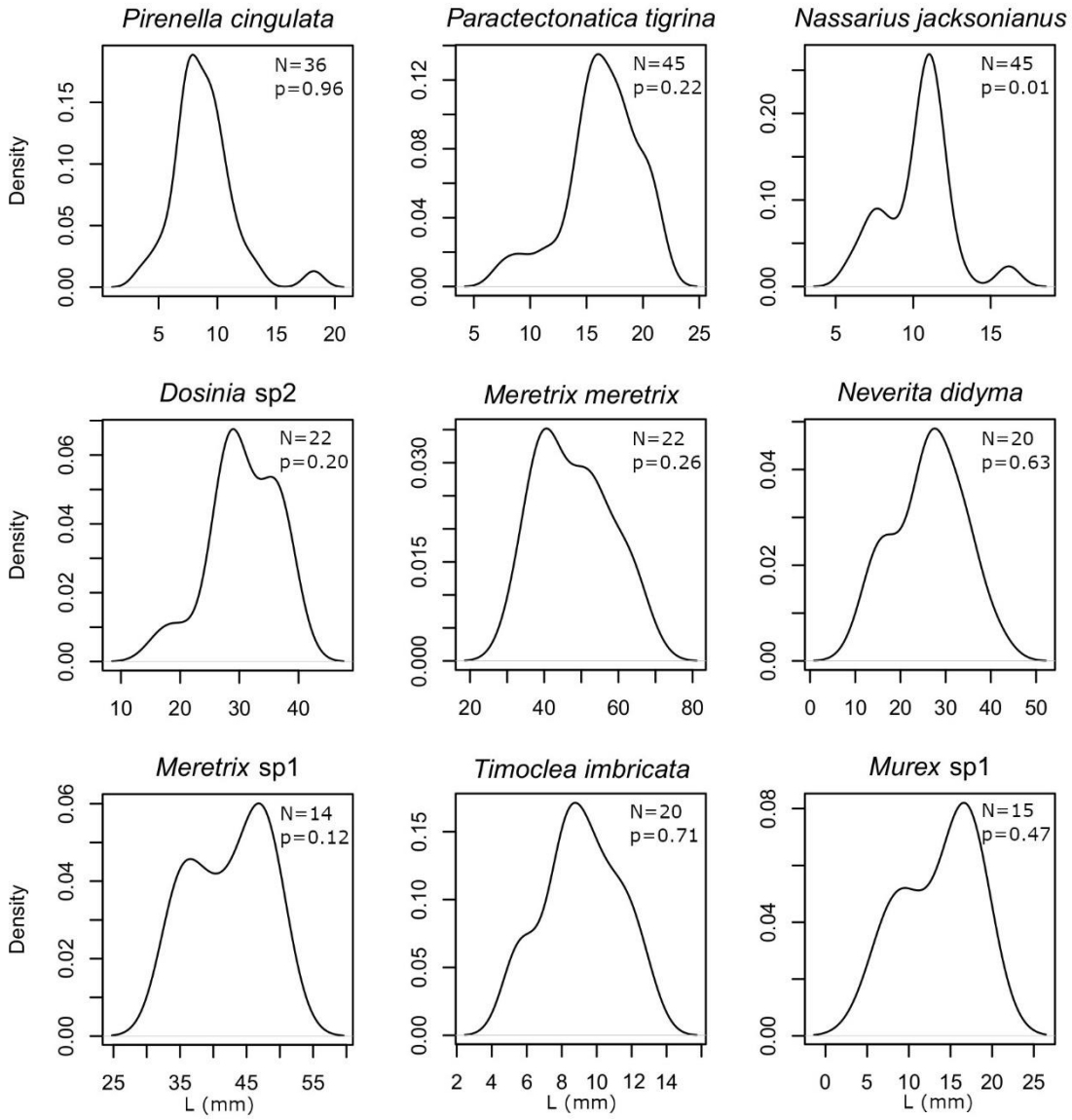

Figure.2. S1. — Size distribution of the live species that have also been found in DA. The sample size is marked as N. The p-value is associated with the Shapiro-Wilk test performed for evaluating the normality of the size distribution.

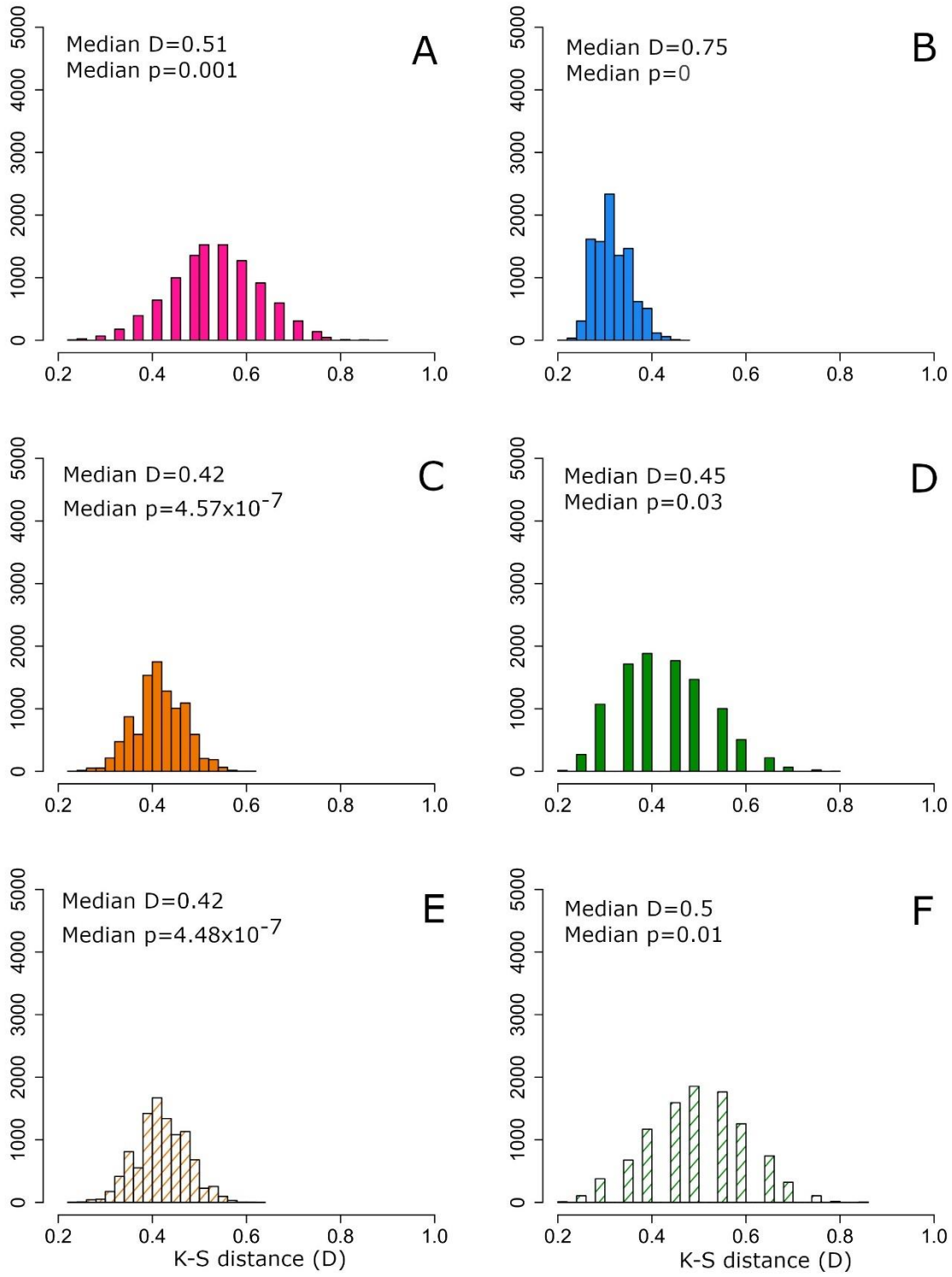

Figure.2.S2. Histograms of D-values from the K-S test between simulated and observed dead size distribution for shared species between LAs and DAs. (A) beach, (B) tidal flat, (C) restricted environment, (D) estuary, (E) restricted environment (with size filter), (F) estuary (with size filter).

R Script 2.S1. R Script for statistical analyses and plots in Chapter 2

(Datafiles used for the codes will be available on request)

```
############################################################
require(vegan)
abundancedata=read.csv("abundance30.4.19.csv", header = T)
abundanceall=abundancedata[1:34,4:60]
abundanceocc=decostand(abundanceall,method="pa")
envall=abundancedata[,1:2]
abundancelive=abundanceall[c(14:21,27:31),1:57]
abundancedead=abundanceall[c(1:13,22:26,32:34),1:57]

par(mfrow=c(1,2))
par(mar=c(15,5,1,0.5))
par(pty="s") ####makes the plot square##################
season=abundancedata[,3]
sites=abundancedata[,2]
env=c(rep("Beach",5),rep("Tidal flat",8),rep("Restricted",5),rep("Estuary",3))
attribute=data.frame(sites,env)

#############Figure 2.3################################
#jpeg("Plot3.jpeg", res = 300)
par(mfrow=c(3,2))
par(mar=c(8, 4.1, 1, 2.1))
#par(mar=c(1, 1, 1, 1))

par(mai = c(1,0.6,0.4,0.1))
spbarplot=read.csv("barplotdatanew.csv",header = T)
Beach=subset(spbarplot,spbarplot$Env=="Beach",select =c(Species,X.))
barplot(Beach$X.,width=0.5,col="deeppink",ylim=c(0,100),las=2,ylab="%",font.axis = 4,names.arg
= Beach$Species,cex.axis = 1.5,cex.names = 1.5,cex.lab=1.5)
#text(seq(1,6,by=1),par("usr")[3]-0.3, srt = 35, adj= 1, xpd = TRUE,labels = Beach$Species, cex=1)
Estuary=subset(spbarplot,spbarplot$Env=="Estuary",select =c(Species,X.))
```

```
barplot(Estuary$X.,col="green4",ylim=c(0,100),las=2,ylab="%",font.axis = 4,names.arg =
Estuary$Species,cex.axis = 1.5,cex.names = 1.5,cex.lab=1.5)

#text(seq(1,6,by=1),par("usr")[3]-0.3, srt = 35, adj= 1, xpd = TRUE,labels = Estuary$Species, cex=1)

Tidal=subset(spbarplot,spbarplot$Env=="Tidal flat",select =c(Species,X.))

barplot(Tidal$X.,col="dodgerblue2",ylim=c(0,100),las=2,ylab="%",font.axis = 4,names.arg
=Tidal$Species,cex.axis = 1.5,cex.names = 1.5,cex.lab=1.5)

#text(seq(1,6,by=1),par("usr")[3]-0.3, srt = 35, adj= 1, xpd = TRUE,labels = Tidal$Species, cex=1)

Restricted=subset(spbarplot,spbarplot$Env=="Restricted",select =c(Species,X.))

barplot(Restricted$X.,col="darkorange2",ylim=c(0,100),las=2,ylab="%",font.axis = 4,names.arg =
Restricted$Species,cex.axis = 1.5,cex.names = 1.5,cex.lab=1.5)

#text(seq(1,6,by=1),par("usr")[3]-0.3, srt = 35, adj= 1, xpd = TRUE,labels = Restricted$Species,
cex=1)

Tidal_live=subset(spbarplot,spbarplot$Env=="Tidal flat live",select =c(Species,X.))

barplot(Tidal_live$X.,col="dodgerblue2",ylim=c(0,100),density=30,angle=11,las=2,ylab="%",font.ax
is = 4,names.arg = Tidal_live$Species,cex.axis = 1.5,cex.names = 1.5,cex.lab=1.5)

#text(seq(1,6,by=1),par("usr")[3]-0.3, srt = 35, adj= 1, xpd = TRUE,labels=Tidal_live$Species,
cex=1)

Restricted_live=subset(spbarplot,spbarplot$Env=="Restricted live",select =c(Species,X.))

barplot(Restricted_live$X.,col="darkorange2",ylim=c(0,100),density=30,angle=11,las=2,ylab="%",fo
nt.axis = 4,names.arg = Restricted_live$Species,cex.axis = 1.5,cex.names = 1.5,cex.lab=1.5)

#text(seq(1,6,by=1),par("usr")[3]-0.3, srt = 35, adj= 1, xpd = TRUE,labels = Restricted_live$Species,
cex=1)


#######Figure 2.4 A#########

##################LA DA richness plot without beach and estuary###########

Dead=rowSums(abundanceocc[c(1:13,22:26,32:34),])

Live1=rowSums(abundanceocc[c(14:21,27:31),])

Live=c(rep(0,5),Live1,rep(0,3))

names=envall[c(1:13,22:26,32:34),2]

richnessdf=cbind(as.character(names),Live,Dead)

richnessdf=cbind(env,richnessdf)

richnessdf=richnessdf[-c((1:5),(19:21)),]

richnessdf=as.data.frame(richnessdf)

colorsenv <- c("darkorange2","dodgerblue2")
```

```
attr.envir <- factor(richnessdf$env)

plot(richnessdf$Live,richnessdf$Dead,type="p",pch=19,col=colorsenv[attr.envir],xlim =
c(0,25),ylim=c(0,25),xlab = "Number of species in LA", ylab = "Number of species
DA",cex=1.5,cex.axis=1.5,cex.lab=1.5)

#text(Live,Dead,labels=names,col=colorsenv[richnessdf$env], cex= 1,pos = 3)

abline(a=0, b=1, col = 1, lty=2)


################################################################################################
###################

env=abundancedata[,1:2]

abundanceLD=abundancedata[,4:60]

abundanceLD=t(abundanceLD)

##################Live vs dead relative abundance in each sample#########################

TF1=abundanceLD[1:57,c(1,9)]

TF1=as.data.frame(TF1)

colnames(TF1)=c("Live","Dead")

Livepercent=TF1$Live/ colSums(TF1[1])*100

Deadpercent=TF1$Dead/ colSums(TF1[2])*100

TF1rel=as.data.frame(cbind(Livepercent,Deadpercent))

rownames(TF1rel)=rownames(abundance_species)

plot(TF1rel$Livepercent,TF1rel$Deadpercent)

cor=cor.test(Livepercent,Deadpercent,method = "spearman")

cor$p.value

cor$estimate


TF2=abundanceLD[1:57,c(2,10)]

TF2=as.data.frame(TF2)

colnames(TF2)=c("Live","Dead")

Livepercent=TF2$Live/ colSums(TF2[1])*100

Deadpercent=TF2$Dead/ colSums(TF2[2])*100

TF2rel=as.data.frame(cbind(Livepercent,Deadpercent))

rownames(TF2rel)=rownames(abundance_species)
```

```
plot(TF2rel$Livepercent,TF2rel$Deadpercent)
cor=cor.test(Livepercent,Deadpercent,method = "spearman")
cor$p.value
cor$estimate

TF3=abundanceLD[,c(3,11)]
TF3=as.data.frame(TF3)
colnames(TF3)=c("Live","Dead")
Livepercent=TF3$Live/ colSums(TF3[1])*100
Deadpercent=TF3$Dead/ colSums(TF3[2])*100
TF3rel=as.data.frame(cbind(Livepercent,Deadpercent))
rownames(TF3rel)=rownames(abundance_species)
plot(TF3rel$Livepercent,TF3rel$Deadpercent)
cor=cor.test(Livepercent,Deadpercent,method = "spearman")
cor$p.value
cor$estimate

TF4=abundanceLD[,c(4,12)]
TF4=as.data.frame(TF4)
colnames(TF4)=c("Live","Dead")
Livepercent=TF4$Live/ colSums(TF4[1])*100
Deadpercent=TF4$Dead/ colSums(TF4[2])*100
TF4rel=as.data.frame(cbind(Livepercent,Deadpercent))
rownames(TF4rel)=rownames(abundance_species)
plot(TF4rel$Livepercent,TF4rel$Deadpercent)
cor=cor.test(Livepercent,Deadpercent,method = "spearman")
cor$p.value
cor$estimate

TF5=abundanceLD[,c(5,13)]
TF5=as.data.frame(TF5)
```

```
colnames(TF5)=c("Live","Dead")
Livepercent=TF5$Live/ colSums(TF5[1])*100
Deadpercent=TF5$Dead/ colSums(TF5[2])*100
TF5rel=as.data.frame(cbind(Livepercent,Deadpercent))
rownames(TF5rel)=rownames(abundance_species)
plot(TF5rel$Livepercent,TF5rel$Deadpercent)
cor=cor.test(Livepercent,Deadpercent,method = "spearman")
cor$p.value
cor$estimate

TF6=abundanceLD[,c(6,14)]
TF6=as.data.frame(TF6)
colnames(TF6)=c("Live","Dead")
Livepercent=TF6$Live/ colSums(TF6[1])*100
Deadpercent=TF6$Dead/ colSums(TF6[2])*100
TF6rel=as.data.frame(cbind(Livepercent,Deadpercent))
rownames(TF6rel)=rownames(abundance_species)
plot(TF6rel$Livepercent,TF6rel$Deadpercent)
cor=cor.test(Livepercent,Deadpercent,method = "spearman")
cor$p.value
cor$estimate

TF7=abundanceLD[,c(7,15)]
TF7=as.data.frame(TF7)
colnames(TF7)=c("Live","Dead")
Livepercent=TF7$Live/ colSums(TF7[1])*100
Deadpercent=TF7$Dead/ colSums(TF7[2])*100
TF7rel=as.data.frame(cbind(Livepercent,Deadpercent))
rownames(TF7rel)=rownames(abundance_species)
plot(TF7rel$Livepercent,TF7rel$Deadpercent)
cor=cor.test(Livepercent,Deadpercent,method = "spearman")
```

```
cor$p.value
cor$estimate

TF8=abundanceLD[,c(8,16)]
TF8=as.data.frame(TF8)
colnames(TF8)=c("Live","Dead")
Livepercent=TF8$Live/ colSums(TF8[1])*100
Deadpercent=TF8$Dead/ colSums(TF8[2])*100
TF8rel=as.data.frame(cbind(Livepercent,Deadpercent))
rownames(TF8rel)=rownames(abundance_species)
plot(TF8rel$Livepercent,TF8rel$Deadpercent)
cor=cor.test(Livepercent,Deadpercent,method = "spearman")
cor$p.value
cor$estimate

###############restricted#####################################
RS1=abundanceLD[,c(17,22)]
RS1=as.data.frame(RS1)
colnames(RS1)=c("Live","Dead")
Livepercent=RS1$Live/ colSums(RS1[1])*100
Deadpercent=RS1$Dead/ colSums(RS1[2])*100
RS1rel=as.data.frame(cbind(Livepercent,Deadpercent))
rownames(RS1rel)=rownames(abundance_species)
plot(RS1rel$Livepercent,RS1rel$Deadpercent)
corRS1=cor.test(Livepercent,Deadpercent,method = "spearman")
corRS1$p.value
corRS1$estimate

RS2=abundanceLD[,c(18,23)]
RS2=as.data.frame(RS2)
colnames(RS2)=c("Live","Dead")
```

```
Livepercent=RS2$Live/ colSums(RS2[1])*100
Deadpercent=RS2$Dead/ colSums(RS2[2])*100
RS2rel=as.data.frame(cbind(Livepercent,Deadpercent))
rownames(RS2rel)=rownames(abundance_species)
plot(RS2rel$Livepercent,RS2rel$Deadpercent)
corRS2=cor.test(Livepercent,Deadpercent,method = "spearman")
corRS2$p.value
corRS2$estimate

RS3=abundanceLD[,c(19,24)]
RS3=as.data.frame(RS3)
colnames(RS3)=c("Live","Dead")
Livepercent=RS3$Live/ colSums(RS3[1])*100
Deadpercent=RS3$Dead/ colSums(RS3[2])*100
RS3rel=as.data.frame(cbind(Livepercent,Deadpercent))
rownames(RS3rel)=rownames(abundance_species)
plot(RS3rel$Livepercent,RS3rel$Deadpercent)
corRS3=cor.test(Livepercent,Deadpercent,method = "spearman")
corRS3$p.value
corRS3$estimate

RS4=abundanceLD[,c(20,25)]
RS4=as.data.frame(RS4)
colnames(RS4)=c("Live","Dead")
Livepercent=RS4$Live/ colSums(RS4[1])*100
Deadpercent=RS4$Dead/ colSums(RS4[2])*100
RS4rel=as.data.frame(cbind(Livepercent,Deadpercent))
rownames(RS4rel)=rownames(abundance_species)
plot(RS4rel$Livepercent,RS4rel$Deadpercent)
corRS4=cor.test(Livepercent,Deadpercent,method = "spearman")
corRS4$p.value
```

```
corRS4$estimate


RS5=abundanceLD[,c(21,26)]
RS5=as.data.frame(RS5)
colnames(RS5)=c("Live","Dead")
Livepercent=RS5$Live/ colSums(RS5[1])*100
Deadpercent=RS5$Dead/ colSums(RS5[2])*100
RS5rel=as.data.frame(cbind(Livepercent,Deadpercent))
rownames(RS5rel)=rownames(abundance_species)
plot(RS5rel$Livepercent,RS5rel$Deadpercent)
corRS5=cor.test(Livepercent,Deadpercent,method = "spearman")
corRS5$p.value
corRS5$estimate

#######################Figure 2.4B################################################
env=abundancedata[,1:2]
abundanceLD=abundancedata[6:31,4:60]
abund=as.data.frame(t(abundanceLD))
Dead=as.data.frame(rowSums(abund[,c(1:8,17:21)]))
Live=as.data.frame(rowSums(abund[,c(9:16,22:26)]))
abundance_species=cbind(Live,Dead)
colnames(abundance_species)=c("Live","Dead")
Livepercent=abundance_species$Live/ colSums(abundance_species[1])*100
Deadpercent=abundance_species$Dead/ colSums(abundance_species[2])*100
rel_abundance=cbind(Livepercent,Deadpercent)
rownames(rel_abundance)=rownames(abundance_species)
write.csv(rel_abundance,file = "rel_abundance.csv")
rel_abundance=read.csv("rel_abundance.csv",header = T)
pchs=c(16,17)

```

```
rel_abundance$Class=factor(rel_abundance$X)

plot(rel_abundance$Livepercent,rel_abundance$Deadpercent,xlim=c(0.01, 10^2), ylim=c(0.01,
10^2),log="xy",xlab="Live abundance (%)", ylab="Dead abundance (%)",
col=c("red","blue"),yaxt="n",xaxt="n",cex=1.5,cex.axis=1.5,cex.lab=1.5,pch=c(16,17),asp = 1)

#text(Livepercent,Deadpercent,labels=rownames(rel_abundance),cex= 0.7,pos = 4)

#legend("bottomright",legend = c("Bivalve","Gastropod"),cex=0.7,pch = c(16,17),bty="n")

at.x=c(0,0.01,0.1,1,10,100)

at.y=c(0,0.01,0.1,1,10,100)

#lab.y <- ifelse(log10(at.y) %% 1 == 0, at.y, NA)

lab.x=c(0,0.01,0.1,1,10,100)

lab.y=c(0,0.01,0.1,1,10,100)

axis(1, at=at.x, labels=lab.x, las=1,cex.lab=1.5,cex.axis=1.5)

axis(2, at=at.y, labels=lab.y, las=1,cex.lab=1.5,cex.axis=1.5)

abline(a=0, b=1, col = 1, lty=2)

cor=cor.test(Livepercent,Deadpercent)

cor$p.value

cor$estimate


###############Figure 2.5#######################

####################Calculating shared species between live and dead for all
sites#####################################################

sharedTF1=length(which(colSums(abundanceocc[c(6,14),])==2))

sharedTF2=length(which(colSums(abundanceocc[c(7,15),])==2))

sharedTF3=length(which(colSums(abundanceocc[c(8,16),])==2))

sharedTF4=length(which(colSums(abundanceocc[c(9,17),])==2))

sharedTF5=length(which(colSums(abundanceocc[c(10,18),])==2))

sharedTF6=length(which(colSums(abundanceocc[c(11,19),])==2))

sharedTF7=length(which(colSums(abundanceocc[c(12,20),])==2))

sharedTF8=length(which(colSums(abundanceocc[c(13,21),])==2))

sharedRS1=length(which(colSums(abundanceocc[c(22,27),])==2))

sharedRS2=length(which(colSums(abundanceocc[c(23,28),])==2))

sharedRS3=length(which(colSums(abundanceocc[c(24,29),])==2))
```

```
sharedRS4=length(which(colSums(abundanceocc[c(25,30),])==2))
sharedRS5=length(which(colSums(abundanceocc[c(26,31),])==2))
#sharedrestricted=length(which(colSums(abundanceocc[c(22:26),c(27:31)])==10))
Sharedsp=rbind(sharedTF1,sharedTF2,sharedTF3,sharedTF4,sharedTF5,sharedTF6,sharedTF7,shared
TF8,sharedRS1,sharedRS2,sharedRS3,sharedRS4,sharedRS5)
sharedsp_vect=c(rep(0,5),Sharedsp,rep(0,3))
richnessdf=as.data.frame(cbind(Live,Dead,sharedsp_vect))
richnessdf$liveonly=richnessdf$Live-richnessdf$sharedsp_vect
richnessdf$deadonly=richnessdf$Dead-richnessdf$sharedsp_vect
subsrichness=richnessdf[6:18,]

par(mfrow=c(1,2))
par(mar=c(20,5,1,0.5))

env1=c(rep("Tidal flat",8),rep("Restricted",5))
subsrichness=cbind(env1,subsrichness)
subsrichness=as.data.frame(subsrichness)

###############calculating F1 and F2
index############################################################
subsrichness$F1=(subsrichness$sharedsp_vect*100)/(subsrichness$liveonly+subsrichness$sharedsp_
vect)
subsrichness$F2=(subsrichness$sharedsp_vect*100)/(subsrichness$deadonly+subsrichness$sharedsp_
vect)
subsrichness=cbind(names[6:18],subsrichness)
row.names(subsrichness)=subsrichness$`names[6:18]`
subsrichness=subsrichness[,-1]
mean(subsrichness$F1)
mean(subsrichness$F2)
colorsenv <- c("darkorange2","dodgerblue2")
plot(subsrichness$Live,subsrichness$F1,col=colorsenv[subsrichness$env1],ylab = "% of LA species
in DAs",xlab="Live S",cex=1.5,pch=16,cex.axis=1.5,cex.lab=1.5)
text(subsrichness$Live,subsrichness$F1,labels=row.names(subsrichness), cex= 0.7,pos = 4)
```

```
plot(subsrichness$Dead,subsrichness$F2,col=colorsenv[subsrichness$env1],ylab = "% of DA species
in LAs",xlab="Dead S",cex=1.5,pch=16,cex.axis=1.5,cex.lab=1.5)
text(subsrichness$Dead,subsrichness$F2,labels=row.names(subsrichness), cex= 0.7,pos = 4)

######################PIE SOURCE CODE####################
#' Calculate probability of interspecific encounter (PIE)
#'
#'  \code{calc_PIE} returns the probability of interspecific  encounter (PIE)
#'  which is also known as Simpson's evenness index and Gini-Simpson index. For
\code{ENS=TRUE},
#'  PIE will be converted to an asymptotic effective number of species (S_PIE).
#'
#' data(inv_comm)
#' calc_PIE(inv_comm)
#' calc_PIE(inv_comm, ENS=TRUE)
calc_PIE = function(x, ENS=FALSE) {
  if (class(x) == 'mob_in') {
    x = x_mob_in$comm
  }
  x = drop(as.matrix(x))
  if (any(x < 0, na.rm = TRUE))
    stop("input data must be non-negative")
  if (length(dim(x)) > 1) {
    total = apply(x, 1, sum)
    S = apply(x, 1, function(x) return(sum(x > 0)))
    x = sweep(x, 1, total, "/")
  } else {
    total = sum(x)
    S = sum(x > 0)
    x = x / total
  }
  x = x * x
```

```
    if (length(dim(x)) > 1) {
      H = rowSums(x, na.rm = TRUE)
    } else {
      H = sum(x, na.rm = TRUE)
    }
    # calculate PIE without replacement (for total >= 2)
    H = ifelse(total < 2, NA, (total / (total - 1) * (1 - H)))
    if (ENS) {
      # convert to effective number of species (except for PIE == 1)
      H = ifelse(H==1| S == total, NA, (1/ (1-H)))
    }
    return(H)
  }
  par(mfrow=c(1,2))
  par(mar=c(20,4.5,0.5,0.5))

  ############Figure 2.6#################################
  ###################Probability of intraspecific encounter###################
  envvector=c(rep("Beach",5),rep("Tidal flat",16),rep("Restricted",10),rep("Estuary",3))
  abundancedata=cbind(envvector,abundancedata)
  abundanceTR=subset(abundancedata,select = c(5:60),envvector=="Tidal
  flat"|envvector=="Restricted")
  TF1=calc_PIE(abundanceTR[c(6,14),])
  TF2=calc_PIE(abundanceTR[c(7,15),])
  TF3=calc_PIE(abundanceTR[c(8,16),])
  TF4=calc_PIE(abundanceTR[c(9,17),])
  TF5=calc_PIE(abundanceTR[c(10,18),])
  TF6=calc_PIE(abundanceTR[c(11,19),])
  TF7=calc_PIE(abundanceTR[c(12,20),])
  TF8=calc_PIE(abundanceTR[c(13,21),])
  RS1=calc_PIE(abundanceTR[c(22,27),])
```

```
RS2=calc_PIE(abundanceTR[c(23,28),])
RS3=calc_PIE(abundanceTR[c(24,29),])
RS4=calc_PIE(abundanceTR[c(25,30),])
RS5=calc_PIE(abundanceTR[c(26,31),])
PIEtable=as.data.frame(rbind(TF1,TF2,TF3,TF4,TF5,TF6,TF7,TF8,RS1,RS2,RS3,RS4,RS5))
PIEtable[is.na(PIEtable)] <- 0
env2=c(rep("Tidal flat",8),rep("Restricted",5))
PIEtable=cbind(env2,PIEtable)
PIEtable=as.data.frame(PIEtable)
colorsenv <- c("darkorange2","dodgerblue2")
plot(PIEtable$`11`,PIEtable$`19`,col=colorsenv[PIEtable$env2],xlab="Dead PIE",ylab="Live
PIE",xlim =c(0,1),ylim=c(0,1),cex=1.5,cex.lab=1.5,cex.axis=1.5,pch=16)
text(PIEtable$`11`,PIEtable$`19`,col=colorsenv[PIEtable$env2],labels=row.names(PIEtable), cex=
1.25,pos = 4)
abline(a=0, b=1, col = 1,lty=2)
cor.test(PIEtable$`11`,PIEtable$`19`,method = "spearman")
################Calculating deltaPIE###############
dPIE=as.numeric(as.character(PIEtable$`11`))
lPIE=as.numeric(as.character(PIEtable$`19`))
PIEtable$delPIE=dPIE-lPIE

######Calculating deltaS=(log10(deadS)-log10(liveS))##########
richnessdfTR=richnessdf[6:18,]
#rownames(richnessdfTR)=richnessdfTR[,2]
#richnessdfTR=richnessdfTR[,-1]
#colnames(richnessdfTR)=c("env","L","D")
richnessdfTR=as.data.frame(richnessdfTR)
D=as.numeric(as.character(richnessdfTR$D))
L=as.numeric(as.character(richnessdfTR$L))
richnessdfTR$delS=log10(D)-log10(L)

########plot delPIE vs delS############
```

```
env2=c(rep("Tidal flat",8),rep("Restricted",5))
richnessdfTR=cbind(env2,richnessdfTR)
richnessdfTR=as.data.frame(richnessdfTR)
colorsenv <- c("darkorange2","dodgerblue2")
plot(richnessdfTR$delS,PIEtable$delPIE,col=colorsenv[richnessdfTR$env2],xlab =
expression(paste(Delta,"S")),ylab =
expression(paste(Delta,"PIE")),cex=1.5,cex.lab=1.5,cex.axis=1.5,pch=16)
text(richnessdfTR$delS,PIEtable$delPIE,col=colorsenv[PIEtable$env2],labels=row.names(PIEtable),
cex= 1.25,pos = 1,offset = 0.2)
abline(v=0.55,lty=1)
abline(h=0.0,lty=1)
cor.test(richnessdfTR$delS,PIEtable$delPIE,method = "spearman")

##################Figure 2.8##############################
################Creating a data frame with seasonal and environmental data for
NMDS############
abundancedata=read.csv("abundance30.4.19.csv", header = T)
abundancedatanew=abundancedata
abundancedatanew=abundancedata[-4,]#####remove B4 locality as it has only 3 specimen##
abundanceallnew=abundanceall[-4,]
abundancedeadnew=abundancedead[-4,]#####remove B4 locality as it has only 3 specimen##
abundancedeadTR=abundancedeadnew[-(1:4),]####deadabundancefor only tidal and
restricted#######
abundancedeadTR=abundancedeadTR[-(14:16),]
season=abundancedatanew[,3]
sites=abundancedatanew[,2]
env=c(rep("Beach",4),rep("Tidal flat",8),rep("Tidal flat live",8),rep("Restricted",5),rep("Restricted
live",5),rep("Estuary",3))
attribute=data.frame(season,sites,env)

par(mar=c(3,5,0.25,0.25))
par(mfrow=c(2,2))
par(pty="s")
```

```
####Figure 2.8A#####################

########################################NMDS of live and dead with seasonal variation#####################

attr.envir <- factor(attribute$env)

div.mds=metaMDS(abundanceallnew, distance = "bray", trace = FALSE)

div.mds

#pchs<- c(4,5,6,7,8,9)

pchs<- c(15,23,17,2,19,1)

col.season <- c("deeppink", "green4", "darkorange2","darkorange2","dodgerblue2","dodgerblue2")

plot(div.mds, type="n",display="sites",xlim=c(-3,5),ylim=c(-3,5),cex=1.5, cex.lab=1,cex.axis=1)

points(div.mds, display="sites", pch=pchs[attr.envir], col = col.season[attr.envir],bg = "green4",cex=1.5,cex.lab=1,cex.axis=1)

treat=c(rep("Treatment1",4),rep("Treatment2",8),rep("Treatment3",8),rep("Treatment4",5),rep("Treatment1",5),rep("Treatment2",3))

ordihull(div.mds,groups=treat,draw="lines",col="grey62",label=F,border=NULL)

#########Figure 2.8B##############

#####################NMDS of live#################################################

attributelive=attribute[c(13:20,26:30),]

#attr.season <- factor(attributelive$season)

attr.envir2 <- factor(attributelive$env)

div.mds=metaMDS(abundancelive, distance = "bray", trace = FALSE)

div.mds

pchs<- c(2,1)

col.season <- c("darkorange2", "dodgerblue2")

plot(div.mds, type="n",display="sites",xlim=c(-3,5),ylim=c(-3,5),cex=1.5,cex.lab=1,cex.axis=1)

points(div.mds, display="sites", pch=pchs[attr.envir2], col = col.season[attr.envir2],cex=1.5)

treat=c(rep("Treatment3",8),rep("Treatment1",5))

ordihull(div.mds,groups=treat,draw="lines",col="grey62",label=F)
```

```
#############Figure 2.8C#############################################################

########################Nmds
dead#####################################################

attributedead=attribute[c(1:12,21:25,31:33),]

#attr.season <- factor(attributedead$season)

attr.envir1 <- factor(attributedead$env)

div.mds=metaMDS(abundancedeadnew, distance = "bray", trace = FALSE)

div.mds

pchs<- c(15,23,17,19)

col.season <- c("deeppink", "green4", "darkorange2","dodgerblue2")

plot(div.mds, type="n",display="sites",xlim=c(-3,5),ylim=c(-3,5),cex=1.5,cex.lab=1,cex.axis=1)

points(div.mds, display="sites", pch=pchs[attr.envir1], col = col.season[attr.envir1],bg =
"green4",cex=1.5)

treat=c(rep("Treatment1",4),rep("Treatment2",8),rep("Treatment4",5),rep("Treatment2",3))

ordihull(div.mds,groups=treat,draw="lines",col="grey62",label=F)


#######Figure 2.8D#########################################

#########################NMDS dead only tidal and restricted#################

attributedead2=attribute[c(5:12,21:25),]

#attr.season <- factor(attributedead$season)

attr.envir1 <- factor(attributedead2$env)

div.mds=metaMDS(abundancedeadTR, distance = "bray", trace = FALSE)

div.mds

pchs<- c(17,19)

col.season <- c("darkorange2","dodgerblue2")

plot(div.mds, type="n",display="sites",xlim=c(-3,5),ylim=c(-3,5),cex=1.5,cex.lab=1,cex.axis=1)

points(div.mds, display="sites", pch=pchs[attr.envir1], col = col.season[attr.envir1],bg =
"green4",cex=1.5)

treat=c(rep("Treatment2",8),rep("Treatment4",5))

ordihull(div.mds,groups=treat,draw="lines",col="grey62",label=F)

#########Figure 2.12 C#############################################################

distdata=read.csv("geographic vs pairwisedist occ - Copy.csv",header = T)
```

```
rownames(distdata)=distdata[,1]

plot(distdata$Geographic.Distance.km.,distdata$Pairwise.distance.bray.,xlab = "Geographic distance
(km)",ylab = "Pairwise distance (Bray
Curtis)",ylim=c(0.60,1.1),pch=16,cex=1.5,cex.lab=1.5,cex.axis=1.5)

text(distdata$Geographic.Distance.km.,distdata$Pairwise.distance.bray.,labels = rownames(distdata),
cex= 1,pos = 3)

distdata=distdata[,-1]

plot(distdata$Geographic.Distance.km.,distdata$Pairwise.distance.euclidean.,xlab = "Geographic
distance (km)",ylab = "Pairwise distance
(Euclidean)",ylim=c(0,58),pch=16,cex=1.5,cex.lab=1.5,cex.axis=1.5)

text(distdata$Geographic.Distance.km.,distdata$Pairwise.distance.euclidean.,labels =
rownames(distdata), cex= 1,pos = 3)

div.ch=as.matrix(vegdist(occeastchandi,"eucl"))

div.ch.bray=as.matrix(vegdist(occeastchandi,"bray"))

cor.test(distdata$Pairwise.distance.bray.,distdata$Geographic.Distance.km.,method = "spearman")

distSE=distdata[7:15,]

plot(distSE$Pairwise.distance.bray.,distSE$Geographic.Distance.km.,ylab = "Geographic distance
(km)",xlab = "Pairwise distance (Bray Curtis)",pch=19,cex=1.5,cex.lab=1,cex.axis=1)

text(distSE$Pairwise.distance.bray.,distSE$Geographic.Distance.km.,labels = distSE$X, cex= 1.5,pos
= 3)

cor.test(distSE$Pairwise.distance.bray.,distSE$Geographic.Distance.km.,method = "spearman")

barplot(distdata$Bray.curtis.similarity,horiz = T,names.arg =
c("8","9","10","11","12","13","14","15","16","17","18","19","20","21"),col="paleturquoise4",
xlab="Bray Curtis similarity",ylab="Latitude",cex.axis = 1.15,cex.names = 1.15,cex.lab=1.15)


#######Figure 2.S1######################

####Size distribution and normalcy test (shapiro-wilk test) of the live species that have also been
found in DA#######

####################cerethium normalcy test#################

library(moments)

mydatalive=read.csv("live measurement - Copy.csv",header=T)###after including subronils
measurements###

cerethium=mydata[ which(mydata$Species=="Cerethium sp1"),]

plot(density(cerethium$L),main=substitute(paste(italic("Pirenella cingulata"),"
(N=36)")),xlim=c(0,25),xlab = "L (mm)")

shapiro.test(cerethium$L)
```

```
skewness(cerethium$L)
######################
tigrina=mydatalive[which(mydatalive$Species=="Notocochlis tigrina"),]
hist(tigrina$L,main=substitute(paste(italic("Paractectonatica tigrina")," (N=45)")),xlim=c(0,25),xlab =
"L (mm)")
shapiro.test(tigrina$L)
skewness(tigrina$L)
##############################
nassarius=mydatalive[which(mydatalive$Species=="Nassarius reticulatus"),]
hist(nassarius$L,main=substitute(paste(italic("Nassarius jacksonianus"),"
(N=45)")),xlim=c(0,25),xlab = "L (mm)")
shapiro.test(nassarius$L)
skewness(nassarius$L)
##################################
Dosinia=mydatalive[which(mydatalive$Species=="Dosinia sp2"),]
hist(Dosinia$L,main=substitute(paste(italic("Dosinia sp2")," (N=22)")),xlab = "L (mm)")
shapiro.test(Dosinia$L)
skewness(Dosinia$L)
#####################################
meretrix=mydatalive[which(mydatalive$Species=="Meretrix meretrix"),]
hist(meretrix$L,main=substitute(paste(italic("Meretrix meretrix")," (N=22)")),xlab = "L (mm)")
shapiro.test(meretrix$L)
skewness(meretrix$L)
#########################################
polynices=mydatalive[which(mydatalive$Species=="Polynices didyma"),]
hist(polynices$L,main=substitute(paste(italic("Neverita didyma")," (N=20)")),xlab = "L (mm)")
shapiro.test(polynices$L)
skewness(meretrix$L)
###################################################
meretrixsp1=mydatalive[which(mydatalive$Species=="Meretrix sp1"),]
hist(meretrixsp1$L,main=substitute(paste(italic("Meretrix sp1")," (N=14)")),xlab = "L (mm)")
shapiro.test(meretrixsp1$L)
```

```
579  ######################################################
580  cardiumsp1=mydatalive[which(mydatalive$Species=="Cardium sp1"),]
581  hist(cardiumsp1$L,main=substitute(paste(italic("Timoclea imbricata")," (N=20)")),xlim=c(4,14),xlab
582  = "L (mm)")
583  shapiro.test(cardiumsp1$L)
584  ######################################################
585  murexsp1=mydatalive[which(mydatalive$Species=="Muricidae sp1"),]
586  hist(murexsp1$L,main=substitute(paste(italic("Murex sp1")," (N=15)")),xlab = "L (mm)")
587  shapiro.test(murexsp1$L)
588  #########code for generating a simulated species-specific SFD after confirming normality of each
589  species SFD for LA####
590  mydata=read.csv("live measurement.csv",header=T)
591  species1=mydata$Species
592  L=mydata$L
593  W=mydata$W
594  mydata1=read.csv("live individual1.csv",header=F)
595  Individuals=mydata1$V2
596  #mydata1=mydata1[-7,]
597  x=c("Cerethium sp1","Notocochlis tigrina","Nassarius reticulatus","Dosinia sp2","Polynices
598  didyma","Natica lineata","Meretrix meretrix","Cardium sp1","Muricidae sp1", "Muricidae
599  sp2","Meretrix sp1",      "Bivalve sp1", "Bivalve sp2")
600  #w=array(0,dim=c(length(x),1))
601  final=c(0,0,0)
602  final=t(as.matrix(final))
603  colnames(final) <- c("c1","L","W")
604  i=0;
605  install.packages("truncnorm")
606  require(truncnorm)
607  for(val in x)
608  {
609    #i=i+1
610    c1=c( )
```

```
611     spsubset=subset(mydata,species1==val,select = c(L,W))
612     Length=spsubset$L
613     Width=spsubset$W
614     plot(Length,Width)
615     mg=lm(Width~Length)
616     C=coefficients(mg)
617     n=dim(spsubset)
618     n=n[1]
619     m=mydata1[which(mydata1[,1]==val),2]
620     if(m>n)
621     {
622       g=m-n
623       g
624       L=rtruncnorm(g, a=min(Length), b=max(Length), mean=mean(Length), sd=sd(Length))
625       W=C[1]+C[2]*L
626       matrix=cbind(L,W)
627       final1=rbind(matrix,spsubset)
628       k=dim(final1)
629       k=k[1]
630       c1[1:k] = val
631       final1=cbind(c1,final1)
632     }
633     else{
634       final1=spsubset
635       k=dim(final1)
636       k=k[1]
637       c1[1:k] = val
638       final1=cbind(c1,final1)
639     }
640     final=rbind(final,final1)
641   }
```

```
final=final[-1,]
final=final[,-1]

#write.table(final,file="livegenerated2019.csv")

############Figure 2.S1#####################
#########################################################
cerethium=mydata[which(mydata$Species=="Cerethium sp1"),]
notocochlis=mydata[which(mydata$Species=="Notocochlis tigrina"),]
nassarius=mydata[which(mydata$Species=="Nassarius reticulatus"),]
dosinia=mydata[which(mydata$Species=="Dosinia sp2"),]
polynices=mydata[which(mydata$Species=="Polynices didyma"),]
meretrix=mydata[which(mydata$Species=="Meretrix meretrix"),]
meresp1=mydata[which(mydata$Species=="Meretrix sp1"),]
cardium=mydata[which(mydata$Species=="Cardium sp1"),]
murexsp1=mydata[which(mydata$Species=="Muricidae sp1"),]
murexsp2=mydata[which(mydata$Species=="Muricidae sp2"),]
murexsp1=rbind(murexsp1,murexsp2)
natica=mydata[which(mydata$Species=="Natica lineata"),]
#########################################################
plot(mfrow=c(3,3))
par(mar=c(2,4,2,1))
mai = c(1, 0.1, 0.1, 0.1)
par(mfrow=c(3,3),mai = c(0.4, 0.1, 0.1, 0.1))
plot(density(cerethium$L),main=substitute(paste(italic("Pirenella cingulata"))),xlab = " ")
plot(density(notocochlis$L),main=substitute(paste(italic("Paractectonatica tigrina"))),xlab = "
",ylab=" ")
plot(density(nassarius$L),main=substitute(paste(italic("Nassarius jacksonianus"))),xlab = " ",ylab="
")
plot(density(dosinia$L),main=substitute(paste(italic("Dosinia")," sp2")),xlab = " ")
plot(density(meretrix$L),main=substitute(paste(italic("Meretrix meretrix"))),xlab = " ",ylab=" ")
plot(density(polynices$L),main=substitute(paste(italic("Neverita didyma"))),xlab = " ",ylab=" ")
```

```
plot(density(meretrixsp1$L),main=substitute(paste(italic("Meretrix")," sp1")),xlab = "L (mm)")

plot(density(cardiumsp1$L),main=substitute(paste(italic("Timoclea imbricata"))),xlab = "L
(mm)",ylab=" ")

plot(density(murexsp1$L),main=substitute(paste(italic("Murex")," sp1")),xlab = "L (mm)",ylab=" ")


######################Figure 2.9################################

################################box plot for shell size
summary################################################

par(pty="s")

beachdead=read.delim("beachnewfinal.csv",header = F)

estuarydead=read.delim("deadestuarynew.txt",header = F)

restricdead=read.delim("deadrestricted.txt",header = F)

tidaldead=read.delim("deadtidalnew.txt",header = F)

restrictlive=read.delim("restriclivemeasure.txt", header=F)

tidallive=read.delim("tidallive.txt",header=F)


Beach=cbind((rep("Beach",239)),beachdead)

colnames(Beach)<-c("Env","Size")

Tidalflat=cbind((rep("Tidal flat",406)),tidaldead)

colnames(Tidalflat)<-c("Env","Size")

Restricted=cbind((rep("Restricted",185)),restricdead)

colnames(Restricted)<-c("Env","Size")

Estuary=cbind((rep("Estuary",84)),estuarydead)

colnames(Estuary)<-c("Env","Size")

Restrictedlive=cbind((rep("Restricted live",38)),restrictlive)

colnames(Restrictedlive)<-c("Env","Size")

Tidalflatlive=cbind((rep("Tidal flat live",121)),tidallive)

colnames(Tidalflatlive)<-c("Env","Size")

sizedf=rbind(Beach,Tidalflat,Tidalflatlive,Restricted,Restrictedlive,Estuary)

plot(sizedf$Env,sizedf$Size,col=c("deeppink",
"dodgerblue2","dodgerblue2","darkorange2","darkorange2","green4"),names = c("Beach", " ", "Tidal
flat", "", "Restricted", "Estuary"),ylab=expression('log '[2]*'(size)'),cex.lab=1.5,cex.axis=1.5,cex=1.5)
```

```
#sizedf2=write.csv(sizedf,"sizedf.csv")

sizedf3=read.csv("sizedf.csv",header = T)

require(ggplot2)

names=c("Beach DA", "Tidal flat DA", "Tidal flat LA", "Restricted DA", "Restricted LA","Estuary
DA")

ggplot(sizedf3, aes(Env, Size,
gcoroup=factor(sizedf3$Env),fill=factor(sizedf3$Env)))+scale_fill_manual(values = c("deeppink",
"dodgerblue2","dodgerblue2","darkorange2","darkorange2","green4")) +
scale_x_discrete(labels=c("Beach DA", "Tidal flat DA", "Tidal flat LA", "Restricted DA", "Restricted
LA","Estuary DA"))+ geom_boxplot() +xlab("Environment")+ ylab(expression('log
'[2]*'(size)'))+theme(panel.grid.major = element_blank(), panel.grid.minor =
element_blank(),panel.background = element_blank())+theme(legend.position =
"none",aspect.ratio=1,panel.border = element_rect(colour = "black", fill=NA, size=0.75))+
theme(axis.text.x = element_text(angle = 90, vjust = 0.5, hjust=1))+theme(strip.text.x =
element_text(size = 27, face = "bold"),strip.text.y = element_text(size = 27, face = "bold"
))+theme(axis.title =  element_text(size = 25))+theme(axis.text =  element_text(size =
25))+theme(aspect.ratio=1)


###########Figure 2.10#############################

###################Comparison of simulated and actual
dead#################################

beachdead=read.csv("beachnewfinal.csv",header = F)

estuarydead=read.delim("deadestuarynew.txt",header = F)

restricdead=read.delim("deadrestricted.txt",header = F)

tidaldead=read.delim("deadtidalnew.txt",header = F)

#live=read.delim("Livemax.txt",header = F)

livegenerated=read.csv("livegenerated2019.csv",header = F)#file generated from the size live file##


require(seewave)

require(base)

################################Beach################################################

 Dist_beach=array(0,c(10000,1))

 pvalue_beach=array(0,c(10000,1))

 for(i in 1:10000)

 {

  D1=sample(t(livegenerated),239,replace = T)
```

```
  Dist_beach[i]=ks.test(t(beachdead),as.matrix(D1))$statistic
  pvalue_beach[i]=ks.test(t(beachdead),as.matrix(D1))$p.value
 }
 pvalue_beach
 Dist_beach
 summary(Dist_beach)

#######################Estuary#################################
 Dist_estuary=array(0,c(10000,1))
 pvalue_estuary=array(0,c(10000,1))
 for(i in 1:10000)
 {
  D1=sample(t(livegenerated),84,replace = T)
  Dist_estuary[i]=ks.test(t(estuarydead),as.matrix(D1))$statistic
  pvalue_estuary[i]=ks.test(t(estuarydead),as.matrix(D1))$p.value
 }
 pvalue_estuary
 Dist_estuary
 summary(Dist_estuary)
 ###################################Tidal flat#############################
 Dist_tidal=array(0,c(10000,1))
 pvalue_tidal=array(0,c(10000,1))
 for(i in 1:10000)
 {
  D1=sample(t(livegenerated),406,replace = T)
  Dist_tidal[i]=ks.test(t(tidaldead),as.matrix(D1))$statistic
  pvalue_tidal[i]=ks.test(t(tidaldead),as.matrix(D1))$p.value
 }
 pvalue_tidal
 Dist_tidal
 summary(Dist_tidal)
```

```
###################################restricted##############################
 Dist_rest=array(0,c(10000,1))
 pvalue_rest=array(0,c(10000,1))
 for(i in 1:10000)
 {
  D1=sample(t(livegenerated),185,replace = T)
  Dist_rest[i]=ks.test(t(restricdead),as.matrix(D1))$statistic
  pvalue_rest[i]=ks.test(t(restricdead),as.matrix(D1))$p.value
 }
 pvalue_rest
 Dist_rest
 summary(Dist_rest)

################################Setting a cutoff size for each
env##############################################
#####################Estuary#########################
 Dist_estuary1=array(0,c(10000,1))
 pvalue_estuary1=array(0,c(10000,1))
 live_filtered = livegenerated[which(livegenerated<4),1]
 for(i in 1:10000)
 {
  D2=sample(live_filtered,84,replace = T)
  Dist_estuary1[i]=ks.test(t(estuarydead),as.matrix(D2))$statistic
  pvalue_estuary1[i]=ks.test(t(estuarydead),as.matrix(D2))$p.value
 }
 pvalue_estuary1
 Dist_estuary1
 summary(Dist_estuary1)

###########################################restricted###################
 Dist_rest1=array(0,c(10000,1))
```

```
pvalue_rest1=array(0,c(10000,1))
live_filtered_restric = livegenerated[which(livegenerated<4.6),1]
for(i in 1:10000)
{
 D2=sample(live_filtered_restric,185,replace = T)
 Dist_rest1[i]=ks.test(t(restricdead),as.matrix(D2))$statistic
 pvalue_rest1[i]=ks.test(t(restricdead),as.matrix(D2))$p.value
}
pvalue_rest1
Dist_rest1
summary(Dist_rest1)

################histograms#############################################################
par(mar=c(4,4,2,2))
par(mfrow=c(3,2))
p1=hist(Dist_beach,breaks = 7)
p2=hist(Dist_tidal,breaks = 12)
p3=hist(Dist_estuary,breaks =19)
p4=hist(Dist_rest)
p13=hist(Dist_estuary1)
 p16=hist(Dist_rest1)
plot(p1,w=10,col=c("deeppink"),xlim = c(0.2,1),ylim = c(0,5000),cex.axis=1.5,ann=FALSE)

plot(p2,col=c("dodgerblue2"),xlim = c(0.2,1),ylim = c(0,5000),cex.axis=1.5,ann=FALSE)
plot(p4,col=c("darkorange2"),xlim = c(0.2,1),ylim = c(0,5000),cex.axis=1.5,ann=FALSE)
 plot(p3,col=c("green4"),xlim = c(0.2,1),ylim = c(0,5000),cex.axis=1.5,ann=FALSE)
plot(p16,col=c("darkorange2"),xlim = c(0.2,1),ylim = c(0,5000),density=50,angle =
30,cex.axis=1.5,ann=FALSE)
 plot(p13,col=c("green4"),xlim = c(0.2,1),ylim = c(0,5000),density=50,angle =
30,cex.axis=1.5,ann=FALSE)
############Figure 2.S2#########################################
 #######Shared species LD simulation ##################
```

```
836     mydata=read.csv("livemeasurementshared.csv",header=T)
837     species1=mydata$Species
838     L=mydata$L
839     W=mydata$W
840     mydata1=read.csv("liveindividualshared.csv",header=F)
841     Individuals=mydata1$V2
842     #mydata1=mydata1[-7,]
843     x=c("Cerethium sp1","Notocochlis tigrina","Nassarius reticulatus","Dosinia sp2","Meretrix
844   meretrix","Cardium sp1","Murex sp1","Meretrix sp1","Polynices didyma")
845     #w=array(0,dim=c(length(x),1))
846     final=c(0,0,0)
847     final=t(as.matrix(final))
848     colnames(final) <- c("c1","L","W")
849     i=0;
850     #install.packages("truncnorm")
851     require(truncnorm)
852     for(val in x)
853     {
854       #i=i+1
855       c1=c( )
856       spsubset=subset(mydata,species1==val,select = c(L,W))
857       Length=spsubset$L
858       Width=spsubset$W
859       plot(Length,Width)
860       mg=lm(Width~Length)
861       C=coefficients(mg)
862       n=dim(spsubset)
863       n=n[1]
864       m=mydata1[which(mydata1[,1]==val),2]
865       if(m>n)
866       {
```

```
867         g=m-n
868         g
869         L=rtruncnorm(g, a=min(Length), b=max(Length), mean=mean(Length), sd=sd(Length))
870         W=C[1]+C[2]*L
871         matrix=cbind(L,W)
872         final1=rbind(matrix,spsubset)
873         k=dim(final1)
874         k=k[1]
875         c1[1:k] = val
876         final1=cbind(c1,final1)
877       }
878       else{
879         final1=spsubset
880         k=dim(final1)
881         k=k[1]
882         c1[1:k] = val
883         final1=cbind(c1,final1)
884       }
885       final=rbind(final,final1)
886     }
887     final=final[-1,]
888     final=final[,-1]
889
890     #write.table(final,file="livegenerated_shared.csv")
891
892     ###################Comparison of simulated and actual
893   dead#################################
894     setwd("F:/Madhura/BACKUP/Madhura/Chandipur/R files")
895     beachdead=read.csv("beachsharednew.csv",header = F)
896     estuarydead=read.csv("estuarysharednew.csv",header = F)
897     restricdead=read.csv("restrictedsharednew.csv",header = F)
```

```
898   tidaldead=read.csv("tidalsharednew.csv",header = F)
899   livegenerated=read.csv("live_generated_shared.csv",header = F)#file generated from the size live
900  file##
901
902   require(seewave)
903   require(base)
904   ################################Beach#################################################
905    Dist_beach=array(0,c(10000,1))
906    pvalue_beach=array(0,c(10000,1))
907    for(i in 1:10000)
908    {
909     D1=sample(t(livegenerated),27,replace = T)
910     Dist_beach[i]=ks.test(t(beachdead),as.matrix(D1))$statistic
911     pvalue_beach[i]=ks.test(t(beachdead),as.matrix(D1))$p.value
912    }
913    pvalue_beach
914    Dist_beach
915    summary(Dist_beach)
916    hist(as.matrix(beachdead))
917   ########################Estuary#################################
918    Dist_estuary=array(0,c(10000,1))
919    pvalue_estuary=array(0,c(10000,1))
920    for(i in 1:10000)
921    {
922     D1=sample(t(livegenerated),20,replace = T)
923     Dist_estuary[i]=ks.test(t(estuarydead),as.matrix(D1))$statistic
924     pvalue_estuary[i]=ks.test(t(estuarydead),as.matrix(D1))$p.value
925    }
926    pvalue_estuary
927    Dist_estuary
928    summary(Dist_estuary)
```

```
929
930  ##################################Tidal flat##############################
931     Dist_tidal=array(0,c(10000,1))
932     pvalue_tidal=array(0,c(10000,1))
933     for(i in 1:10000)
934     {
935       D1=sample(t(livegenerated),123,replace = T)
936       Dist_tidal[i]=ks.test(t(tidaldead),as.matrix(D1))$statistic
937       pvalue_tidal[i]=ks.test(t(tidaldead),as.matrix(D1))$p.value
938     }
939     pvalue_tidal
940     Dist_tidal
941     summary(Dist_tidal)
942     hist(as.matrix(tidaldead))
943     hist(Dist_tidal)
944
945   ######################################restricted############################
946     Dist_rest=array(0,c(10000,1))
947     pvalue_rest=array(0,c(10000,1))
948     for(i in 1:10000)
949     {
950       D1=sample(t(livegenerated),87,replace = T)
951       Dist_rest[i]=ks.test(t(restricdead),as.matrix(D1))$statistic
952       pvalue_rest[i]=ks.test(t(restricdead),as.matrix(D1))$p.value
953     }
954     pvalue_rest
955     Dist_rest
956     summary(Dist_rest)
957
958   ##################################Setting a cutoff size for each
959  env#############################################
```

```
960  ##############################Beach#################################################
961  livebeachfiltered=read.csv("beachbivalvefiltered.csv",header = F)
962
963    Dist_beachbiv=array(0,c(10000,1))
964    pvalue_beachbiv=array(0,c(10000,1))
965    for(i in 1:10000)
966    {
967      D1=sample(t(livebeachfiltered),27,replace = T)
968      Dist_beachbiv[i]=ks.test(t(beachdead),as.matrix(D1))$statistic
969      pvalue_beachbiv[i]=ks.test(t(beachdead),as.matrix(D1))$p.value
970    }
971    pvalue_beachbiv
972    Dist_beachbiv
973    summary(Dist_beachbiv)
974
975  ######################Estuary#########################
976    Dist_estuary1=array(0,c(10000,1))
977    pvalue_estuary1=array(0,c(10000,1))
978    live_filtered = livegenerated[which(livegenerated<4),1]
979    for(i in 1:10000)
980    {
981      D2=sample(live_filtered,20,replace = T)
982      Dist_estuary1[i]=ks.test(t(estuarydead),as.matrix(D2))$statistic
983      pvalue_estuary1[i]=ks.test(t(estuarydead),as.matrix(D2))$p.value
984    }
985    pvalue_estuary1
986    Dist_estuary1
987    summary(Dist_estuary1)
988
989  ######################################Beach#########################
990    Dist_beach1=array(0,c(10000,1))
```

```
pvalue_beach1=array(0,c(10000,1))
live_filtered_beach = livegenerated[which(livegenerated<20),1]
for(i in 1:10000)
{
  D2=sample(t(live_filtered_beach),27,replace = T)
  Dist_beach1[i]=ks.test(t(beachdead),as.matrix(D2))$statistic
  pvalue_beach1[i]=ks.test(t(beachdead),as.matrix(D2))$p.value
}
pvalue_beach1
Dist_beach1
summary(Dist_beach1)

##############################################tidal flat#########################
Dist_tidal1=array(0,c(10000,1))
pvalue_tidal1=array(0,c(10000,1))
live_filtered_tidal = livegenerated[which(livegenerated<12),1]
for(i in 1:10000)
{
  D2=sample(live_filtered_tidal,123,replace = T)
  Dist_tidal1[i]=ks.test(t(tidaldead),as.matrix(D2))$statistic
  pvalue_tidal1[i]=ks.test(t(tidaldead),as.matrix(D2))$p.value
}
pvalue_tidal1
Dist_tidal1
summary(Dist_tidal1)

##############################################restricted#####################
Dist_rest1=array(0,c(10000,1))
pvalue_rest1=array(0,c(10000,1))
live_filtered_restric = livegenerated[which(livegenerated<4.6),1]
for(i in 1:10000)
```

```
1022        {
1023          D2=sample(live_filtered_restric,87,replace = T)
1024          Dist_rest1[i]=ks.test(t(restricdead),as.matrix(D2))$statistic
1025          pvalue_rest1[i]=ks.test(t(restricdead),as.matrix(D2))$p.value
1026        }
1027        pvalue_rest1
1028        Dist_rest1
1029        summary(Dist_rest1)
1030      ##############################################################################
1031       par(mar=c(4,4,2,2))
1032       par(mfrow=c(3,2))
1033       p1=hist(Dist_beach,breaks = 24)
1034       p2=hist(Dist_tidal,breaks = 12)
1035       p3=hist(Dist_estuary,breaks =23)
1036       p4=hist(Dist_rest,breaks = 15)
1037       p13=hist(Dist_estuary1,breaks = 25)
1038       p16=hist(Dist_rest1,breaks = 15)
1039       plot(p1,col=c("deeppink"),xlim = c(0.2,1),ylim = c(0,5000),cex.axis=1.5,ann=FALSE)
1040        plot(p2,col=c("dodgerblue2"),xlim = c(0.2,1),ylim = c(0,5000),cex.axis=1.5,ann=FALSE)
1041        plot(p4,col=c("darkorange2"),xlim = c(0.2,1),ylim = c(0,5000),cex.axis=1.5,ann=FALSE)
1042         plot(p3,col=c("green4"),xlim = c(0.2,1),ylim = c(0,5000),cex.axis=1.5,ann=FALSE)
1043
1044        plot(p16,col=c("darkorange2"),xlim = c(0.2,1),ylim = c(0,5000),density=50,angle =
1045      30,cex.axis=1.5,ann=FALSE)
1046        plot(p13,col=c("green4"),xlim = c(0.2,1),ylim = c(0,5000),density=50,angle =
1047      30,cex.axis=1.5,ann=FALSE)
```

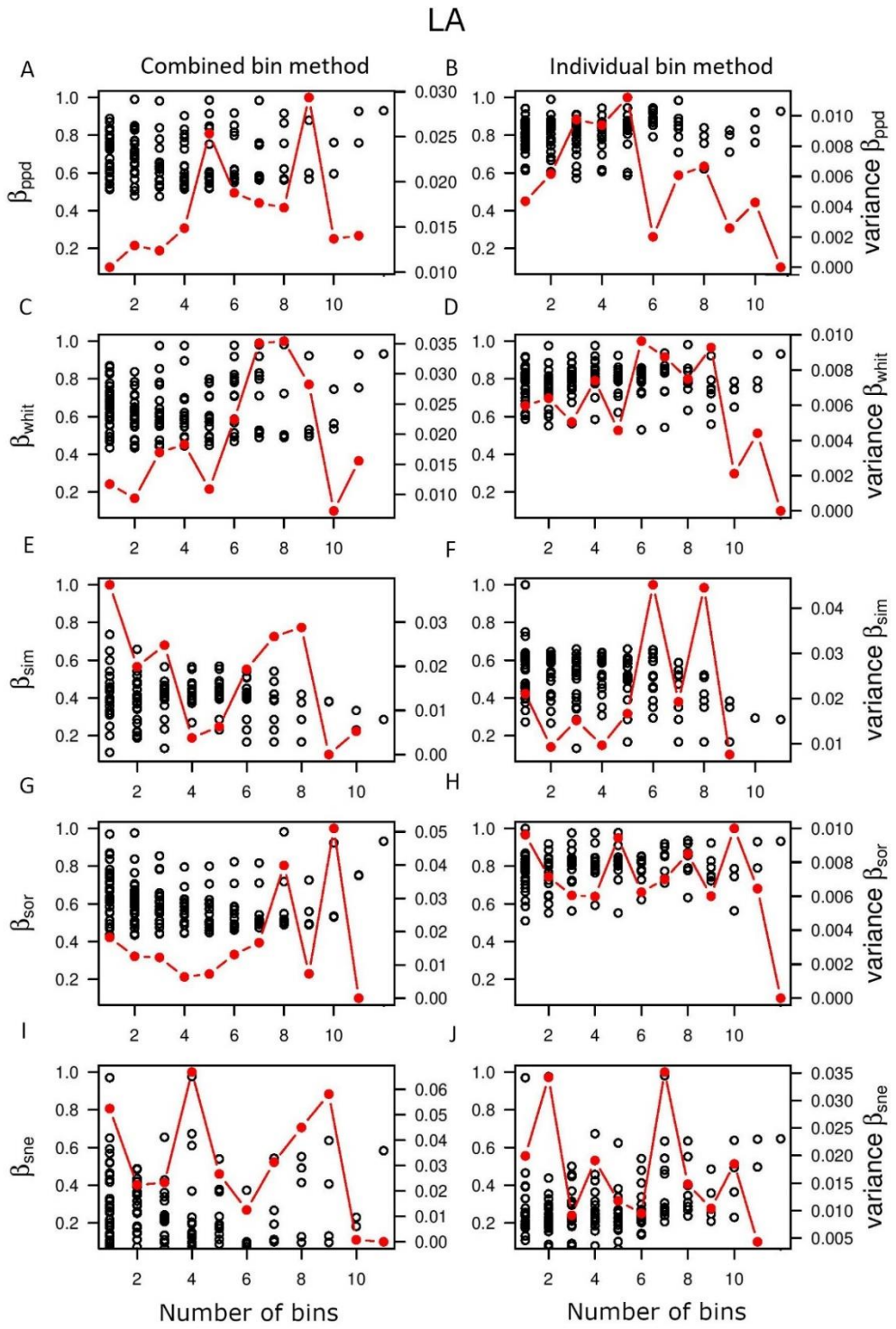

Figure 3.S1: Null model predicted mean (black circles) and variance of beta diversity (red dash) with number of bins based on LA data. The left column represents "combined bin method" and the right column represents "individual bin method". The indices of beta diversity used here include Bray-Curtis (β_{ppd}) (A-B), Whittaker index (β_{whit}) (C-D), Simpson index (β_{sim}) (E-F), Sorenson index (β_{sor}) (G-H), Nestedness component of Sorenson (β_{sne}) (I-J).

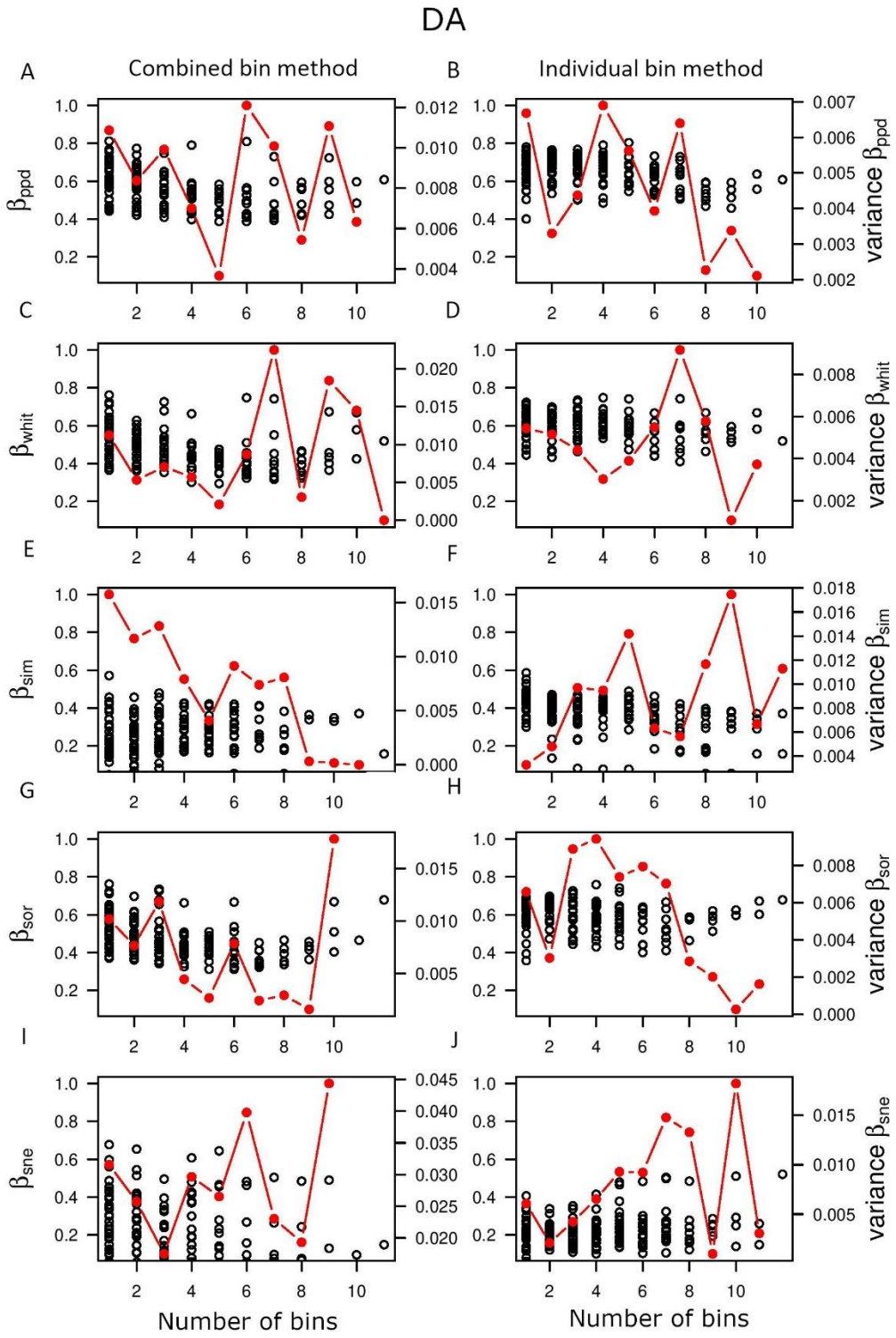

Figure 3.S2: Null model predicted mean (black circles) and variance of beta diversity (red dash) with number of bins based on DA data. The left column represents "combined bin method" and the right column represents "individual bin method". The indices of beta diversity used here include Bray-Curtis (β_{ppd}) (A-B), Whittaker index (β_{whit}) (C-D), Simpson index (β_{sim}) (E-F), Sorenson index (β_{sor}) (G-H), Nestedness component of Sorenson (β_{sne}) (I-J).

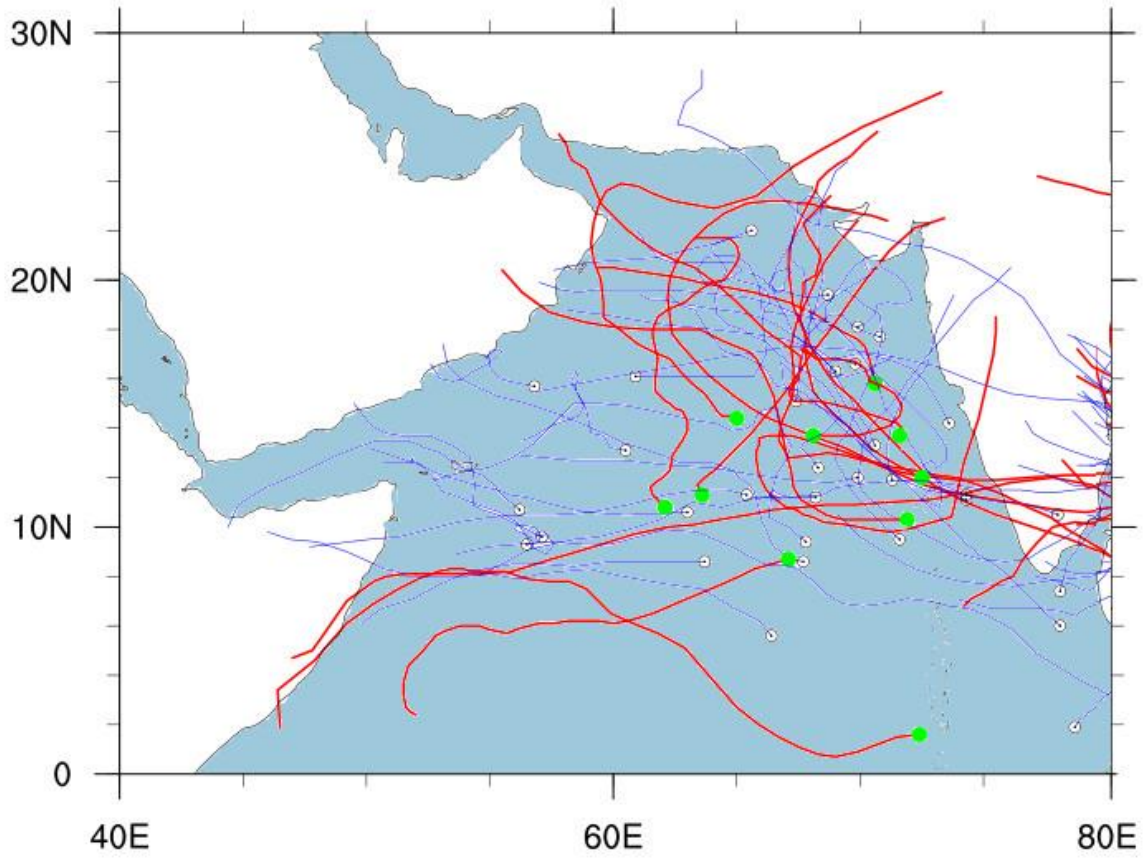

Figure. 3.S3. Tracks of cyclones passing through the western coast of India from years 1977–2014. Cyclones with higher intensity (>60 knots) have bolder lines and marked in red and cyclones with lower intensity (<60 knots) are marked in blue.

Table 3.S1. Significance (p-values) of Spearman rank correlation test between environmental variables. The significant results are in bold.

	Productivity (mean)	Productivity (range)	Salinity (mean)	Salinity (range)	Temperature (mean)	Temperature (range)	Oxygen	Cyclones	Shelf area
Productivity (mean)	0.692	0.059	**0.001**	**0.002**	**0.003**	0.923	0.817	0.061	0.081
Productivity (range)	NA	**0.002**	0.056	**0.045**	0.533	0.056	0.852	0.538	**0.005**
Salinity (mean)		NA	**0.011**	**0.000**	0.274	0.375	0.970	0.874	**0.000**
Salinity (range)			NA	**0.002**	0.049	0.180	0.573	0.224	0.015
Temperature (mean)				NA	0.056	0.817	0.887	0.278	**0.004**
Temperature (range)					NA	0.203	0.887	0.240	0.197
Oxygen concentration						NA	0.185	0.809	0.533
Cyclones							NA	0.910	0.817
Shelf area								NA	0.320

R Script 3.S1. R Script for statistical analyses and plots in Chapter 3 are available in the Supplemental files of the preprint version uploaded in the biorxiv

MS ID Number: BIORXIV/2022/514806

MS Title: Controls of spatial grain size and environmental variables on observed beta diversity of molluscan assemblage at a regional scale.

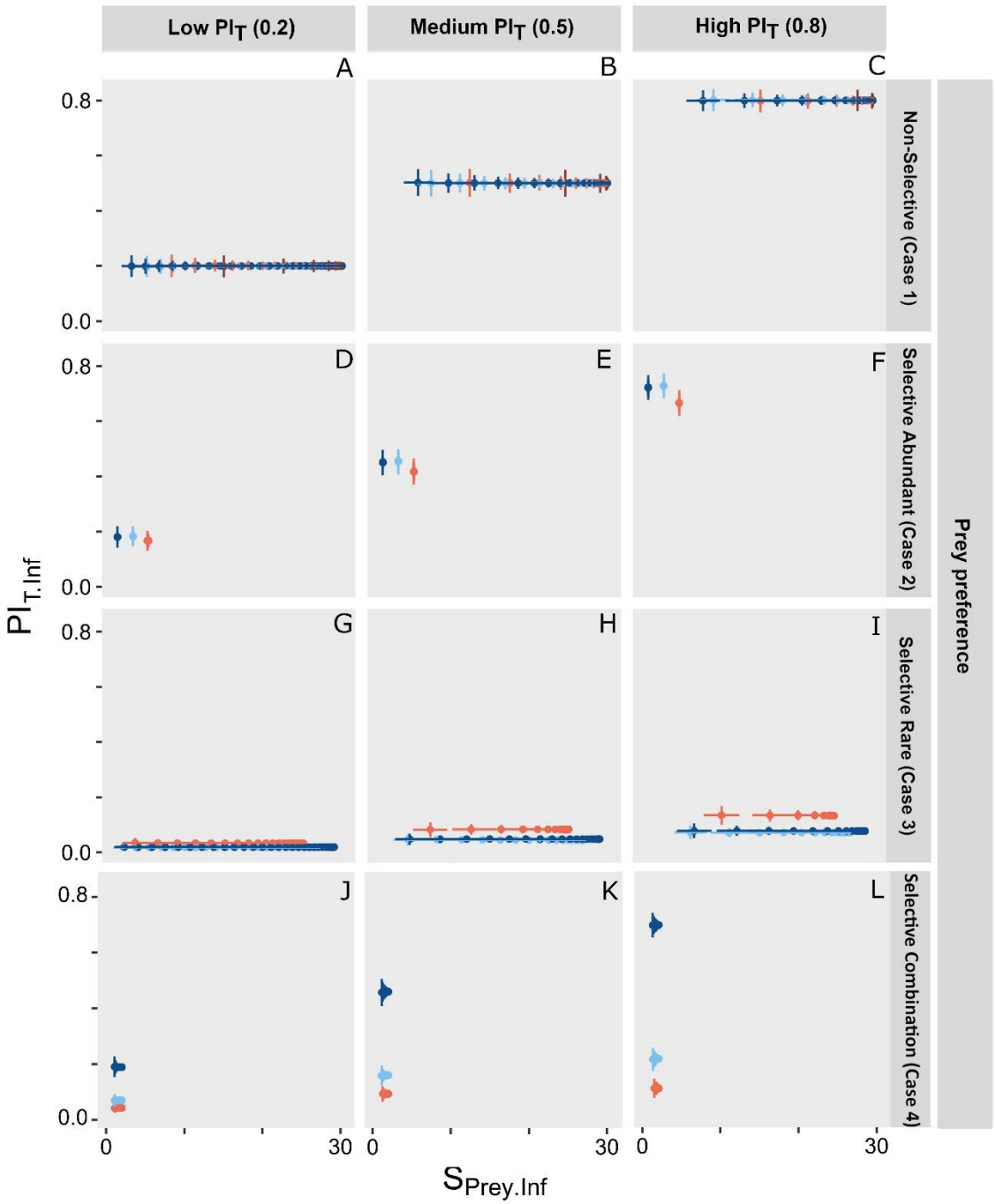

Figure 4. S1. The plot showing variation in inferred predation intensity ($PI_{T.inf}$) and inferred the number of prey species ($S_{prey.inf}$) with specific sample sizes for different model assemblages. The rows represent different degrees of selectivity of predation and the columns indicate predation intensity in the original assemblage (PI_T). The warmer colors represent higher evenness.

R Script 4.S1. R Script for statistical analyses and plots in Chapter 4 are available in the Supplemental files of the preprint version uploaded in the biorxiv

MS ID Number: BIORXIV/2022/500550

MS Title: Community structure and sample size affect estimates of predation intensity and prey selection: A model-based validation.

Bibliography

Abrams, P. A. 2015: Why ratio dependence is (still) a bad model of predation. Biological Reviews 90:794–814.

Albano, P. G., and B. Sabelli. 2011: Comparison between death and living molluscs assemblages in a Mediterranean infralittoral off-shore reef. Palaeogeography, Palaeoclimatology, Palaeoecology 310:206–215.

Alexander, R. R., and G. P. Dietl. 2003: The Fossil Record of Shell-Breaking Predation on Marine Bivalves and Gastropods. Pp.141–176 *in* P. H. Kelley, M. Kowalewski, and T. A. Hansen, eds. Predator—Prey Interactions in the Fossil Record. Springer US, Boston, MA.

———. 2003: The Fossil Record of Shell-Breaking Predation on Marine Bivalves and Gastropods. Pp.141–176 *in* P. H. Kelley, M. Kowalewski, and T. A. Hansen, eds. Predator—Prey Interactions in the Fossil Record. Springer US, Boston, MA.

———. 2005: Non-Predatory Shell Damage in Neogene Western Atlantic Deep-Burrowing Bivalves. PALAIOS 20:280–295.

Ali, A. 1996: Vulnerability of Bangladesh to Climate Change and Sea Level Rise through Tropical Cyclones and Storm Surges. Pp.171–179 *in* L. Erda, W. C. Bolhofer, S. Huq, S. Lenhart, S. K. Mukherjee, J. B. Smith, and J. Wisniewski, eds. Climate Change Vulnerability and Adaptation in Asia and the Pacific: Manila, Philippines, 15–19 January 1996. Springer Netherlands, Dordrecht.

Ali, A. 1999: Climate change impacts and adaptation assessment in Bangladesh. Climate Research 12:109–116.

Allen, J. R. L. 1984: Experiments on the settling, overturning and entrainment of bivalve shells and related models. Sedimentology 31:227–250.

Anderson, M. J., K. E. Ellingsen, and B. H. McArdle. 2006: Multivariate dispersion as a measure of beta diversity. Ecology Letters 9:683–693.

Anderson, M. J., T. O. Crist, J. M. Chase, M. Vellend, B. D. Inouye, A. L. Freestone, N. J. Sanders, H. V. Cornell, L. S. Comita, K. F. Davies, S. P. Harrison, N. J. B. Kraft, J. C. Stegen, and N. G. Swenson. 2011: Navigating the multiple meanings of β diversity: a roadmap for the practicing ecologist. Ecology Letters 14:19–28.

Apte, D. 1998: The book of Indian shells. Oxford University Press.

Arias-González, J. E., P. Legendre, and F. A. Rodríguez-Zaragoza. 2008: Scaling up beta diversity on Caribbean coral reefs. Journal of Experimental Marine Biology and Ecology 366:28–36.

Astorga, A., R. Death, F. Death, R. Paavola, M. Chakraborty, and T. Muotka. 2014: Habitat heterogeneity drives the geographical distribution of beta diversity: the case of New Zealand stream invertebrates. Ecology and Evolution 4:2693–2702.

Balaguru, K., S. Taraphdar, L. R. Leung, and G. R. Foltz. 2014: Increase in the intensity of postmonsoon Bay of Bengal tropical cyclones. Geophysical Research Letters 41:3594–3601.

Barnes, C., D. Maxwell, D. C. Reuman, and S. Jennings. 2010: Global patterns in predator–prey size relationships reveal size dependency of trophic transfer efficiency. Ecology 91:222–232.

Barton, P. S., S. A. Cunningham, A. D. Manning, H. Gibb, D. B. Lindenmayer, and R. K. Didham. 2013: The spatial scaling of beta diversity. Global Ecology and Biogeography 22:639–647.

Barwell, L. J., N. J. B. Isaac, and W. E. Kunin. 2015: Measuring β-diversity with species abundance data. Journal of Animal Ecology 84:1112–1122.

Baselga, A. 2007: Disentangling Distance Decay of Similarity from Richness Gradients: Response to Soininen et al. 2007. Ecography 30:838–841.

———. 2010: Partitioning the turnover and nestedness components of beta diversity. Global Ecology and Biogeography 19:134–143.

Baselga, A., and C. D. L. Orme. 2012: betapart: an R package for the study of beta diversity. Methods in Ecology and Evolution 3:808–812.

Baselga, A., J. M. Lobo, J.-C. Svenning, P. Aragón, and M. B. Araújo. 2012: Dispersal ability modulates the strength of the latitudinal richness gradient in European beetles. Global Ecology and Biogeography 21:1106–1113.

Baumiller, T. K., M. A. Salamon, P. Gorzelak, R. Mooi, C. G. Messing, and F. J. Gahn. 2010: Post-Paleozoic crinoid radiation in response to benthic predation preceded the Mesozoic marine revolution. Proceedings of the National Academy of Sciences 107:5893–5896.

Beck, J., J. D. Holloway, and W. Schwanghart. 2013: Undersampling and the measurement of beta diversity. Methods in Ecology and Evolution 4:370–382.

Becking, L. E., D. F. R. Cleary, N. J. de Voogd, W. Renema, M. de Beer, R. W. M. van Soest, and B. W. Hoeksema. 2006: Beta diversity of tropical marine benthic assemblages in the Spermonde Archipelago, Indonesia. Marine Ecology 27:76–88.

Behrensmeyer, A. K. 1978: Taphonomic and ecologic information from bone weathering. Paleobiology 4:150–162.
Behrensmeyer, A. K., S. M. Kidwell, and R. A. Gastaldo. 2000: Taphonomy and paleobiology. Paleobiology 26:103–147.
Belley, R., and P. V. R. Snelgrove. 2016: Relative Contributions of Biodiversity and Environment to Benthic Ecosystem Functioning. Frontiers in Marine Science 3.
Bennington, J. B. 2003: Transcending Patchiness in the Comparative Analysis of Paleocommunities: A Test Case from the Upper Cretaceous of New Jersey. PALAIOS 18:22–33.
Berryman, A. A. 1992: The Orgins and Evolution of Predator-Prey Theory. Ecology 73:1530–1535.
Bhattacherjee, M., D. Chattopadhyay, B. Som, A. S. Sankar, and S. Mazumder. 2021: Molluscan Live-Dead fidelity of a storm-dominated shallow-marine setting and its implications. Palaios 36:77–93.
Bicknell, R. D. C., and J. R. Paterson. 2018: Reappraising the early evidence of durophagy and drilling predation in the fossil record: implications for escalation and the Cambrian Explosion: Reappraising the early evidence of predation. Biological Reviews 93:754–784.
Bicknell, R. D. C., and B. Holland. 2020: Injured trilobites within a collection of dinosaurs: Using the Royal Tyrrell Museum of Palaeontology to document Cambrian predation. Palaeontologia Electronica 23: a33.
Bleich, S., M. Powilleit, T. Seifert, and G. Graf. 2011: β-diversity as a measure of species turnover along the salinity gradient in the Baltic Sea, and its -consistency with the Venice System. Marine Ecology Progress Series 436:101–118.
Blundon, J. A., and V. S. Kennedy. 1982: Refuges for infaunal bivalves from blue crab, Callinectes sapidus (Rathbun), predation in Chesapeake Bay. Journal of Experimental Marine Biology and Ecology 65:67–81.
Bonelli, J. R., C. E. Brett, A. I. Miller, and J. B. Bennington. 2006: Testing for faunal stability across a regional biotic transition: quantifying stasis and variation among recurring coral-rich biofacies in the Middle Devonian Appalachian Basin. Paleobiology 32:20–37.

Boström, C., and E. Bonsdorff. 1997: Community structure and spatial variation of benthic invertebrates associated with Zostera marina (L.) beds in the northern Baltic Sea. Journal of Sea Research 37:153–166.
Bouchet, P., P. Lozouet, P. Maestrati, and V. Heros. 2002: Assessing the magnitude of species richness in tropical marine environments: exceptionally high numbers of molluscs at a New Caledonia site. Biological Journal of the Linnean Society 75:421–436.
Boucot, A. J. 1953: Life and death assemblages among fossils. American Jour. Sci. 251:25–40.
Bray, J. R., and J. T. Curtis. 1957: An Ordination of the Upland Forest Communities of Southern Wisconsin. Ecological Monographs 27:326–349.
Brett, C. E. 1995: Sequence Stratigraphy, Biostratigraphy, and Taphonomy in Shallow Marine Environments. Palaios 10:597–616.
———. 1998: Sequence stratigraphy, paleoecology, and evolution; biotic clues and responses to sea-level fluctuations. Palaios 13:241–262.
Brett, C. E., and G. C. Baird. 1993: Taphonomic approaches to temporal resolution in stratigraphy: examples from Paleozoic marine mudrocks. Short Courses in Paleontology 6:251–274.
Brett, C. E., and G. C. Baird. 1997: Epiboles, Outages, and Ecological Evolutionary Bioevents: Taphonomic. Paleontological events: stratigraphic, ecological, and evolutionary implications:249.
Bries, J. M., A. O. Debrot, and D. L. Meyer. 2004: Damage to the leeward reefs of Curacao and Bonaire, Netherlands Antilles from a rare storm event: Hurricane Lenny, November 1999. Coral Reefs 23:297–307.
Broitman, B. R., S. A. Navarrete, F. Smith, and S. D. Gaines. 2001: Geographic variation of southeastern Pacific intertidal communities. Marine Ecology Progress Series 224:21–34.
Brown, J. H. 2014: Why are there so many species in the tropics? Journal of Biogeography 41:8–22.
Budd, G. E., and R. P. Mann. 2019: Modeling durophagous predation and mortality rates from the fossil record of gastropods. Paleobiology 45:246–264.
Bürkli, A., and A. B. Wilson. 2017: Explaining high-diversity death assemblages: Undersampling of the living community, out-of-habitat transport, time-averaging of rare

taxa, and local extinction. Palaeogeography, Palaeoclimatology, Palaeoecology 466:174–183.

Burrows, M. T., and R. N. Hughes. 1991: Optimal Foraging Decisions by Dogwhelks, Nucella lapillus (L.): Influences of Mortality Risk and Rate-Constrained Digestion. Functional Ecology 5:461.

Bustamante, R., and G. Branch. 1996: Large scale patterns and trophic structure of southern African rocky shores: the roles of geographic variation and wave exposure. Journal of Biogeography 23:339–351.

Callender, W. R., E. N. Powell, G. M. Staff, and D. J. Davies. 1992: Distinguishing autochthony, parautochthony and allochthony using taphofacies analysis: Can cold seep assemblages be discriminated from assemblages of the nearshore and continental shelf? Palaios:409–421.

Carriker, M. R. 1951: Observations on the Penetration of Tightly Closing Bivalves by Busycon and Other Predators. Ecology 32:73–83.

Casey, M. M., and D. Chattopadhyay. 2008: Clumping behavior as a strategy against drilling predation: Implications for the fossil record. Journal of Experimental Marine Biology and Ecology 367:174–179.

Chandroth, A., and D. Chattopadhyay. 2022: Micromorphy Offers Effective Defense Against Predation: Insights from Cost-Benefit Analyses of the Miocene Microgastropod Predation Record from Kerala, India. Contributions from the Museum of Paleontology, University of Michigan 34:63–81.

Chao, A., R. L. Chazdon, R. K. Colwell, and T.-J. Shen. 2005: A new statistical approach for assessing similarity of species composition with incidence and abundance data. Ecology letters 8:148–159.

Chattopadhyay, D., and T. K. Baumiller. 2010: Effect of durophagy on drilling predation: a case study of Cenozoic molluscs from North America. Historical Biology 22:367–379.

Chattopadhyay, D., and S. Dutta. 2013: Prey selection by drilling predators: A case study from Miocene of Kutch, India. Palaeogeography, Palaeoclimatology, Palaeoecology 374:187–196.

Chattopadhyay, D., A. Rathie, and A. Das. 2013a: The effect of morphology on postmortem transportation of bivalves and its taphonomic implications. Palaios 28:203–209.

Chattopadhyay, D., M. Zuschin, and A. Tomašových. 2015: How effective are ecological traits against drilling predation? Insights from recent bivalve assemblages of the northern Red Sea. Palaeogeography, Palaeoclimatology, Palaeoecology 440:659–670.
Chattopadhyay, D., V. G. S. Kella, and D. Chattopadhyay. 2020: Effectiveness of small size against drilling predation: Insights from lower Miocene faunal assemblage of Quilon Limestone, India. Palaeogeography, Palaeoclimatology, Palaeoecology 551:109742.
Chattopadhyay, D., D. Sarkar, and M. Bhattacherjee. 2021: The Distribution Pattern of Marine Bivalve Death Assemblage From the Western Margin of Bay of Bengal and Its Oceanographic Determinants. Frontiers in Marine Science 8.
Chattopadhyay, D., A. Rathie, D. J. Miller, and T. K. Baumiller. 2013b: Hydrodynamic effects of drill holes on postmortem transportation of bivalve shells and its taphonomic implications. Palaios 28:875–884.
Chattopadhyay, D., D. Sarkar, S. Dutta, and S. R. Prasanjit. 2014: What controls cannibalism in drilling gastropods? A case study on Natica tigrina. Palaeogeography, Palaeoclimatology, Palaeoecology 410:126–133.
Chattopadhyay, D., M. Zuschin, S. Dominici, and J. A. Sawyer. 2016: Patterns of drilling predation in relation to stratigraphy, locality and sieve size: Insights from the Eocene molluscan fauna of the Paris Basin. Palaeogeography, Palaeoclimatology, Palaeoecology 459:86–98.
Cheng, C., J. de Smit, G. Fivash, S. Hulscher, B. W. Borsje, and K. Soetaert. 2021: Sediment shell-content diminishes current-driven sand ripple development and migration. Earth Surface Dynamics 9:1335–1346.
Chojnacki, N. C., and L. R. Leighton. 2014: Comparing predatory drillholes to taphonomic damage from simulated wave action on a modern gastropod. Historical Biology 26:69–79.
Clapham, M. E., and N. P. James. 2008: Paleoecology Of Early–Middle Permian Marine Communities In Eastern Australia: Response To Global Climate Change In the Aftermath Of the Late Paleozoic Ice Age. PALAIOS 23:738–750.
Clapham, M. E., D. J. Bottjer, C. M. Powers, N. Bonuso, M. L. Fraiser, P. J. Marenco, S. Q. Dornbos, and S. B. Pruss. 2006: Assessing the ecological dominance of Phanerozoic marine invertebrates. Palaios 21:431–441.
Cleary, D. F. R. 2003: An examination of scale of assessment, logging and ENSO-induced fires on butterfly diversity in Borneo. Oecologia 135:313–321.

Cleary, D. F. R., A. Ø. Mooers, K. A. O. Eichhorn, J. Van Tol, R. De Jong, and S. B. J. Menken. 2004: Diversity and community composition of butterflies and odonates in an ENSO-induced fire affected habitat mosaic: a case study from East Kalimantan, Indonesia. Oikos 105:426–448.

Collins, M. J. 1991: Growth rate and substrate-related mortality of a benthic brachiopod population. Lethaia 24:1–11.

Condit, R., N. Pitman, E. G. Leigh, J. Chave, J. Terborgh, R. B. Foster, P. Núñez, S. Aguilar, R. Valencia, G. Villa, H. C. Muller-Landau, E. Losos, and S. P. Hubbell. 2002: Beta-Diversity in Tropical Forest Trees. Science 295:666–669.

Cooper, R. A., P. A. Maxwell, J. S. Crampton, A. G. Beu, C. M. Jones, and B. A. Marshall. 2006: Completeness of the fossil record: Estimating losses due to small body size. Geology 34:241–244.

Corte, G. N., T. A. Schlacher, H. H. Checon, C. A. M. Barboza, E. Siegle, R. A. Coleman, and A. C. Z. Amaral. 2017: Storm effects on intertidal invertebrates: increased beta diversity of few individuals and species. PeerJ 5:e3360.

Crist, T. O., J. A. Veech, J. C. Gering, and K. S. Summerville. 2003: Partitioning Species Diversity across Landscapes and Regions: A Hierarchical Analysis of α, β, and γ Diversity. The American Naturalist 162:734–743.

Cummins, H., E. N. Powell, R. J. Stanton Jr, and G. Staff. 1986: The size-frequency distribution in palaeoecology: effects of taphonomic processes during formation of molluscan death assemblages in Texas bays. Palaeontology 29:495–518.

Da Silva, R., A. Mazumdar, T. Mapder, A. Peketi, R. K. Joshi, A. Shaji, P. Mahalakshmi, B. Sawant, B. G. Naik, M. A. Carvalho, and S. K. Molletti. 2017: Salinity stratification controlled productivity variation over 300 ky in the Bay of Bengal. Scientific Reports 7:14439.

Darwin, C. 1909: The origin of species. New York: PF Collier & son., p.

Davidar, P., B. Rajagopal, D. Mohandass, J.-P. Puyravaud, R. Condit, S. J. Wright, and E. G. Leigh Jr. 2007: The effect of climatic gradients, topographic variation and species traits on the beta diversity of rain forest trees. Global Ecology and Biogeography 16:510–518.

DeAngelis, D. L., R. A. Goldstein, and R. V. O'Neill. 1975: A Model for Tropic Interaction. Ecology 56:881–892.

DeAngelis, D. L., J. A. Kitchell, and W. M. Post. 1985: The Influence of Naticid Predation on Evolutionary Strategies of Bivalve Prey: Conclusions from a Model. The American Naturalist 126:817–842.
Dettinger, M. 2011: Climate change, atmospheric rivers, and floods in California–a multimodel analysis of storm frequency and magnitude changes 1. JAWRA Journal of the American Water Resources Association 47:514–523.
Dey, S. 2003: Incipient motion of bivalve shells on sand beds under flowing water. Journal of engineering mechanics 129:232–240.
Dietl, G. P. 2003: Coevolution of a marine gastropod predator and its dangerous bivalve prey. Biological Journal of the Linnean Society 80:409–436.
Dietl, G. P., and R. R. Alexander. 2000: Post-Miocene Shift in Stereotypic Naticid Predation on Confamilial Prey from the Mid-Atlantic Shelf: Coevolution with Dangerous Prey. PALAIOS 15:414–429.
Dietl, G. P., and R. R. Alexander. 2009: Patterns of unsuccessful shell-crushing predation along a tidal gradient in two geographically separated salt marshes. Marine Ecology 30:116–124.
Dietl, G. P., and M. Kosloski. 2013: On the measurement of repair frequency: how important is data standardization? Palaios 28:394–402.
Dietl, G. P., G. S. Herbert, and G. J. Vermeij. 2004: Reduced Competition and Altered Feeding Behavior Among Marine Snails After a Mass Extinction. Science 306:2229–2231.
Dominici, S., and M. Zuschin. 2005: Infidelities of fossil assemblages. Lethaia 38:381–382.
Donovan, S. K. 2002: Island shelves, downslope transport and shell assemblages. Lethaia 35:277–277.
Downes, B. J., P. s. Lake, and E. s. g. Schreiber. 1993: Spatial variation in the distribution of stream invertebrates: implications of patchiness for models of community organization. Freshwater Biology 30:119–132.
Duivenvoorden, J. F., J.-C. Svenning, and S. J. Wright. 2002: Beta Diversity in Tropical Forests. Science 295:636–637.
Dyer, A. D., E. R. Ellis, D. J. Molinaro, and L. R. Leighton. 2018: Experimental fragmentation of gastropod shells by sediment compaction: Implications for interpreting

drilling predation intensities in the fossil record. Palaeogeography, Palaeoclimatology, Palaeoecology 511:332–340.
Ebert, M., M. Kölbl-Ebert, and J. A. Lane. 2015: Fauna and Predator-Prey Relationships of Ettling, an Actinopterygian Fish-Dominated Konservat-Lagerstätte from the Late Jurassic of Southern Germany. PLOS ONE 10:e0116140.
Ehret, D. J., B. J. Macfadden, and R. Salas-Gismondi. 2009: Caught in the act: trophic interactions between a 4-million-year-old white shark (Carcharodon) and mysticete whale from Peru. PALAIOS 24:329–333.
Ellingsen, K. E. 2001: Biodiversity of a continental shelf soft-sediment macrobenthos community. Marine Ecology Progress Series 218:1–15.
———. 2002: Soft-sediment benthic biodiversity on the continental shelf in relation to environmental variability. Marine Ecology Progress Series 232:15–27.
Ellingsen, Karie., and J. s. Gray. 2002: Spatial patterns of benthic diversity: is there a latitudinal gradient along the Norwegian continental shelf? Journal of Animal Ecology 71:373–389.
Ferrier, S., G. Manion, J. Elith, and K. Richardson. 2007: Using generalized dissimilarity modelling to analyse and predict patterns of beta diversity in regional biodiversity assessment. Diversity and Distributions 13:252–264.
Fick, C., E. Puhl, and E. E. Toldo Jr. 2020: Threshold of motion of bivalve and gastropod shells under oscillatory flow in flume experiments. Sedimentology 67:627–648.
Finnegan, S., and M. L. Droser. 2008: Reworking diversity: effects of storm deposition on evenness and sampled richness, Ordovician of the Basin and Range, Utah and Nevada, USA. Palaios 23:87–96.
Fleishman, E., C. J. Betrus, and R. B. Blair. 2003: Effects of spatial scale and taxonomic group on partitioning of butterfly and bird diversity in the Great Basin, USA. Landscape Ecology 18:675–685.
Flessa, K. W., and M. Kowalewski. 1994: Shell survival and time-averaging in nearshore and shelf environments: estimates from the radiocarbon literature. Lethaia 27:153–165.
Fluck, I. E., N. Cáceres, C. D. Hendges, M. do N. Brum, and C. S. Dambros. 2020: Climate and geographic distance are more influential than rivers on the beta diversity of passerine birds in Amazonia. Ecography 43:860–868.

Forcino, F. L. 2013: How many fossils, how to count them, and where to collect them: Examinations of the most appropriate methods for community paleoecological research - ProQuest.University of Alberta, Edmonton, Alberta, 149pp.
Fournier, E., and M. Loreau. 2001: Respective roles of recent hedges and forest patch remnants in the maintenance of ground-beetle (Coleoptera: Carabidae) diversity in an agricultural landscape. Landscape Ecology 16:17–32.
Freestone, A. L., R. W. Osman, G. M. Ruiz, and M. E. Torchin. 2011: Stronger predation in the tropics shapes species richness patterns in marine communities. Ecology 92:983–993.
Freestone, A. L., E. W. Carroll, K. J. Papacostas, G. M. Ruiz, M. E. Torchin, and B. J. Sewall. 2020: Predation shapes invertebrate diversity in tropical but not temperate seagrass communities. Journal of Animal Ecology 89:323–333.
Fürisch, F. T., and M. Aberhan. 1990: Significance of time-averaging for palaeocommunity analysis. Lethaia 23:143–152.
Fürsich, F. T. 1978: The influence of faunal condensation and mixing on the preservation of fossil benthic communities. Lethaia 11:243–250.
Fürsich, F. T., and K. W. Flessa. 1987: Taphonomy of tidal flat molluscs in the northern Gulf of California: paleoenvironmental analysis despite the perils of preservation. The Paleontological Society Special Publications 2:200–237.
Gabriel, D., I. Roschewitz, T. Tscharntke, and C. Thies. 2006: Beta Diversity at Different Spatial Scales: Plant Communities in Organic and Conventional Agriculture. Ecological Applications 16:2011–2021.
Gallmetzer, I., A. Haselmair, A. Tomašovỳch, A.-K. Mautner, S.-M. Schnedl, D. Cassin, R. Zonta, and M. Zuschin. 2019: Tracing origin and collapse of Holocene benthic baseline communities in the northern Adriatic Sea. Palaios 34:121–145.
García-Ramos, D. A., P. G. Albano, M. Harzhauser, W. E. Piller, and M. Zuschin. 2016: High dead-live mismatch in richness of molluscan assemblages from carbonate tidal flats in the Persian (Arabian) Gulf. Palaeogeography, Palaeoclimatology, Palaeoecology 457:98–108.
Gaston, K. J. 1994: Measuring Geographic Range Sizes. Ecography 17:198–205.
Gehling, J. G., and M. L. Droser. 2018: Ediacaran scavenging as a prelude to predation. Emerging Topics in Life Sciences 2:213–222.

Gerhard C Cadée. 1991: The history of taphonomy. Pp.3–21 *in* The Processes of Fossilization. Columbia University Press.
Gering, J. C., T. O. Crist, and J. A. Veech. 2003: Additive Partitioning of Species Diversity across Multiple Spatial Scales: Implications for Regional Conservation of Biodiversity. Conservation Biology 17:488–499.
Giribet, G. 2008: Bivalvia. Pp.105–141 *in* Phylogeny and Evolution of the Mollusca. University of California Press.
Goodsell, P. J., and S. D. Connell. 2002: Can habitat loss be treated independently of habitat configuration? Implications for rare and common taxa in fragmented landscapes. Marine Ecology Progress Series 239:37–44.
Gordillo, S., and F. Archuby. 2014: Live-Live and Live-Dead Interactions in Marine Death Assemblages: The Case of the Patagonian Clam Venus antiqua. Acta Palaeontologica Polonica 59:429–442.
Gordillo, S., and M. E. Malvé. 2021: Drilling predation on Antarctic tusk shells: first records on Recent scaphopods from the Southern Hemisphere. Antarctic Science 33:344–348.
Gordillo, S., G. A. Morán, and M. E. Malvé. 2022: Octopuses and drilling snails as the main suspects of predation traces on shelled molluscs in West Antarctica. Polar Biology 45:127–141.
Gorzelak, P., M. A. Salamon, and T. K. Baumiller. 2012: Predator-induced macroevolutionary trends in Mesozoic crinoids. Proceedings of the National Academy of Sciences 109:7004–7007.
Gorzelak, P., M. A. Salamon, D. Trzęsiok, and R. Niedźwiedzki. 2013: Drill Holes and Predation Traces versus Abrasion-Induced Artifacts Revealed by Tumbling Experiments. PLoS ONE 8: e58528.
Gray, J. S. 2000: The measurement of marine species diversity, with an application to the benthic fauna of the Norwegian continental shelf. Journal of Experimental Marine Biology and Ecology 250:23–49.
Grey, M., E. G. Boulding, and M. E. Brookfield. 2006a: Estimating multivariate selection gradients in the fossil record: a naticid gastropod case study. Paleobiology 32:100–108.
———. 2006b: Estimating multivariate selection gradients in the fossil record: a naticid gastropod case study. Paleobiology 32:100–108.

Haque, M. 2012: Existence of complex patterns in the Beddington–DeAngelis predator–prey model. Mathematical Biosciences 239:179–190.
Harborne, A. R., P. J. Mumby, K. ZŻychaluk, J. D. Hedley, and P. G. Blackwell. 2006: Modeling the Beta Diversity of Coral Reefs. Ecology 87:2871–2881.
Harper, E. M. 2016: Uncovering the holes and cracks: from anecdote to testable hypotheses in predation studies. Palaeontology 59:597–609.
Harper, E. M., J. A. Crame, and C. E. Sogot. 2018: "Business as usual": Drilling predation across the K-Pg mass extinction event in Antarctica. Palaeogeography, Palaeoclimatology, Palaeoecology 498:115–126.
Harrison, S., S. J. Ross, and J. H. Lawton. 1992: Beta Diversity on Geographic Gradients in Britain. Journal of Animal Ecology 61:151–158.
Hattab, T., C. Albouy, F. Ben Rais Lasram, F. Le Loc'h, F. Guilhaumon, and F. Leprieur. 2015: A biogeographical regionalization of coastal Mediterranean fishes. Journal of Biogeography 42:1336–1348.
Hattori, K. E., P. H. Kelley, G. P. Dietl, N. O. Moore, S. L. Simpson, A. M. Zappulla, K. J. Ottens, and C. C. Visaggi. 2014: Validation of taxon-specific sampling by novice collectors for studying drilling predation in fossil bivalves. Palaeogeography, Palaeoclimatology, Palaeoecology 412:199–207.
Hausmann, I. M., H. Domanski, and M. Zuschin. 2018: Influence of setting, sieve size, and sediment depth on multivariate and univariate assemblage attributes of coral reef-associated mollusc death assemblages from the Gulf of Aqaba. Facies 64:20.
Heim, N. A. 2009: Stability of regional brachiopod diversity structure across the Mississippian/Pennsylvanian boundary. Paleobiology 35:393–412.
Hereu, B., M. Zabala, and E. Sala. 2008: Multiple Controls of Community Structure and Dynamics in a Sublittoral Marine Environment. Ecology 89:3423–3435.
Hewitt, J. E., S. F. Thrush, J. Halliday, and C. Duffy. 2005: The Importance of Small-Scale Habitat Structure for Maintaining Beta Diversity. Ecology 86:1619–1626.
Hewitt, J. E., S. F. Thrush, P. K. Dayton, and E. Bonsdorff. 2007: The Effect of Spatial and Temporal Heterogeneity on the Design and Analysis of Empirical Studies of Scale-Dependent Systems. The American Naturalist 169:398–408.
Hohenegger, J., and E. Yordanova. 2001: Depth–transport functions and erosion–deposition diagrams as indicators of slope inclination and time-averaged traction forces: applications in tropical reef environments. Sedimentology 48:1025–1046.

Hortal, J., N. Roura-Pascual, N. J. Sanders, and C. Rahbek. 2010: Understanding (insect) species distributions across spatial scales. Ecography 33:51–53.
Hubbard, D. K. 1992: Hurricane-induced sediment transport in open-shelf tropical systems; an example from St. Croix, US Virgin Islands. Journal of Sedimentary Research 62:946–960.
Hughes, R. N. 1980: Optimal foraging theory in the marine context. Oceanography and Marine Biology: An Annual Review 18:423–481.
Huntley, J. W., and M. Kowalewski. 2007: Strong coupling of predation intensity and diversity in the Phanerozoic fossil record. Proceedings of the National Academy of Sciences 104:15006–15010.
Hurlbert, S. H. 1971: The Nonconcept of Species Diversity: A Critique and Alternative Parameters. Ecology 52:577–586.
Hutchings, J. A., and G. S. Herbert. 2013: No honor among snails: Conspecific competition leads to incomplete drill holes by a naticid gastropod. Palaeogeography, Palaeoclimatology, Palaeoecology 379–380:32–38.
Hutchinson, S., and L. E. Hawkins. 1992: Quantification of the physiological responses of the European flat oyster *Ostrea edulis* l. to temperature and salinity. Journal of Molluscan Studies 58:215–226.
Jablonski, D. 1998: Geographic Variation in the Molluscan Recovery from the End-Cretaceous Extinction. Science 279:1327–1330.
Jankowski, J. E., A. L. Ciecka, N. Y. Meyer, and K. N. Rabenold. 2009: Beta diversity along environmental gradients: implications of habitat specialization in tropical montane landscapes. Journal of Animal Ecology 78:315–327.
Jayaraj, J., A. Wan, M. Rahman, and Z. K. Punja. 2008: Seaweed extract reduces foliar fungal diseases on carrot. Crop Protection 27:1360–1366.
Josefson, A. B. 2009: Additive partitioning of estuarine benthic macroinvertebrate diversity across multiple spatial scales. Marine Ecology Progress Series 396:283–292.
Josefson, A. B., and C. Göke. 2013: Disentangling the effects of dispersal and salinity on beta diversity in estuarine benthic invertebrate assemblages. Journal of Biogeography 40:1000–1009.
Joydas, T. V., and R. Damodaran. 2009: Infaunal macrobenthos along the shelf waters of the west coast of India, Arabian Sea. IJMS Vol.38(2) [June 2009].

Joydas, T. V., and R. Damodaran. 2014: Infaunal macrobenthos of the oxygen minimum zone on the Indian western continental shelf. Marine Ecology 35:22–35.
Jurasinski, G. 2007: Spatio-Temporal Patterns of Biodiversity and their Drivers - Method Development and Application.Doctoral thesis, Bayreuthpp.
Kase, T., and M. Ishikawa. 2003: Mystery of naticid predation history solved: Evidence from a “living fossil” species. Geology 31:403.
Keen, T. R., S. J. Bentley, W. Chad Vaughan, and C. A. Blain. 2004: The generation and preservation of multiple hurricane beds in the northern Gulf of Mexico. Marine Geology 210:79–105.
Kelley, P. H., and T. A. Hansen. 1993: Evolution of the Naticid Gastropod Predator-Prey System: An Evaluation of the Hypothesis of Escalation. PALAIOS 8:358–375.
———. 2003: The Fossil Record of Drilling Predation on Bivalves and Gastropods. Pp.113–139 *in* P. H. Kelley, M. Kowalewski, and T. A. Hansen, eds. Predator—Prey Interactions in the Fossil Record. Springer US, Boston, MA.
Khan, A., S. Manokaran, S. Lyla, and Z. Nazeer. 2010: Biodiversity of epibenthic community in the inshore waters of southeast coast of India. Biologia 65:704–713.
Kidwell, S., and A. Tomasovych. 2013a: Implications of Time-Averaged Death Assemblages for Ecology and Conservation Biology. Annual Review of Ecology Evolution and Systematics 44:539–563.
Kidwell, S. M. 1998: Time-averaging in the marine fossil record: overview of strategies and uncertainties. Oceanographic Literature Review 9:1546–1547.
Kidwell, S. M. 2001: Preservation of Species Abundance in Marine Death Assemblages. Science 294:1091–1094.
———. 2002a: Mesh-size effects on the ecological fidelity of death assemblages: a meta-analysis of molluscan live–dead studies. Geobios 35:107–119.
———. 2002b: Time-averaged molluscan death assemblages: palimpsests of richness, snapshots of abundance. Geology 30:803–806.
———. 2007: Discordance between living and death assemblages as evidence for anthropogenic ecological change. Proceedings of the National Academy of Sciences 104:17701–17706.
———. 2008: Ecological fidelity of open marine molluscan death assemblages: effects of post-mortem transportation, shelf health, and taphonomic inertia. Lethaia 41:199–217.

———. 2013: Time-averaging and fidelity of modern death assemblages: building a taphonomic foundation for conservation palaeobiology. Palaeontology 56:487–522.
Kidwell, S. M., and D. Bosence. 1991: Taphonomy and time averaging of marine shelly faunas. Pp.115–209 *in* Taphonomy: Releasing the Data Locked in the Fossil Record. Plenum, New York.
Kidwell, S. M., and K. W. Flessa. 1995: The Quality of the Fossil Record: Populations, Species, and Communities. Annual Review of Ecology and Systematics 26:269–299.
Kidwell, S. M., and S. M. Holland. 2002: The Quality of the Fossil Record: Implications for Evolutionary Analyses. Annual Review of Ecology and Systematics 33:561–588.
Kidwell, S. M., and A. Tomasovych. 2013b: Implications of time-averaged death assemblages for ecology and conservation biology. Annual Review of Ecology, Evolution, and Systematics 44:539–563.
Kidwell, S. M., T. A. Rothfus, and M. M. Best. 2001: Sensitivity of taphonomic signatures to sample size, sieve size, damage scoring system, and target taxa. Palaios 16:26–52.
Kidwell, S. M., D. W. Bosence, P. A. Allison, and D. E. G. Briggs. 1991: Taphonomy and time-averaging of marine shelly faunas. Pp.115–209 *in* Taphonomy: Releasing the Data Locked in the Fossil Record. Plenum, New York, US.
Kitchell, J. A., and J. F. Kitchell. 1980: Size-selective predation, light transmission, and oxygen stratification: Evidence from the recent sediments of manipulated lakes1. Limnology and Oceanography 25:389–402.
Kitchell, J. A., C. H. Boggs, J. F. Kitchell, and J. A. Rice. 1981: Prey Selection by Naticid Gastropods: Experimental Tests and Application to Application to the Fossil Record. Paleobiology 7:533–552.
Klompmaker, A. A., and P. H. Kelley. 2015: Shell ornamentation as a likely exaptation: evidence from predatory drilling on Cenozoic bivalves. Paleobiology 41:187–201.
Klompmaker, A. A., and S. Finnegan. 2018: Extreme rarity of competitive exclusion in modern and fossil marine benthic ecosystems. Geology 46:723–726.
Klompmaker, A. A., and N. H. Landman. 2021: Octopodoidea as predators near the end of the Mesozoic Marine Revolution. Biological Journal of the Linnean Society 132:894–899.

Klompmaker, A. A., M. Kowalewski, J. W. Huntley, and S. Finnegan. 2017: Increase in predator-prey size ratios throughout the Phanerozoic history of marine ecosystems. Science 356:1178–1180.
Klompmaker, A. A., P. H. Kelley, D. Chattopadhyay, J. C. Clements, J. W. Huntley, and M. Kowalewski. 2019a: Predation in the marine fossil record: Studies, data, recognition, environmental factors, and behavior. Earth-Science Reviews 194:472–520.
———. 2019b: Predation in the marine fossil record: Studies, data, recognition, environmental factors, and behavior. Earth-Science Reviews 194:472–520.
Koleff, P., K. J. Gaston, and J. J. Lennon. 2003: Measuring beta diversity for presence–absence data. Journal of Animal Ecology 72:367–382.
Korpanty, C. A., and P. H. Kelley. 2014: Molluscan live–dead agreement in anthropogenically stressed seagrass habitats: Siliciclastic versus carbonate environments. Palaeogeography, Palaeoclimatology, Palaeoecology 410:113–125.
Kosloski, M. 2011: Recognizing biotic breakage of the hard clam, Mercenaria mercenaria caused by the stone crab, Menippe mercenaria: An experimental taphonomic approach. Journal of Experimental Marine Biology and Ecology 396:115–121.
Kosloski, M. E., G. P. Dietl, and G. S. Herbert. 2008: Are museum collections adequate to test the escalation hypothesis?: A preliminary case study using the Plio-Pleistocene Strombus alatus species complex from Florida. Geological Society of America, Abstracts with Program 40:373.
Kosnik, M. A., D. Jablonski, R. Lockwood, and P. M. Novack-Gottshall. 2006: Quantifying molluscan body size in evolutionary and ecological analyses: maximizing the return on data-collection efforts. Palaios 21:588–597.
Kosnik, M. A., Q. Hua, D. S. Kaufman, and R. A. Wüst. 2009: Taphonomic bias and time-averaging in tropical molluscan death assemblages: differential shell half-lives in Great Barrier Reef sediment. Paleobiology 35:565–586.
Kotta, J., T. Wernberg, H. Jänes, I. Kotta, K. Nurkse, M. Pärnoja, and H. Orav-Kotta. 2018: Novel crab predator causes marine ecosystem regime shift. Scientific Reports 8:4956.
Kowalewski, M. 1996: Time-Averaging, Overcompleteness, and the Geological Record. The Journal of Geology 104:317–326.
Kowalewski, M. 2002: The Fossil Record of Predation: An Overview of Analytical Methods. The Paleontological Society Papers 8:3–42.

Kowalewski, M. 2004: Drill holes produced by the predatory gastropod Nucella lamellosa (Muricidae): Palaeobiological and ecological implications. Journal Molluscan Studies 70:359–370.
Kowalewski, M., and A. P. Hoffmeister. 2003: Sieves and Fossils: Effects of Mesh Size on Paleontological Patterns. PALAIOS 18:460–469.
Kowalewski, M., and R. K. Bambach. 2008: The Limits of Paleontological Resolution. Pp.1–48 *in* P. J. Harries, ed. High-Resolution Approaches in Stratigraphic Paleontology. Springer Netherlands, Dordrecht.
Kowalewski, M., and P. Novack-Gottshall. 2010: Resampling Methods in Paleontology. The Paleontological Society Papers 16:19–54.
Kowalewski, M., A. Dulai, and F. T. Fürsich. 1998: A fossil record full of holes: The Phanerozoic history of drilling predation. Geology 26:1091.
Kowalewski, M., G. E. A. Serrano, K. W. Flessa, and G. A. Goodfriend. 2000: Dead delta's former productivity: two trillion shells at the mouth of the Colorado River. Geology 28:1059–1062.
Kowalewski, M., A. P. Hoffmeister, T. K. Baumiller, and R. K. Bambach. 2005: Secondary Evolutionary Escalation Between Brachiopods and Enemies of Other Prey. Science 308:1774–1777.
Kowalewski, M., D. G. Lazo, M. Carroll, C. Messina, L. Casazza, S. Puchalski, N. S. Gupta, T. A. Rothfus, B. Hannisdal, J. Sälgeback, A. Hendy, J. Stempien, R. A. Krause Jr., R. C. Terry, M. LaBarbera, and A. Tomašových. 2003: Quantitative fidelity of brachiopod-mollusk assemblages from modern subtidal environments of San Juan Islands, USA. Journal of Taphonomy.
Kraft, N. J. B., L. S. Comita, J. M. Chase, N. J. Sanders, N. G. Swenson, T. O. Crist, J. C. Stegen, M. Vellend, B. Boyle, M. J. Anderson, H. V. Cornell, K. F. Davies, A. L. Freestone, B. D. Inouye, S. P. Harrison, and J. A. Myers. 2011: Disentangling the Drivers of β Diversity Along Latitudinal and Elevational Gradients. Science 333:1755–1758.
Kudrass, H., K. Michels, M. Wiedicke, and A. Suckow. 1998: Cyclones and tides as feeders of a submarine canyon off Bangladesh. Geology 26:715–718.
Kuehl, S. A., T. M. Hariu, and W. S. Moore. 1989: Shelf sedimentation off the Ganges-Brahmaputra river system: Evidence for sediment bypassing to the Bengal fan. Geology 17:1132–1135.

Kumar, S. P., and T. G. Prasad. 1996: Winter cooling in the northern Arabian Sea. Current Science 71:834–841.

Kumar, T. S., R. Mahendra, S. Nayak, K. Radhakrishnan, and K. Sahu. 2010: Coastal vulnerability assessment for Orissa State, east coast of India. Journal of Coastal research 26:523–534.

Lafferty, A. G., A. I. Miller, and C. E. Brett. 1994: Comparative Spatial Variability in Faunal Composition along Two Middle Devonian Paleoenvironmental Gradients. PALAIOS 9:224–236.

Lande, R. 1996: Statistics and Partitioning of Species Diversity, and Similarity among Multiple Communities. Oikos 76:5–13.

Langerhans, R. B. 2007: Evolutionary consequences of predation: avoidance, escape, reproduction, and diversification. Pp.177–220 *in* A. M. T. Elewa, ed. Predation in Organisms: A Distinct Phenomenon. Springer, Berlin, Heidelberg.

Lee, D., J. Lindqvist, A. Beu, J. Robinson, M. Ayress, H. Morgans, and J. Stein. 2014: Geological setting and diverse fauna of a Late Oligocene rocky shore ecosystem, Cosy Dell, Southland. New Zealand Journal of Geology and Geophysics 57:195–208.

Legendre, P. 2014: Interpreting the replacement and richness difference components of beta diversity. Global Ecology and Biogeography 23:1324–1334.

Legendre, P., and L. Legendre. 1998: Numerical Ecology: Volume 20. Elsevier Science & Technology, p.

Leighton, L., N. Chojnacki, E. Stafford, C. Tyler, and C. Schneider. 2016: Categorization of shell fragments provides a proxy for environmental energy and predation intensity. Journal of the Geological Society 173: 2015-086.

Leighton, L. R. 2001: New example of Devonian predatory boreholes and the influence of brachiopod spines on predator success. Palaeogeography, Palaeoclimatology, Palaeoecology 165:53–69.

———. 2002: Inferring predation intensity in the marine fossil record. Paleobiology 28:328–342.

Leonard-Pingel, J. S., and J. B. Jackson. 2013: Drilling Intensity Varies Among Neogene Tropical American Bivalvia in Relation to Shell Form and Life Habit. Bulletin of Marine Science 89:905–919.

Leprieur, F., P. A. Tedesco, B. Hugueny, O. Beauchard, H. H. Dürr, S. Brosse, and T. Oberdorff. 2011: Partitioning global patterns of freshwater fish beta diversity reveals contrasting signatures of past climate changes. Ecology Letters 14:325–334.
Lerosey-Aubril, R., and J. S. Peel. 2018: Gut evolution in early Cambrian trilobites and the origin of predation on infaunal macroinvertebrates: evidence from muscle scars in Mesolenellus. Palaeontology 61:747–760.
Levin, L. A., J. D. Gage, C. Martin, and P. A. Lamont. 2000: Macrobenthic community structure within and beneath the oxygen minimum zone, NW Arabian Sea. Deep Sea Research Part II: Topical Studies in Oceanography 47:189–226.
Levin, S. A. 1992: The Problem of Pattern and Scale in Ecology: The Robert H. MacArthur Award Lecture. Ecology 73:1943–1967.
Lin, N., K. Emanuel, M. Oppenheimer, and E. Vanmarcke. 2012: Physically based assessment of hurricane surge threat under climate change. Nature Climate Change 2:462–467.
Lindo, Z., and N. N. Winchester. 2008: Scale dependent diversity patterns in arboreal and terrestrial oribatid mite (Acari: Oribatida) communities. Ecography 31:53–60.
Lockwood, R., and L. R. Chastant. 2006: Quantifying taphonomic bias of compositional fidelity, species richness, and rank abundance in molluscan death assemblages from the upper Chesapeake Bay. Palaios 21:376–383.
Loiseau, N., G. Legras, M. Kulbicki, B. Mérigot, M. Harmelin-Vivien, N. Mazouni, R. Galzin, and J. c. Gaertner. 2017: Multi-component β-diversity approach reveals conservation dilemma between species and functions of coral reef fishes. Journal of Biogeography 44:537–547.
Mac Arthur, R. H., and E. O. Wilson. 1967: The Theory of Island Biogeography. Princeton University Press, p.
Madhupratap, M., S. P. Kumar, P. M. A. Bhattathiri, M. D. Kumar, S. Raghukumar, K. K. C. Nair, and N. Ramaiah. 1996: Mechanism of the biological response to winter cooling in the northeastern Arabian Sea. Nature 384:549–552.
Martinelli, J. C., M. A. Kosnik, and J. S. Madin. 2015: Encounter frequency does not predict predation frequency in tropical dead-shell assemblages. PALAIOS 30:818–826.
Maxwell, M. F., F. Leprieur, J. P. Quimbayo, S. R. Floeter, and M. G. Bender. 2022: Global patterns and drivers of beta diversity facets of reef fish faunas. Journal of Biogeography 49:954–967.

McClain, C., and M. Rex. 2001: The relationship between dissolved oxygen concentration and maximum size in deep-sea turrid gastropods: an application of quantile regression. Marine Biology 139:681–685.
McClain, C. R., A. P. Allen, D. P. Tittensor, and M. A. Rex. 2012: Energetics of life on the deep seafloor. Proceedings of the National Academy of Sciences 109:15366–15371.
McNamara, K. J. 1994a: Diversity of Cenozoic marsupiate echinoids as an environmental indicator. Lethaia 27:257–268.
McNamara, K. J. 1994b: The significance of gastropod predation to patterns of evolution and extinction in Australian Tertiary echinoids. Pp.*in* Echinoderms through Time. CRC Press.
Melo, A. S., T. F. L. V. B. Rangel, and J. A. F. Diniz-Filho. 2009a: Environmental drivers of beta-diversity patterns in New-World birds and mammals. Ecography 32:226–236.
———. 2009b: Environmental drivers of beta-diversity patterns in New-World birds and mammals. Ecography 32:226–236.
Mendelsohn, R., K. Emanuel, S. Chonabayashi, and L. Bakkensen. 2012: The impact of climate change on global tropical cyclone damage. Nature climate change 2:205–209.
Michels, K., H. Kudrass, C. Hübscher, A. Suckow, and M. Wiedicke. 1998: The submarine delta of the Ganges–Brahmaputra: cyclone-dominated sedimentation patterns. Marine Geology 149:133–154.
Miller, J. H., A. K. Behrensmeyer, A. Du, S. K. Lyons, D. Patterson, A. Tóth, A. Villaseñor, E. Kanga, and D. Reed. 2014: Ecological fidelity of functional traits based on species presence-absence in a modern mammalian bone assemblage (Amboseli, Kenya). Paleobiology 40:560–583.
Miller, K. B., C. E. Brett, and K. M. Parsons. 1988: The paleoecologic significance of storm-generated disturbance within a Middle Devonian muddy epeiric sea. Palaios:35–52.
Milliman, J. D., and R. H. Meade. 1983: World-wide delivery of river sediment to the oceans. The Journal of Geology 91:1–21.
Mohanty, P. K., U. S. Panda, P. Mishra, H. Takada, and T. Sugimoto. 2004: Tropical cyclones associated changes along Orissa coast, East coast of India. Pp.1–8 *in* Asian And Pacific Coasts 2003: (With CD-ROM). World Scientific.
Mohapatra, M., and U. Mohanty. 2004: Some characteristics of low pressure systems and summer monsoon rainfall over Orissa. Current science:1245–1255.

Molinaro, D. J., B. M. Collins, M. E. Burns, E. S. Stafford, and L. R. Leighton. 2013: Do predatory drill holes influence the transport and deposition of gastropod shells? Lethaia 46:508–517.

Mondal, S., J. A. Hutchings, and G. S. Herbert. 2014: A note on edge drilling predation by naticid gastropods. Journal of Molluscan Studies 80:206–212.

Mondal, S., and U. Sarkar. 2021: Predatory Drilling Traces on Recent Foraminifera from Chandipur Coast, India. Journal of Foraminiferal Research 51:286–293.

Mukhopadhyay, A., S. Hazra, D. Mitra, C. Hutton, A. Chanda, and S. Mukherjee. 2016: Characterizing the multi-risk with respect to plausible natural hazards in the Balasore coast, Odisha, India: a multi-criteria analysis (MCA) appraisal. Natural Hazards 80:1495–1513.

Nebelsick, J. 1999: Taphonomic legacy of predation on echinoids. Pp.347–352 .

Nilsen, E., D. Christianson, J.-M. Gaillard, D. Halley, J. Linnell, M. Odden, M. Panzacchi, C. Toïgo, and B. Zimmermann. 2012: Describing food habits and predation: field methods and statistical considerations. Carnivore Ecology and Conservation - a handbook of techniques:256–272.

Olivera, A. M., and W. L. Wood. 1997: Hydrodynamics of bivalve shell entrainment and transport. Journal of Sedimentary Research 67:514–526.

Olszewski, T. D. 2004a: A unified mathematical framework for the measurement of richness and evenness within and among multiple communities. Oikos 104:377–387.

Olszewski, T. D. 2004b: Modeling the Influence of Taphonomic Destruction, Reworking, and Burial on Time-Averaging in Fossil Accumulations. PALAIOS 19:39–50.

———. 2012: Remembrance of things past: modelling the relationship between species' abundances in living communities and death assemblages. Biology Letters 8:131–134.

Olszewski, T. D., and M. E. Patzkowsky. 2001: Measuring Recurrence of Marine Biotic Gradients: A Case Study from the Pennsylvanian-Permian Midcontinent. PALAIOS 16:444–460.

Olszewski, T. D., and S. M. Kidwell. 2007: The preservational fidelity of evenness in molluscan death assemblages. Paleobiology 33:1–23.

Ottens, K. J., G. P. Dietl, P. H. Kelley, and S. D. Stanford. 2012: A comparison of analyses of drilling predation on fossil bivalves: Bulk- vs. taxon-specific sampling and the role of collector experience. Palaeogeography, Palaeoclimatology, Palaeoecology 319–320:84–92.

Pahari, A., S. Mondal, S. Bardhan, D. Sarkar, S. Saha, and D. Buragohain. 2016: Subaerial naticid gastropod drilling predation by Natica tigrina on the intertidal molluscan community of Chandipur, Eastern Coast of India. Palaeogeography, Palaeoclimatology, Palaeoecology 451:110–123.

Palmqvist, P., B. Martínez-Navarro, and A. Arribas. 1996: Prey selection by terrestrial carnivores in a lower Pleistocene paleocommunity. Paleobiology 22:514–534.

Pandolfi, J. 2002: Coral community dynamics at multiple scales. Coral Reefs 21.

Pandolfi, J. M. 1992: Evolution and the Fossil Record. Evolution 46:1589–1592.

Parsons, K. M., and C. E. Brett. 1991: Taphonomic processes and biases in modern marine environments: an actualistic perspective on fossil assemblage preservation. The processes of fossilization.:22–65.

Parsons-Hubbard, K. M., W. R. Callender, E. N. Powell, C. E. Brett, S. E. Walker, A. L. Raymond, and G. M. Staff. 1999: Rates of burial and disturbance of experimentally-deployed molluscs; implications for preservation potential. PALAIOS 14:337–351.

Parulekar, A. H., and A. B. Wagh. 1975: Quantitative studies on benthic macrofauna of north-eastern Arabian Sea shelf. IJMS Vol.04(2) [December 1975].

Patra, S. K., P. Mishra, P. Mohanty, U. Pradhan, U. Panda, R. Murthy, V. S. Kumar, and B. Nair. 2016: Cyclone and monsoonal wave characteristics of northwestern Bay of Bengal: long-term observations and modeling. Natural Hazards 82:1051–1073.

Patzkowsky, M. E., and S. M. Holland. 2012a: Stratigraphic Paleobiology: Understanding the Distribution of Fossil Taxa in Time and Space. University of Chicago Press, p.

———. 2012b: 6 The Ecology of Fossil Taxa through Time. Pp.113–130 *in* 6 The Ecology of Fossil Taxa through Time. University of Chicago Press.

Peixoto, F. P., F. Villalobos, A. S. Melo, J. a. F. Diniz-Filho, R. Loyola, T. F. Rangel, and M. V. Cianciaruso. 2017: Geographical patterns of phylogenetic beta-diversity components in terrestrial mammals. Global Ecology and Biogeography 26:573–583.

Petsios, E., R. W. Portell, L. Farrar, S. Tennakoon, T. B. Grun, M. Kowalewski, and C. L. Tyler. 2021: An asynchronous Mesozoic marine revolution: the Cenozoic intensification of predation on echinoids. Proceedings of the Royal Society B: Biological Sciences 288:20210400.

Poirier, C., P.-G. Sauriau, E. Chaumillon, and X. Bertin. 2010: Influence of hydro-sedimentary factors on mollusc death assemblages in a temperate mixed tide-and-wave

dominated coastal environment: implications for the fossil record. Continental Shelf Research 30:1876–1890.
Ponder, W., and D. R. Lindberg. 2008: Phylogeny and Evolution of the Mollusca. University of California Press, p.
Powell, E. N., W. R. Callender, G. M. Staff, K. M. Parsons-Hubbard, C. E. Brett, S. E. Walker, A. Raymond, and K. A. Ashton-Alcox. 2008: Molluscan Shell Condition After Eight Years on the Sea Floor—Taphonomy in the Gulf of Mexico and Bahamas. Journal of Shellfish Research 27:191–225.
Powell, E. N., G. M. Staff, W. R. Callender, K. A. Ashton-Alcox, C. E. Brett, K. M. Parsons-Hubbard, S. E. Walker, and A. Raymond. 2011: Taphonomic degradation of molluscan remains during thirteen years on the continental shelf and slope of the northwestern Gulf of Mexico. Palaeogeography, Palaeoclimatology, Palaeoecology 312:209–232.
Powell, E. N., K. M. Parsons-Hubbard, W. R. Callender, G. M. Staff, G. T. Rowe, C. E. Brett, S. E. Walker, A. Raymond, D. D. Carlson, S. White, and E. A. Heise. 2002: Taphonomy on the continental shelf and slope: two-year trends – Gulf of Mexico and Bahamas. Palaeogeography, Palaeoclimatology, Palaeoecology 184:1–35.
Pringle, R. M., T. R. Kartzinel, T. M. Palmer, T. J. Thurman, K. Fox-Dobbs, C. C. Y. Xu, M. C. Hutchinson, T. C. Coverdale, J. H. Daskin, D. A. Evangelista, K. M. Gotanda, N. A. Man in ’t Veld, J. E. Wegener, J. J. Kolbe, T. W. Schoener, D. A. Spiller, J. B. Losos, and R. D. H. Barrett. 2019: Predator-induced collapse of niche structure and species coexistence. Nature 570:58–64.
Pruden, M. J., S. E. Mendonca, and L. R. Leighton. 2018: The effects of predation on the preservation of ontogenetically young individuals. Palaeogeography, Palaeoclimatology, Palaeoecology 490:404–414.
Purvis, A., and A. Hector. 2000: Getting the measure of biodiversity. Nature 405:212–219.
Pyke, G. H. 1984: Optimal Foraging Theory: A Critical Review. Annual Review of Ecology and Systematics 15:523–575.
Qian, H., and R. E. Ricklefs. 2007: A latitudinal gradient in large-scale beta diversity for vascular plants in North America. Ecology Letters 10:737–744.
Qian, H., and M. Xiao. 2012: Global patterns of the beta diversity–energy relationship in terrestrial vertebrates. Acta Oecologica 39:67–71.

Qian, H., R. E. Ricklefs, and P. S. White. 2005: Beta diversity of angiosperms in temperate floras of eastern Asia and eastern North America. Ecology Letters 8:15–22.
Qian, H., Y. Jin, F. Leprieur, X. Wang, and T. Deng. 2020: Geographic patterns and environmental correlates of taxonomic and phylogenetic beta diversity for large-scale angiosperm assemblages in China. Ecography 43:1706–1716.
Quinn, G. P., and M. J. Keough. 2002: Experimental Design and Data Analysis for Biologists. Cambridge University Press, p.
Rahel, F. J. 1990: The Hierarchical Nature of Community Persistence: A Problem of Scale. The American Naturalist 136:328–344.
Rajeevan, M., J. Srinivasan, K. Niranjan Kumar, C. Gnanaseelan, and M. M. Ali. 2013: On the epochal variation of intensity of tropical cyclones in the Arabian Sea. Atmospheric Science Letters 14:249–255.
Randle, E., and R. S. Sansom. 2019: Bite marks and predation of fossil jawless fish during the rise of jawed vertebrates. Proceedings of the Royal Society B: Biological Sciences 286:20191596.
Rao, N. S. 2017: Indian seashells: part-2 bivalvia. Zoological Survey of India, p.
Redman, C. M., L. R. Leighton, S. A. Schellenberg, C. N. Gale, J. L. Nielsen, D. L. Dressler, and M. K. Klinger. 2007: Influence of spatiotemporal scale on the interpretation of paleocommunity structure: lateral variation in the Imperial formation of California. Palaios 22:630–641.
Ritter, M., and F. Erthal. 2013: Fidelity bias in mollusk assemblages from coastal lagoons of southern Brazil. Revista Brasileira de Paleontologia 16:225–236.
Roden, V. J., M. Zuschin, A. Nützel, I. M. Hausmann, and W. Kiessling. 2020: Drivers of beta diversity in modern and ancient reef-associated soft-bottom environments. PeerJ 8:e9139.
Rojas, A., Cabrera, Fernanda, M. Verde, D. Urteaga, F. Scarabino, and S. Martínez. 2014: The first predatory drillhole on a fossil chiton plate: an occasional prey item or an erroneous attack? PALAIOS 29:414–419.
Rosenzweig, M. L. 1995: Species diversity in space and time. Cambridge University Press, p.
Roy, K., D. J. Miller, and M. Labarbera. 1994: Taphonomic Bias in Analyses of Drilling Predation: Effects of Gastropod Drill Holes on Bivalve Shell Strength. PALAIOS 9:413.

Ryer, C. H., and B. L. Olla. 1995: Influences of food distribution on fish foraging behaviour. Animal Behaviour 49:411–418.
Salamon, M. A., T. Brachaniec, and P. Gorzelak. 2020: Durophagous fish predation traces versus tumbling-induced shell damage—a paleobiological perspective. PALAIOS 35:37–47.
Sarkar, D., M. Bhattacherjee, and D. Chattopadhyay. 2019: Influence of regional environment in guiding the spatial distribution of marine bivalves along the Indian coast. Journal of the Marine Biological Association of the United Kingdom 99:163–177.
Schemske, D. W., G. G. Mittelbach, H. V. Cornell, J. M. Sobel, and K. Roy. 2009: Is There a Latitudinal Gradient in the Importance of Biotic Interactions? Annual Review of Ecology, Evolution, and Systematics 40:245–269.
Segre, H., R. Ron, N. De Malach, Z. Henkin, M. Mandel, and R. Kadmon. 2014: Competitive exclusion, beta diversity, and deterministic vs. stochastic drivers of community assembly. Ecology Letters 17:1400–1408.
Seitz, R. D., R. N. Lipcius, A. H. Hines, and D. B. Eggleston. 2001: Density-Dependent Predation, Habitat Variation, and the Persistence of Marine Bivalve Prey. Ecology 82:2435–2451.
Senft, R. L., M. B. Coughenour, D. W. Bailey, L. R. Rittenhouse, O. E. Sala, and D. M. Swift. 1987: Large Herbivore Foraging and Ecological Hierarchies. BioScience 37:789–799.
Signor, P. W., and C. E. Brett. 1984: The Mid-Paleozoic Precursor to the Mesozoic Marine Revolution. Paleobiology 10:229–245.
Sime, J. A., and P. H. Kelley. 2016: Common mollusk genera indicate interactions with their predators were ecologically stable across the Plio-Pleistocene extinction. Palaeogeography, Palaeoclimatology, Palaeoecology 463:216–229.
Simpson, G. G. 1943: Mammals and the nature of continents. American Journal of Science 241:1–31.
Sims, D. W., M. J. Witt, A. J. Richardson, E. J. Southall, and J. D. Metcalfe. 2006: Encounter success of free-ranging marine predator movements across a dynamic prey landscape. Proceedings of the Royal Society B: Biological Sciences 273:1195–1201.
Sivadas, S. K., D. P. Singh, and R. Saraswat. 2020: Functional and taxonomic (α and β) diversity patterns of macrobenthic communities along a depth gradient (19–2639 m): A

case study from the southern Indian continental margin. Deep Sea Research Part I: Oceanographic Research Papers 159:103250.
Sivadas, S. K., G. V. M. Gupta, S. Kumar, and B. S. Ingole. 2021: Trait-based and taxonomic macrofauna community patterns in the upwelling ecosystem of the southeastern Arabian sea. Marine Environmental Research 170:105431.
Slater, R. D. 1984: Controls of dissolved oxygen distribution and organic carbon deposition in the Arabian Sea. Geology and Oceanography of the Arabian Sea and Coastal Pakistan:305–313.
Smith, A. B., and R. B. J. Benson. 2013: Marine diversity in the geological record and its relationship to surviving bedrock area, lithofacies diversity, and original marine shelf area. Geology 41:171–174.
Smith, A. M., and C. S. Nelson. 2003: Effects of early sea-floor processes on the taphonomy of temperate shelf skeletal carbonate deposits. Earth-Science Reviews 63:1–31.
Smith, J. A., J. C. Handley, and G. P. Dietl. 2018a: Effects of dams on downstream molluscan predator–prey interactions in the Colorado River estuary. Proceedings of the Royal Society B: Biological Sciences 285:20180724.
———. 2018b: On drilling frequency and Manly's alpha: towards a null model for predator preference in paleoecology. PALAIOS 33:61–68.
Smith, J. A., G. P. Dietl, and J. C. Handley. 2019: Durophagy bias: The effect of shell destruction by crushing predators on drilling frequency. Palaeogeography, Palaeoclimatology, Palaeoecology 514:690–694.
Smith, J. A., J. C. Handley, and G. P. Dietl. 2022: Accounting for uncertainty from zero inflation and overdispersion in paleoecological studies of predation using a hierarchical Bayesian framework. Paleobiology 48:65–82.
Soininen, J., J. J. Lennon, and H. Hillebrand. 2007: A Multivariate Analysis of Beta Diversity Across Organisms and Environments. Ecology 88:2830–2838.
Souza, C. A. de, B. E. Beisner, L. F. M. Velho, P. de Carvalho, A. Pineda, and L. C. G. Vieira. 2021: Impoundment, environmental variables and temporal scale predict zooplankton beta diversity patterns in an Amazonian river basin. Science of The Total Environment 776:145948.
Spencer, D. W. 1963: The interpretation of grain size distribution curves of clastic sediments. Journal of Sedimentary Research 33:180–190.

Staff, G. M., R. J. Stanton JR., E. N. Powell, and H. Cummins. 1986: Time-averaging, taphonomy, and their impact on paleocommunity reconstruction: Death assemblages in Texas bays. GSA Bulletin 97:428–443.
Stafford, E. S., and L. R. Leighton. 2011: Vermeij Crushing Analysis: A new old technique for estimating crushing predation in gastropod assemblages. Palaeogeography, Palaeoclimatology, Palaeoecology 305:123–137.
Stanley, S. M. 2008: Predation defeats competition on the seafloor. Paleobiology 34:1–21.
Steinbauer, M. J., K. Dolos, B. Reineking, and C. Beierkuhnlein. 2012: Current measures for distance decay in similarity of species composition are influenced by study extent and grain size. Global Ecology and Biogeography 21:1203–1212.
Stendera, S. E. S., and R. K. Johnson. 2005: Additive partitioning of aquatic invertebrate species diversity across multiple spatial scales. Freshwater Biology 50:1360–1375.
Stephens, D. W., and J. R. Krebs. 2019: Foraging Theory. Princeton University Press, p.
Subrahmanyam, B., K. H. Rao, N. Srinivasa Rao, V. S. N. Murty, and R. J. Sharp. 2002: Influence of a tropical cyclone on Chlorophyll-a Concentration in the Arabian Sea. Geophysical Research Letters 29:22-1-22–24.
Subramanian, V., L. Van't Dack, and R. Van Grieken. 1985: Chemical composition of river sediments from the Indian sub-continent. Chemical Geology 48:271–279.
Summerville, K. S., M. J. Boulware, J. A. Veech, and T. O. Crist. 2003: Spatial Variation in Species Diversity and Composition of Forest Lepidoptera in Eastern Deciduous Forests of North America. Conservation Biology 17:1045–1057.
Sundborg, Å. 1956: The river Klarälven a study of fluvial processes. Geografiska annaler 38:125–316.
Svenning, J.-C., C. Fløjgaard, and A. Baselga. 2011: Climate, history and neutrality as drivers of mammal beta diversity in Europe: insights from multiscale deconstruction. Journal of Animal Ecology 80:393–402.
Ter Braak, C. J. F. 1986: Canonical Correspondence Analysis: A New Eigenvector Technique for Multivariate Direct Gradient Analysis. Ecology 67:1167–1179.
Terry, R. C. 2010: On raptors and rodents: testing the ecological fidelity and spatiotemporal resolution of cave death assemblages. Paleobiology 36:137–160.

Tittensor, D. P., C. Mora, W. Jetz, H. K. Lotze, D. Ricard, E. V. Berghe, and B. Worm. 2010: Global patterns and predictors of marine biodiversity across taxa. Nature 466:1098–1101.

Tokeshi, M. 2009: Species Coexistence: Ecological and Evolutionary Perspectives. John Wiley & Sons, p.

Tomašových, A. 2004: Postmortem Durability and Population Dynamics Affecting the Fidelity of Brachiopod Size-Frequency Distributions. PALAIOS 19:477–496.

Tomašových, A., and S. M. Kidwell. 2009a: Preservation of spatial and environmental gradients by death assemblages. Paleobiology 35:119–145.

———. 2009b: Fidelity of variation in species composition and diversity partitioning by death assemblages: time-averaging transfers diversity from beta to alpha levels. Paleobiology 35:94–118.

———. 2010a: Predicting the effects of increasing temporal scale on species composition, diversity, and rank-abundance distributions. Paleobiology 36:672–695.

———. 2010b: The Effects of Temporal Resolution on Species Turnover and on Testing Metacommunity Models. The American Naturalist 175:587–606.

———. 2011: Accounting for the effects of biological variability and temporal autocorrelation in assessing the preservation of species abundance. Paleobiology 37:332–354.

Tomašovỳch, A., I. Gallmetzer, A. Haselmair, D. S. Kaufman, B. Mavrič, and M. Zuschin. 2019: A decline in molluscan carbonate production driven by the loss of vegetated habitats encoded in the Holocene sedimentary record of the Gulf of Trieste. Sedimentology 66:781–807.

Tomašových, A., I. Gallmetzer, A. Haselmair, D. S. Kaufman, M. Kralj, D. Cassin, R. Zonta, and M. Zuschin. 2018: Tracing the effects of eutrophication on molluscan communities in sediment cores: outbreaks of an opportunistic species coincide with reduced bioturbation and high frequency of hypoxia in the Adriatic Sea. Paleobiology 44:575–602.

Tuomisto, H. 2010: A diversity of beta diversities: straightening up a concept gone awry. Part 1. Defining beta diversity as a function of alpha and gamma diversity. Ecography 33:2–22.

Tuomisto, H., K. Ruokolainen, and M. Yli-Halla. 2003: Dispersal, Environment, and Floristic Variation of Western Amazonian Forests. Science 299:241–244.

Tyler, C. L., and M. Kowalewski. 2017: Surrogate taxa and fossils as reliable proxies of spatial biodiversity patterns in marine benthic communities. Proceedings of the Royal Society B: Biological Sciences 284:20162839.

Tyler, C. L., L. R. Leighton, S. J. Carlson, J. W. Huntley, and M. Kowalewski. 2013: Predation on Modern and Fossil Brachiopods: Assessing Chemical Defenses and Palatability. PALAIOS 28:724–735.

Ulrich, W., and N. J. Gotelli. 2007: Null Model Analysis of Species Nestedness Patterns. Ecology 88:1824–1831.

Vermeij, G. J. 1977: The Mesozoic Marine Revolution: Evidence from Snails, Predators and Grazers. Paleobiology 3:245–258.

———. 1983: Shell-Breaking Predation through Time. Pp.649–669 *in* M. J. S. Tevesz and P. L. McCall, eds. Biotic Interactions in Recent and Fossil Benthic Communities. Springer US, Boston, MA.

———. 1993: Evolution and Escalation: An Ecological History of Life. Princeton University Press

Vermeij, G. J., D. E. Schindel, and E. Zipser. 1981: Predation Through Geological Time: Evidence from Gastropod Shell Repair. Science 214:1024–1026.

Visaggi, C. C., and L. C. Ivany. 2010: The influence of data selection and type of analysis on interpretations of temporal stability in Oligocene Faunas of Mississippi. PALAIOS 25:769–779.

W Schäfer. 1962: *Aktuo-Palaeontologie nach studien in der nordsee.* on 2 September 2022.

Wagner, H. H., O. Wildi, and K. C. Ewald. 2000: Additive partitioning of plant species diversity in an agricultural mosaic landscape. Landscape Ecology 15:219–227.

Walker, K., and R. K. Bambach. 1971: The significance of fossil assemblages from fine-grained sediments: time-averaged communities.

Warwick, R., and J. Light. 2002: Death assemblages of molluscs on St Martin's Flats, Isles of Scilly: a surrogate for regional biodiversity? Biodiversity & Conservation 11:99–112.

Warwick, R., and S. Turk. 2002: Predicting climate change effects on marine biodiversity: comparison of recent and fossil molluscan death assemblages. Journal of the Marine Biological Association of the United Kingdom 82:847–850.

Webber, A. J. 2005: The Effects of Spatial Patchiness on the Stratigraphic Signal of Biotic Composition (Type Cincinnatian Series; Upper Ordovician). PALAIOS 20:37–50.
Weber, K., and M. Zuschin. 2013: Delta-associated molluscan life and death assemblages in the northern Adriatic Sea: implications for paleoecology, regional diversity and conservation. Palaeogeography, Palaeoclimatology, Palaeoecology 370:77–91.
Western, D., and A. K. Behrensmeyer. 2009: Bone Assemblages Track Animal Community Structure over 40 Years in an African Savanna Ecosystem. Science 324:1061–1064.
Westrop, S. R. 1986: Taphonomic versus ecologic controls on taxonomic relative abundance patterns in tempestites. Lethaia 19:123–132.
Whittaker, R. H. 1960: Vegetation of the Siskiyou Mountains, Oregon and California. Ecological Monographs 30:279–338.
Whittaker, R. H., and G. E. Likens. 1975: The Biosphere and Man. Pp.305–328 *in* H. Lieth and R. H. Whittaker, eds. Primary Productivity of the Biosphere. Springer, Berlin, Heidelberg.
Whittaker, R. J., K. J. Willis, and R. Field. 2001: Scale and species richness: towards a general, hierarchical theory of species diversity. Journal of Biogeography 28:453–470.
With, K. A., and T. O. Crist. 1995: Critical Thresholds in Species' Responses to Landscape Structure. Ecology 76:2446–2459.
Wolda, H. 1981: Similarity indices, sample size and diversity. Oecologia 50:296–302.
Womack, T., M. Hannah, and J. Crampton. 2020: Spatial scaling of beta diversity in the shallow-marine fossil record. Paleobiology.
Wright, D. H., and J. H. Reeves. 1992: On the meaning and measurement of nestedness of species assemblages. Oecologia 92:416–428.
Yanes, Y. 2012: Anthropogenic effect recorded in the live-dead compositional fidelity of land snail assemblages from San Salvador Island, Bahamas. Biodiversity and Conservation 21:3445–3466.
Zambito, J. J., IV, C. E. Mitchell, and H. D. Sheets. 2008: A Comparison of Sampling and Statistical Techniques for Analyzing Bulk-sampled Biofacies Composition. Palaios 23:313–321.
Zenetos, A. 1990: Discrimination of autochthonous vs. allochthonous assemblages in the Eden Estuary, Fife, Scotland, UK. Estuarine, Coastal and Shelf Science 30:525–540.

Zinger, L., L. A. Amaral-Zettler, J. A. Fuhrman, M. C. Horner-Devine, S. M. Huse, D. B. M. Welch, J. B. H. Martiny, M. Sogin, A. Boetius, and A. Ramette. 2011: Global Patterns of Bacterial Beta-Diversity in Seafloor and Seawater Ecosystems. PLOS ONE 6:e24570.
Zlotnik, M., and T. Ceranka. 2005: Patterns of drilling predation of cassid gastropods preying on echinoids from the Middle Miocene of Poland. Acta Palaeontologica Polonica 50.
Zorzal-Almeida, S., L. M. Bini, and D. C. Bicudo. 2017: Beta diversity of diatoms is driven by environmental heterogeneity, spatial extent and productivity. Hydrobiologia 800:7–16.
Zuschin, M., and R. J. Stanton. 2002: Paleocommunity Reconstruction from Shell Beds: A Case Study from the Main Glauconite Bed, Eocene, Texas. PALAIOS 17:602–614.
Zuschin, M., and P. G. Oliver. 2003: Fidelity of molluscan life and death assemblages on sublittoral hard substrata around granitic islands of the Seychelles. Lethaia 36:133–149.
Zuschin, M., and P. G. Oliver. 2005: Diversity patterns of bivalves in a coral dominated shallow-water bay in the northern Red Sea–high species richness on a local scale. Marine Biology Research 1:396–410.
Zuschin, M., and C. Ebner. 2015: Actuopaleontological characterization and molluscan biodiversity of a protected tidal flat and shallow subtidal at the northern Red Sea. Facies 61:1–13.
Zuschin, M., J. Hohenegger, and F. F. Steininger. 2000: A comparison of living and dead molluscs on coral reef associated hard substrata in the northern Red Sea—implications for the fossil record. Palaeogeography, Palaeoclimatology, Palaeoecology 159:167–190.
Zuschin, M., M. Stachowitsch, and R. J. Stanton. 2003: Patterns and processes of shell fragmentation in modern and ancient marine environments. Earth-Science Reviews 63:33–82.
Zuschin, M., M. Harzhauser, and O. Mandic. 2005: Influence of size-sorting on diversity estimates from tempestitic shell beds in the middle Miocene of Austria. Palaios 20:142–158.
Zuschin, M., M. Harzhauser, and K. Sauermoser. 2006: Patchiness of local species richness and its implication for large-scale diversity patterns: an example from the middle Miocene of the Paratethys. Lethaia 39:65–80.

List of publications of Madhura Bhattacherjee

Journal

1. **M Bhattacherjee**, D Chattopadhyay, B Som, AS Sankar, S Mazumder (2021): Molluscan live-dead fidelity of a storm-dominated shallow-marine setting and its implications, *Palaios* 36 (2), 77-93

2. Chattopadhyay, D., Sarkar, D., & **Bhattacherjee, M.** (2021). The distribution pattern of marine bivalve death assemblage from the western margin of Bay of Bengal and its oceanographic determinants. *Frontiers in Marine Science*, 8, 675344.

3. Sarkar, D., **Bhattacherjee, M.**, & Chattopadhyay, D. (2019). Influence of regional environment in guiding the spatial distribution of marine bivalves along the Indian coast. *Journal of the Marine Biological Association of the United Kingdom*, 99 (1), 163-177.

Preprint:

1. Bhattacherjee, M., & Chattopadhyay, D. (2022). Controls of spatial grain size and environmental variables on observed beta diversity of molluscan assemblage at a regional scale. bioRxiv. doi: https://doi.org/10.1101/2022.11.02.514806

2. Bhattacherjee, M., & Chattopadhyay, D. (2022). Community evenness and sample size affect estimates of predation intensity and prey selection: A model-based validation. bioRxiv. doi: https://doi.org/10.1101/2022.07.18.500550